In vivo imaging of the degenerating and regenerating nervous system

Dissertation
zur Erlangung des Grades eines Doktors
der Naturwissenschaften

der Fakultät für Biologie
der Ludwig-Maximilians-Universität München

vorgelegt
von

Ali Ertürk

München, Jan 2008

Erklärung und ehrenwörtliche Versicherung:

Ich versichere, dass ich die vorliegende Arbeit selbstständig durchgeführt habe und keine anderen als die aufgeführten Hilfsmittel und Quellen benutzt habe. Hiermit erkläre ich, dass ich mich einer Doktorprüfung anderweitig ohne Erfolg nicht unterzogen habe.

Ali Ertürk

München, January 9, 2008

DISSERTATION

submitted to the
Biology Faculty of Ludwig-Maximilians University of Munich,
Germany
for the degree of
Doctor of Natural Sciences

Presented by

Ali Ertürk

Born in Sakarya, Turkey

Declaration

I declare that this thesis is my own original work was carried out between October 2003 and October 2007 under the supervision of Dr. Frank Bradke at the Max-Planck-Institute of Neurobiology in Martinsried. It is submitted as PhD to the Biology Faculty of Ludwig-Maximilians University in Munich. No part of this research has been submitted in the past, or is being submitted, for a degree or examination at any other University.

Ali Ertürk

München, January 9, 2008

First Referee : **Prof. Dr. Rüdiger Klein**
Second Referee : **PD Dr. Angelika Böttger**

The exam date : **26th February, 2008**

The following article has been published based on my thesis:

Erturk A, Hellal F, Enes J, Bradke F (2007) Disorganized microtubules underlie the formation of retraction bulbs and the failure of axonal regeneration. J Neurosci 27:9169-9180.

Acknowledgments

It would have been impossible to carry out this project without the help of several people to whom I am very grateful. I would like to express my sincere gratitude to:

Dr. Frank Bradke for giving me the opportunity of working in his marvelous group at Max-Planck-Institute of Neurobiology. Besides being a great supervisor and supporting me during each step of my PhD work, his friendly and candid behaviors created a warm atmosphere which I enjoyed very much. I am also grateful to him for letting me to do my own ideas as well…

the members of my PhD thesis committee, **PD Dr. Mark Hübener, Prof. Dr. Ferdinando Rossi** and **Prof. Dr. med. Nikolaus Plesnila** for extremely helpful and encouraging discussions and advices…

Prof. Dr. Rüdiger Klein for being my doctor-father and his supports for my fellowship…

Marianne Braun, Dietmute Büringer, James P. Chalcroft, Robert Schorner and **EDV** group for technical support…

Tara Keck, Fabien Nadrigny, PD Dr. Frank Kirchhoff, Christoph Mauch and **Prof. Hans Ulrich-Dodt** for opening their facilities to collaborate…

all Bradke group members, **Liane Meyn, Farida Hellal, Joana Enes, Bhavna Ylera, Sabina Tahirovic, Boyan Garvalov, Harald Witte, Susana Gomis-Rüth, Dorothee Neukirchen, Michael Stiess** for creating wonderful working atmosphere and elegant friendships with the all funny lunches, coffee breaks and movie clubs…

Dr. Gaia Tavosanis and her group for useful discussions in the lab meetings…

all close friends especially to **Oguzhan, Erkan, Öner, Fatih, Hüseyin** and **Cihan** for their spiritual supports…

my family, for all their generous supports to my life and to **Melisa** the cutie of the family...

EU for feeding me through the NSR-RTN Marie Curie fellowship…

all my NSR colleagues and supervisors in the network for the gorgeous friendship and incredibly educative workshops…

In vivo imaging of the degenerating and regenerating nervous system

Dissertation
zur Erlangung des Grades eines Doktors
der Naturwissenschaften

der Fakultät für Biologie
der Ludwig-Maximilians-Universität München

vorgelegt
von

Ali Ertürk

München, Jan 2008

Erklärung und ehrenwörtliche Versicherung:

Ich versichere, dass ich die vorliegende Arbeit selbstständig durchgeführt habe und keine anderen als die aufgeführten Hilfsmittel und Quellen benutzt habe. Hiermit erkläre ich, dass ich mich einer Doktorprüfung anderweitig ohne Erfolg nicht unterzogen habe.

Ali Ertürk

München, January 9, 2008

DISSERTATION

submitted to the
Biology Faculty of Ludwig-Maximilians University of Munich,
Germany
for the degree of
Doctor of Natural Sciences

Presented by

Ali Ertürk

Born in Sakarya, Turkey

Declaration

I declare that this thesis is my own original work was carried out between October 2003 and October 2007 under the supervision of Dr. Frank Bradke at the Max-Planck-Institute of Neurobiology in Martinsried. It is submitted as PhD to the Biology Faculty of Ludwig-Maximilians University in Munich. No part of this research has been submitted in the past, or is being submitted, for a degree or examination at any other University.

Ali Ertürk

München, January 9, 2008

First Referee : **Prof. Dr. Rüdiger Klein**
Second Referee : **PD Dr. Angelika Böttger**

The exam date : **26th February, 2008**

The following article has been published based on my thesis:

Erturk A, Hellal F, Enes J, Bradke F (2007) Disorganized microtubules underlie the formation of retraction bulbs and the failure of axonal regeneration. J Neurosci 27:9169-9180.

Acknowledgments

It would have been impossible to carry out this project without the help of several people to whom I am very grateful. I would like to express my sincere gratitude to:

Dr. Frank Bradke for giving me the opportunity of working in his marvelous group at Max-Planck-Institute of Neurobiology. Besides being a great supervisor and supporting me during each step of my PhD work, his friendly and candid behaviors created a warm atmosphere which I enjoyed very much. I am also grateful to him for letting me to do my own ideas as well…

the members of my PhD thesis committee, **PD Dr. Mark Hübener, Prof. Dr. Ferdinando Rossi** and **Prof. Dr. med. Nikolaus Plesnila** for extremely helpful and encouraging discussions and advices…

Prof. Dr. Rüdiger Klein for being my doctor-father and his supports for my fellowship…

Marianne Braun, Dietmute Büringer, James P. Chalcroft, Robert Schorner and **EDV** group for technical support…

Tara Keck, Fabien Nadrigny, PD Dr. Frank Kirchhoff, Christoph Mauch and **Prof. Hans Ulrich-Dodt** for opening their facilities to collaborate…

all Bradke group members, **Liane Meyn, Farida Hellal, Joana Enes, Bhavna Ylera, Sabina Tahirovic, Boyan Garvalov, Harald Witte, Susana Gomis-Rüth, Dorothee Neukirchen, Michael Stiess** for creating wonderful working atmosphere and elegant friendships with the all funny lunches, coffee breaks and movie clubs…

Dr. Gaia Tavosanis and her group for useful discussions in the lab meetings…

all close friends especially to **Oguzhan, Erkan, Öner, Fatih, Hüseyin** and **Cihan** for their spiritual supports…

my family, for all their generous supports to my life and to **Melisa** the cutie of the family...

EU for feeding me through the NSR-RTN Marie Curie fellowship…

all my NSR colleagues and supervisors in the network for the gorgeous friendship and incredibly educative workshops…

Table of content

Table of content....1
List of figures....3
Summary....6
Abbreviations....9
1 Introduction 12
1.1 "Neurons in the CNS do not regenerate", the view is changing 12
1.2 Inhibitors of axonal regeneration in the CNS 12
1.2.1 Intrinsic growth competence 13
1.2.2 Inhibitory environment of the injured CNS 16
1.3 Retraction bulbs versus growth cones 21
1.4 Model of SCI 24
1.5 *In vivo* imaging to study SCI 26
2 Material and Methods 29
2.1 Mice 29
2.2 Laminectomy and Unilateral Dorsal Column Lesion 29
2.3 *In vivo* Imaging of Dorsal Column Axons 32
2.4 Sciatic Nerve Lesion and Peripheral Nerve Live Imaging 33
2.5 Perfusion and Whole Tissue Dissection for Tracing 35
2.6 Nocodazole Treatment of Peripheral Axons *in vivo* 35
2.7 Taxol Treatment of Central Axons *in vivo* 36
2.8 Immunohistochemistry 36
2.9 Confocal Imaging 37
2.10 Electron Microscopy 37
2.11 DRG Neurons Culture and Nocodazole Application 37
2.12 Cerebellar Granule Neurons Culture and Taxol Application 40
2.13 Size, Distance and Length Quantifications, Image Processing and Data Evaluation 41
3 Results 43

3.1 Characterization of retraction bulbs compared to growth cones 43
3.1.1 Morphological changes of growth cones and retraction bulbs 43
3.1.2 Retraction bulbs contain mitochondria and trans-Golgi-Network (TGN)-derived vesicles 48
3.1.3 Retraction bulbs contain disorganized microtubules 50
3.1.4 Microtubule destabilization converts a growth cone into a retraction-bulb-like structure and halts axonal growth *in vivo* 55
3.1.5 Microtubule destabilization induces the formation of bulbous axon terminals and restricts axon outgrowth in cell culture 60
3.1.6 Microtubule stabilization interferes with the formation of retraction bulbs 65
3.1.7 Microtubule stabilization enhances the growth capacity of neurons cultured on myelin 70
3.1.8 Retraction bulbs contain disorganized actin cytoskeleton 72
3.2 *In vivo* imaging of pre and reverse-conditioned axons 74
3.2.1 *In vivo* imaging of axonal degeneration and regeneration in the injured spinal cord 74
3.2.2 *In vivo* imaging of conditioned and unconditioned axons on the same animal ... 78
3.2.3 Crossing axons possess slim growth cones 80
3.2.4 Reverse-conditioned axons carry the potentials to cross the lesion site 82
4 Discussion 90
4.1 The basic intracellular events of retraction bulb formation and maintenance 90
4.2 Manipulating the microtubule network to convert the end-structures 92
4.3 Putative signaling mechanisms underlying microtubule disorganization 94
4.4 *In vivo* imaging 95
4.5 Pre-conditioning lesion 96
4.6 Reverse-conditioning lesion 98
4.7 Overview and Outlook 100
4.7.1 Characterization of retraction bulbs compared to growth cones 100
4.7.2 *In vivo* imaging of pre and reverse-conditioned axons 103

5 References 106

Curriculum Vitae.....119

List of the figures

Introduction

Figure 1 The localization of the DRG neurons and their central and peripheral extensions 14

Figure 2. Schematic representation of the CNS lesion site after a large stab injury 17

Figure 3. GFAP staining of 21 days post injury spinal cord 19

Figure 4. The responses of PNS and CNS axon terminals to the injury *in vivo* 22

Materials and Methods

Figure 5. *In vivo* imaging setup 30

Figure 6. *In vivo* imaging of sciatic nerve axons before and after lesion 34

Results

Figure 7. End-structures of PNS and CNS axons following lesion 44

Figure 8. Retraction bulbs, but not growth cones, increase in size over time 46

Figure 9. Typical appearance of growth cones of DRG Neurons in culture 47

Figure 10. Retraction bulbs contain mitochondria and *trans*-Golgi-Network (TGN)-derived vesicles 49

Figure 11. Retraction bulbs have dispersed and disorganized microtubules 53

Figure 12. Retraction bulbs have dispersed and disorganized stable and dynamic microtubules 54

Figure 13. Nocodazole application converts a growth cone into a retraction-bulb-like structure and restricts axonal growth *in vivo* 57

Figure 14. Low concentrations of nocodazole neither caused retraction bulb formation nor inhibited the growth of injured peripheral axons 59

Figure 15. Nocodazole application converts the axon terminals into retraction-bulb-like swellings and inhibits axonal growth *in vitro* 62

Figure 16. Co-immuno-staining of *in vitro* growth cones and nocodazole induced bulbous ending with tyrosinated and de-tyrosinated tubulin antibodies 64

Figure 17. Taxol application interferes with the formation of retraction bulbs 67

Figure 18. Taxol treatment does not alter the growth capacity of the peripheral axons 69

Figure 19. Taxol treatment increases the growth capacity of neurons in culture 71

Figure 20. Actin cytoskeleton of retraction bulbs *in vitro* and *in vivo* 73

Figure 21. *In vivo* imaging of regenerating sprouts after pre-conditioning lesion 75

Figure 22. Quantification of regenerating pre-conditioning sprouts 76

Figure 23. *In vivo* tissue tracing of the sciatic nerve axons 77

Figure 24. *In vivo* imaging of pre-conditioned and unconditioned (control) on the same animal 79

Figure 25. Regenerating sprouts possess growth cones 81

Figure 26. Reverse-conditioned axons cross the fresh lesion site devoid of the glial scar 84

Figure 27. 2-photon lesioned, reverse-conditioned axons cross the fresh lesion site devoid of the glial scar 87

Figure 28. Two-photon lesion induces minimal glial cell response 89

Discussion

Figure 29. Model for retraction bulb formation versus growth cone mediated regeneration 91

Summary

The current knowledge about the failure of axonal regeneration in the central nervous system (CNS) is not sufficient to treat axonal injuries. Each contribution from different laboratories sheds light on one aspect of this complicated problem. The work presented in this thesis aims to explore the underlying mechanisms of failure of axonal regeneration in the CNS from a unique perspective to find new therapeutic interventions. For this, I studied SCI *in vivo*, and used new technical approaches which allowed an accurate and quick exploration of the formulated hypothesis.

In this thesis, first, I investigated the underlying cellular mechanisms of injured CNS axon terminals, namely retraction bulbs, which are the hallmarks of regeneration failure in the CNS. While the last 10 years have seen the identification and characterization of many of the key inhibitory proteins present in the CNS myelin and the glial scar, the underlying intracellular mechanisms causing a lesioned CNS axon to stall remain poorly defined. Thus, whereas we now have a good comprehension of the “stop-signals” that axons encounter in the lesioned CNS, we do not understand the nature of the intracellular “brake” that halts axonal growth. One of the main reasons for this lies in the lack of knowledge about retraction bulbs, the non-growing counterparts of growth cones that are present at the tip of injured axons of the CNS. Whereas growth cones contain the machinery for locomotion and axonal extension, it remains elusive which part of this machinery misfunctions in retraction bulbs. Up until recent years, retraction bulbs have been neglected because the tools to study them thoroughly *in vivo* have only recently become available. Here we reported the analysis of the morphological and intracellular responses of injured axons in the CNS in comparison to those in the peripheral nervous system (PNS). We showed that retraction bulbs of injured CNS axons increase in size over time, whereas growth cones of injured PNS axons remain constant. Retraction bulbs contain a disorganized microtubule network, while growth cones possess the typical bundling of

microtubules. Using *in vivo* imaging, we found that pharmacological disruption of microtubules in growth cones transforms them into retraction-bulb-like structures, the growth of which is consequently inhibited. Likewise, microtubule destabilization of sensory neurons in cell culture induces retraction bulb formation. Conversely, microtubule stabilization prevents the formation of retraction bulbs and decreases axonal degeneration *in vivo*. Finally, microtubule stabilization enhances the growth capacity of CNS neurons cultured on myelin. Thus, the stability and organization of microtubules define the fate of lesioned axonal stumps to become either advancing growth cones or non-growing retraction bulbs. Our data pinpoint microtubules as a key regulatory target for axonal regeneration.

Next, using recent *in vivo* imaging techniques developed in our laboratory, we studied axonal regeneration after conditioning lesions. It has already been shown that the limited regeneration capacity of dorsal root ganglia (DRG) neurons can be elevated by certain manipulations. The best characterized manipulation, namely “pre-conditioning lesion”, occurs by performing a lesion at the peripheral branches of the sensory neurons prior to the central lesioning that results in a better regeneration of central axonal branches. Unfortunately, a clinically more useful approach, is “reverse-conditioning”, that requires a peripheral lesion to be made after the CNS injury has been shown to be ineffective in boosting the regeneration. However, it has been shown that reverse-conditioning like pre-conditioning upregulates the known regeneration associated genes. This suggests that regeneration failure of the reverse-conditioned axons might be due to the inhibitory external environment, e.g. glial scar, rather than the intrinsic insufficiency. In this work, I analyzed the effect of pre-conditioning lesion and relevance of the reverse-conditioning lesion in a glial scar free environment. Using recent *in vivo* imaging techniques, we demonstrated that the boosting effect of pre-conditioning lesion can be observed as early as 48 hours, much earlier than reported previously. The axonal tips of the crossing sprouts of the conditioned axons were growth cones unlike the tips of non-crossing sprouts which were mostly retraction bulbs. Moreover, reverse-conditioning of previously lesioned axons induces the formation of crossing sprouts within 48 hours through the fresh lesion area. Finally, we used a two-photon (2-photon) laser to transect a single axon thus

avoiding the formation of scar tissue. Our results demonstrated that when a transected axon is reverse-conditioned, it regenerates more than an unconditioned control axon. Hence, the formation of a glial scar after spinal cord lesions is an essential obstacle in axonal regeneration even though their intrinsic capacities can be elevated. This finding is surprising and demonstrates for the first time that if reverse-conditioning is combined with inhibitors of glial scar formation, the approach might favor axonal regeneration.

In conclusion, the work presented in this thesis provides further insight into the reasons of the underlying mechanisms that stall axonal regeneration in the CNS and suggests new approaches to enhance the limited regeneration capacity of CNS neurons.

Abbreviations

2-photon	two-photon
B.B.B	Basso-Beattie-Bresnahan locomotor rating scale
cAMP	cyclic adenosine-5'-monophosphate
CFP	cyan fluorescent protein
CGNs	cerebellar granule neurons
CNS	Central Nervous System
CREB	Ca2+/cAMP-responsive element binding protein
CRMP-2	collapsin response mediator protein-2
CSF	cerebrospinal fluid
CSPGs	chondroitin sulphate proteoglycans
CST	corticospinal track
DC	dorsal columns
DMSO	dimethyl sulfoxide
DREZ	dorsal root entry zone
DRG	dorsal root ganglia
DSPG	dermatan sulphate proteoglycan
ECM	extra cellular matrix
EM	electron microscope
GAG	gylcosaminoglycan
GC	growth cone

GFAP	glial fibrillary acidic protein
GFP	green fluorescent protein
Glu-tubulin	glutamated tubulin
GTPase	Guanosine-5'-triphosphatease
hrs	hours
HSPG	heparan sulphate proteoglycan
IL-6	Interleukin-6
JAK	janus kinases
KSPG	keratan sulphate proteoglycan
L1	lumbar vertebra 1
LIF	leukemia inhibitory factor
MAG	myelin-associated glycoprotein
MAP	microtubule associated proteins
mRNA	messenger ribonucleic acid
MTs	microtubules
NYU	New York University
OMgp	oligodendrocyte myelin glycoprotein
PBS	phosphate buffer solution
PFA	paraformaldehyde
pi	post injury
PNS	Peripheral Nervous System
RAGs	regeneration associated genes
RB	retraction bulb

RFP	red fluorescent protein
s.e.m.	standard error of the mean
SC	sciatic nerve
STAT	Signal Transducers and Activators of Transcription
T8	thoracic vertebra 8
TGN	*trans*-Golgi-network
Tyr-tubulin	tyrosinated tubulin
YFP	yellow fluorescent protein

1 Introduction

1.1 "Neurons in the CNS do not regenerate", the view is changing

Spinal cord injury (SCI) is a non-curable disorder that can affect both the physical and psychological wellbeing of its patients. After SCI, severed axons either do not grow at all or perform only limited re-growth which mostly results in permanent functional deficits such as paralysis or loss of sensation. For decades, SCI has been seen as incurable. However, this view is changing now. In particular, the discovery of inhibitory molecules of regeneration present in the CNS environment and manipulations that can expand the restricted intracellular regeneration capacity of CNS neurons make it possible to design new strategies that might treat the disease. In light of these exciting findings, it is essential that we address the challenges that lie ahead, which once overcome, will lead to complete functional recovery of the patients. We need to find out how to promote even more robust axonal regeneration; what the targets of the re-growing axons are; where they have to contact to re-establish the original function; how axons grow to the targets and how they can form the new synapses with the targets. To this end, we need to acquire a comprehensive understanding of the events underlying axon stalling in the CNS. One important challenge in SCI research has been the presence of adequate animal experimental models to study axonal regeneration. Due to the complexity of the nervous system working on CNS injuries requires technically complicated and challenging experimental procedures. For instance, it was necessary to kill the animals to trace the target axons to assess their regeneration. Nowadays, with the development of new tools, we are able to design more accurate experimental approaches which brings us closer to solving the problem.

1.2 Inhibitors of axonal regeneration in the CNS

Why do the neurons of the PNS regenerate but not those of the CNS? Over the last decades several findings have shown that there are at least two basic requirements necessary for successful regeneration to occur in the CNS: 1) the presence of intrinsic growth capacity and 2)

a permissive environment. Nowadays it has been commonly accepted that both aspects need to be manipulated to stimulate axonal regeneration.

1.2.1 Intrinsic growth competence

Embryonic nervous tissue possesses a high regeneration capacity but this ability declines in the CNS neurons during maturation (Chen et al., 1995; Goldberg et al., 2002). Conversely, adult PNS tissue still retains the ability to regenerate. Even though this transition in development is associated with essential changes in the overall properties of the nervous tissue microenvironment (Ferretti et al., 2003), there are intrinsic events occurring in the nerve cells that modify their competence for outgrowth (Goldberg, 2004). The best characterized intrinsic neuronal change is probably the decrease in the intracellular concentration of cyclic adenosine monophosphate (cAMP) (Filbin, 2003). The decrease in content of cAMP during the aging of neurons changes the effect of myelin-associated glycoprotein (MAG) on cerebellar neurons from growth promoting to growth-inhibitory (Cai et al., 2001) and the response of retinal axons to netrin-1 from attraction to repulsion (Shewan et al., 2002). The short term effect of secondary messenger cAMP is to cause local activations in the growth cone. The long term effect, on the other hand, comes via regulating the transcription of growth-related genes through the activation of the cAMP responsive element binding protein (CREB) (Gao et al., 2004). We still do not know the reasons for the remarkable decrease of intracellular cAMP at the end of development but it is clear that this contributes to regeneration failure of CNS neurons by making them less prone to grow and more sensitive to environmental inhibitors (Filbin, 2003).

Certain modifications on CNS neurons were shown to increase regeneration of the CNS axons suggesting that the intrinsic regeneration capacity is not permanently shut down but restricted. I will discuss the pre-conditioning lesion and increasing the cAMP levels, which are best characterized manipulations so far.

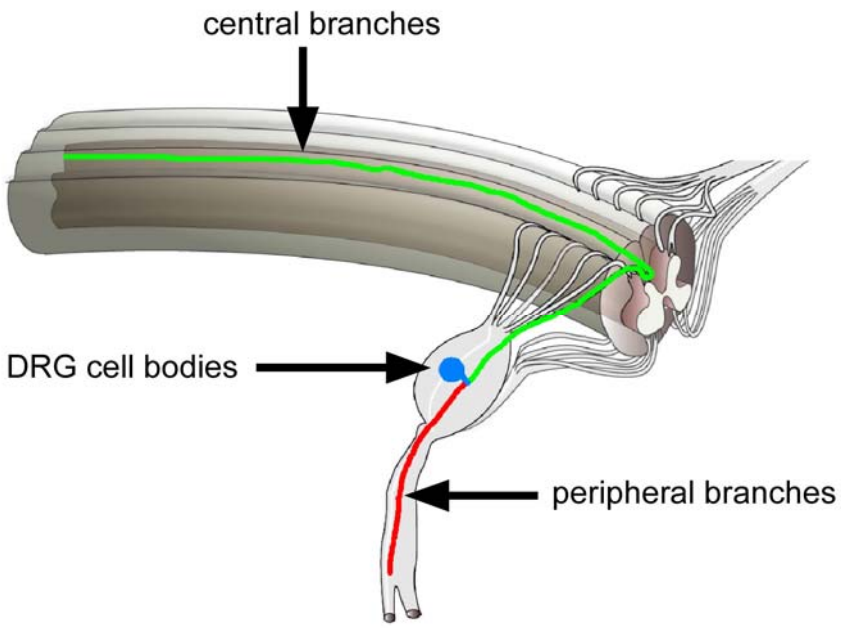

Figure 1. The localization of the DRG neurons and their central and peripheral extensions.

The cell bodies of DRG neurons reside in the ganglion, which is located outside of the spinal cord. The axonal extension coming out from the cell body branches into two extensions in the ganglion. One branch goes into the spinal cord and the other one into the periphery. The peripheral branches regenerate after injury but the central branches do not.

DRG neurons possess a pseudo-unipolar axonal extension, one branch extends into the PNS and regenerates after a lesion while the other extends into the CNS but does not regenerate after lesion (Fig. 1). Local environments surrounding the two different branches differ significantly and, therefore, are partially responsible for different responses to injury. However, lesioning peripheral branches of the DRG neurons about one week prior to lesioning the central branches has been shown to induce a robust regeneration of central axons into and beyond the lesion site (Neumann and Woolf, 1999). The underlying mechanisms of this response are not well characterized. In a simple scenario, injury to the peripheral branches disrupts retrograde transportation which activates a signaling mechanism in the cell bodies that in turn induce expression of regeneration associated genes which are normally not expressed when central branches are injured. Supporting this hypothesis, blocking retrograde axonal transport produced the same effect as pre-conditioning (Smith and Skene, 1997). In addition it has also

been demonstrated that injury induces up-regulation of importin-β leading to the formation of a high-affinity nuclear-localization-signal-binding-complex that is retrogradely transported and induces expression of regeneration associated genes (RAGs) (Hanz et al., 2003). The RAGs are effectively upregulated upon peripheral lesioning but not central lesioning (Bulsara et al., 2002; Seijffers et al., 2006). It has been shown that the order of the central and peripheral lesion is important since the clinically more relevant order which is performing the conditioning peripheral lesion after the central lesion shown to be ineffective (Richardson and Issa, 1984; Neumann and Woolf, 1999). Why does reverse-conditioning or mimicking its effect does not work? Do the neurons have a different intrinsic response after reverse-conditioning compared to the conditioning lesion? If not, what is the role of the glial scar in the reverse-conditioning?

On the other hand, one important signaling pathway that regulates intrinsic growth competence appears to be the cAMP. Increasing the intracellular levels of cAMP enhances the regeneration of CNS axons (Neumann et al., 2002). Initial evidence came from studies on *Xenopus* showing that addition of cAMP to culture media can reverse the repulsion effect of MAG to attraction (Song et al., 1998). Subsequent studies show that the presence of cAMP blocks the inhibition of neurite outgrowth from cerebellar, as well as, DRG neurons when grown on MAG (Cai et al., 2001). In light of these evidences, *in vivo* studies demonstrated that elevating intracellular cAMP levels induces axonal regeneration after SCI (Neumann et al., 2002; Qiu et al., 2002) through the activation of transcription factors such as CREB (Gao et al., 2004). Interestingly, older neurons have decreased levels of cAMP that correlates with the decrease in their ability to regenerate (Shewan et al., 2002).

In conclusion, mature CNS neurons restrict some signaling pathways which are necessary for regeneration. The cAMP pathway seems to be one of these essential signaling pathways. Re-establishment of the cAMP levels results in a more robust regeneration of the CNS axons. Hence, targeting the key intracellular signaling cascades of regeneration such as the cAMP

pathway is a promising approach to reactivate the suppressed regeneration capacity of the neurons.

1.2.2 Inhibitory environment of the injured CNS

Unlike injured PNS tissue, damaging CNS tissue forms a reactive glial scar in the lesion area which has been shown to be a barrier to axonal regeneration (Schwab and Bartholdi, 1996; Silver and Miller, 2004). After spinal cord injury, the lesion site is filled with blood, meningeal cells and macrophages which are the source of many inhibitory molecules (Pasterkamp et al., 2001; Niclou et al., 2003) (Fig. 2). Schwann cells (Zhang et al., 2005) migrate into the lesion and oligodendrocytes extend several processes. Accumulation of many hyperactive astrocytes into the lesion site contribute to the formation of the reactive gliosis (Davies et al., 1999; Tang et al., 2003) (Fig. 2 and Fig. 3). The injured axons encountering these extrinsic inhibitory factors do not grow further and usually form retraction bulbs (terminal structures of the green axons in Fig. 2). Detection of enlarged and shape-transformed astrocytes in very close proximity to dystrophic axonal end bulbs support the idea that reactive glia are involved in the failure of regeneration, presumably by the formation of a physical barrier.

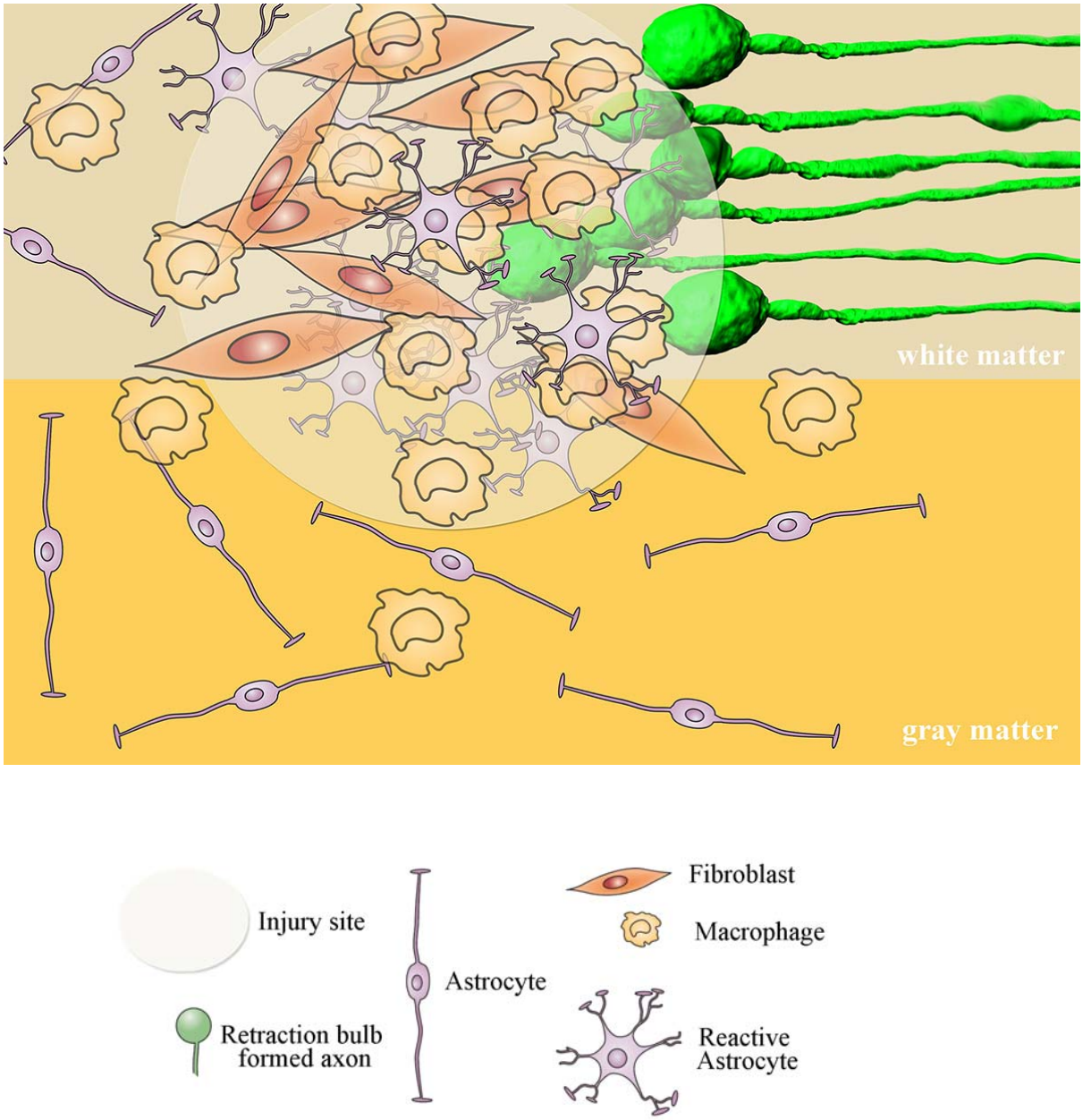

Figure 2. Schematic representation of the CNS lesion site after a large stab injury.

Immediately after the lesion, the blood-brain barrier is completely disrupted. Fibroblast and macrophages invade the lesion; astrocyte alignment is altered at the lesion site and they produce CSPGs; cavitation occurs at the center of lesion. The axons form dystrophic terminal swellings which are highly repelled by the lesion core.

Astrocytes produce a class of molecules known as proteoglycans (Gallo et al., 1987; Gallo and Bertolotto, 1990). Proteoglycans are extra cellular matrix (ECM) molecules which consist of a

protein core linked by four sugar moieties to a sulphated gylcosaminoglycan (GAG) chain containing repeating disaccharide units. So far, it has been shown that astrocytes produce and secrete four classes of proteoglycan; heparan sulphate proteoglycan (HSPG), dermatan sulphate proteoglycan (DSPG), keratan sulphate proteoglycan (KSPG) and chondroitin sulphate proteoglycan (CSPG) (Johnson-Green et al., 1991). There are many members of CSPGs (aggrecan, brevican, neurocan, NG2, phosphacan and versican) all of which have chondroitin sulphate side chains but differ in the protein core, as well as, the number, length and pattern of sulphation of the side chains (Margolis and Margolis, 1993; Grimpe and Silver, 2002; Morgenstern et al., 2002). It has been shown that the levels of CSPGs increase in the glial scar, brain and spinal cord of mature animals (McKeon et al., 1999; Jones et al., 2003; Tang et al., 2003). Several studies showed that CSPGs are inhibitory to CNS axonal extension, e.g. in the developing roof plate of the spinal cord (Katoh-Semba et al., 1995), at the dorsal root entry zone (DREZ) (Pindzola et al., 1993), and at the optic chiasm and distal optic tract (Becker and Becker, 2002). Chondroitinase an enzyme, which selectively removes a large portion of the CSPG GAG side chains, renders CSPGs less inhibitory (Krekoski et al., 2001; Bradbury et al., 2002; Morgenstern et al., 2002; Steinmetz et al., 2005). In mature mammals, CSPGs are secreted as early as 24 hours after injury and persist for several months (Silver and Miller, 2004). Importantly, embryonic reactive astroglia do not upregulate chondroitin sulfate proteoglycans CSPGs after injury (McKeon et al., 1991), however, how CSPGs exert their effect is still unknown. Possible signaling mechanisms involve RhoA GTPase, which is also a target of other inhibitory signal pathways.

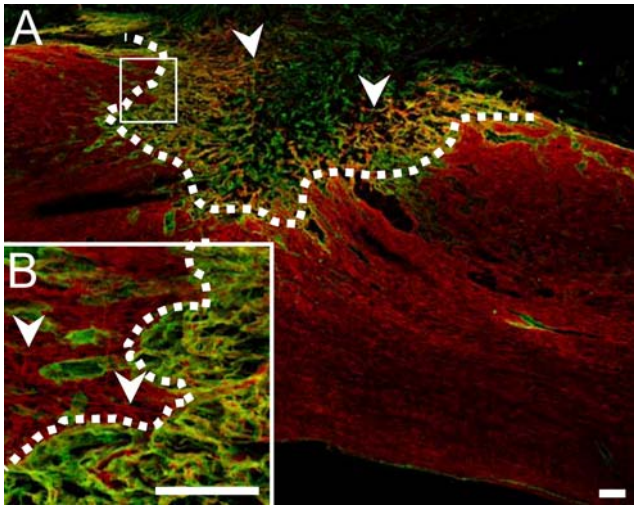

Figure 3. GFAP staining of 21 days post injury spinal cord.

A dorsal column hemi-section has been performed to transect all the axons within the dorsal columns. Twenty one days after the lesion, the animal was killed and stained with GFAP antibody (red) for reactive astrocytes and with laminin antibody for fibrotic scar (green). The dashed line in (A) outlines the lesion area and the arrowheads remark some of the astrocytes, which penetrate into the lesion area. (B) shows the inset in (A). The arrowheads in (B) mark an area dense in reactive astrocytes. The scale bars represent 150 µm. The image is courtesy of Dr. Farida Hellal.

Do reactive astrocytes of injured CNS tissue play only an inhibitory role? Recent studies revealed that mice show less functional recovery in the absence of reactive astrocytes which is associated with widespread infiltration of inflammatory, neuronal disruption and demyelination (Okada et al., 2006). These findings showed that astrocytes play an essential role in the healing of the lesion, particularly in the reformation of the blood-brain-barrier (Faulkner et al., 2004). Therefore, for an effective therapy, the amount of reactive astroglia may be needed to be reduced but not completely eliminated.

On the other hand, differences between PNS and CNS myelin sheaths are shown to contribute towards regeneration failure in the CNS. Several studies presented evidence supporting the crucial role of myelin-associated neurite growth inhibitors in preventing CNS regeneration. Firstly, eliminating oligodendrocytes or myelin improved the regeneration of descending tracts

(Schwab and Bartholdi, 1996). Secondly, antibodies against Nogo-A (IN-1 antigen) applied via the cerebrospinal fluid induced the formation of regenerative sprouts and long-distance elongation (Schnell and Schwab, 1990; Brosamle et al., 2000). Finally, when mice or rats were immunized with myelin or spinal cord homogenates they formed several regenerative sprouts after spinal cord lesions (Huang et al., 1999).

During the early phases of injury, it has been shown that along with MAG, Nogo and oligodendrocyte myelin glycoprotein (OMgp), there are several myelin associated growth inhibitors expressed by oligodendrocytes (Schwab and Bartholdi, 1996; Filbin, 2003). These molecules interact with axonal receptors resulting in growth cone collapse *in vitro* and blockade of regeneration *in vivo* (Harel and Strittmatter, 2006). Interestingly, the age at which most species lose the ability to regenerate their spinal cord coincides with spinal cord myelination (Schwab and Bartholdi, 1996). Besides, at this age the critical periods for experience-dependent plasticity declines (McGee et al., 2005). It has been suggested that myelination might be responsible for the decrease in levels of intracellular cAMP (Filbin, 2006). Therefore, in addition to their well characterized growth cone collapsing activity (Filbin, 2003; Schwab, 2004), myelin-associated proteins might induce a more global inhibitory effect on intrinsic neuronal growth properties.

Among the myelin-associated inhibitors, Nogo is the most characterized. It is a member of the reticulon family of membrane proteins, and, at least, three isoforms are generated by alternative splicing: Nogo -A, -B and -C (Fournier et al., 2002). It has been shown that Nogo and other myelin associated inhibitory cues converge downstream of their receptors onto signaling pathways of the Rho GTPases (Dubreuil et al., 2003; Fournier et al., 2003; Schweigreiter et al., 2004), which, besides the actin cytoskeleton, also affect microtubule stability and dynamics (Etienne-Manneville, 2004; Mimura et al., 2006). These findings suggest that the cytoskeleton of neurons is one of the main targets of inhibitory signaling pathways.

In summary, injured spinal cord, unlike PNS, produces many inhibitory molecules that restrict axonal regeneration. Most of these inhibitory signaling pathways seem to converge on RhoA signaling and finally onto the cytoskeleton. Therefore, the cytoskeleton would be a promising target for therapeutical intervention to bypass the intermediate steps of regeneration blockage induced by inhibitory pathways.

1.3 Retraction bulbs versus growth cones

After an injury, PNS axon terminals transform into growth cones for regeneration similar to the growth of axons during the development of the nervous system. The growth cones comprise both the engine which produces the movement and the steering apparatus, which directs the axonal tips along the proper paths (Fig. 4A). Unlike PNS neurons, CNS neurons do not generate advancing growth cones after injury. Instead, injured CNS axon terminals retract and form retraction bulbs (Fig. 4B) that are also referred to as “frustrated growth cones” due to their failure to regenerate (Ramon y Cajal, 1928; Li and Raisman, 1995; Hill et al., 2001). Although there is a growing interest to identify the intrinsic mechanisms, which prevent axonal regeneration in these end structures (Silver and Miller, 2004; Tom et al., 2004; Steinmetz et al., 2005) the current knowledge about retraction bulbs remains fragmentary.

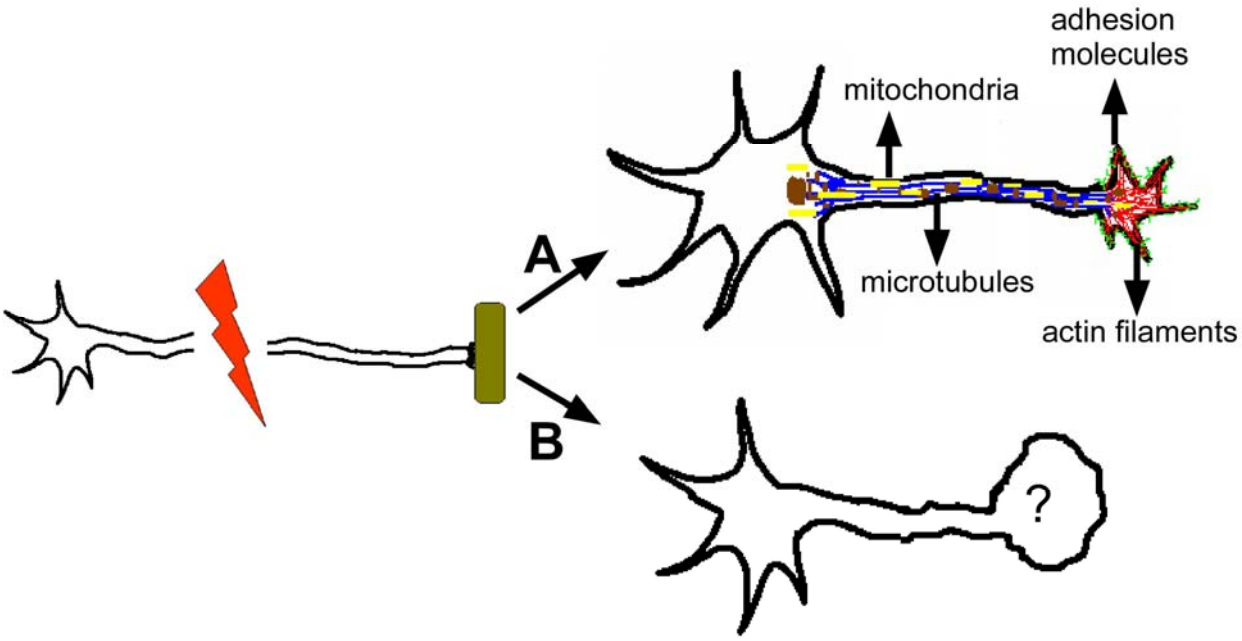

Figure 4. The responses of PNS and CNS axon terminals to the injury *in vivo*.

(A) Injured PNS neurons form a growth cone at its transected proximal terminal, where the axon advances towards the target. This process is highly dynamic and requires fast cytoskeleton polymerization/depolymerization, anterograde and retrograde transport of structural proteins, mitochondria and guidance/adhesion molecules. (B) When a CNS axon is transected it cannot form a growth cone, instead it retracts and transforms into a retraction bulb.

Growth cones possess several lamellipodia and filopodia in various sizes and numbers conferring them a hand-like structure whereas retraction bulbs are oval swellings. In addition, the lamellipodia and filopodia of growth cones are dynamic structures and undergo rapid morphological alterations by extending and retracting many times during their growth (Bray and Chapman, 1985; Dent and Gertler, 2003). The advance of growth cones and their subsequent axonal elongation is supported by a complex interplay between different intracellular mechanisms. Axon formation needs energy provided by mitochondria that are concentrated in the growing axon (Morris and Hollenbeck, 1993; Chada and Hollenbeck, 2003). Axonal growth also depends on a continuous membrane supply to support the surface expansion of the growing axon (Jareb and Banker, 1997). The bulk of the membrane supply is derived from post-Golgi vesicles, which are transported from the *trans*-Golgi-network located in

the cell body to the distal tips of the axon tip, where they are integrated in the plasma membrane at the site of the growth cone (Bray, 1970; Griffin et al., 1981; Pfenninger and Maylie-Pfenninger, 1981; Lockerbie et al., 1991; Craig et al., 1995; Dai and Sheetz, 1995; Vogt et al., 1996; Bradke and Dotti, 1997). In addition, the cytoskeleton, notably, the microtubules and their dynamic rearrangements, are essential for initiating and maintaining axonal growth (Bamburg et al., 1986; Forscher and Smith, 1988; Sabry et al., 1991; Tanaka and Kirschner, 1991; Sabry et al., 1995; Dent and Gertler, 2003). How do these cellular events occur in the retraction bulbs?

To gain a better understanding of regeneration failure in the CNS, it is necessary to elucidate the cellular and molecular mechanisms of retraction bulbs since they are the equivalent structure of growth cones in non-regenerating neurons. One important reason explaining why retraction bulbs have been neglected so far is that they appear only under *in vivo* conditions and have not been observed during *in vitro* studies probably due to the absence of a native CNS environment in the cultures. For instance, axotomy to cultured hippocampal neurons never caused the formation of retraction bulbs (Bradke and Dotti, 1997, 2000). Growth cones of cultured neurons collapse when growth inhibitors, including semaphoring (Kikuchi et al., 2003), Nogo (Huber and Schwab, 2000; Ng and Tang, 2002) and MAG (Li et al., 1996; Tang et al., 1997), are added to the environment. Growth cone collapse is a process involving a net loss of actin filaments from the leading edge, which associates with the retraction of filopodia and lamellipodia and a loss of internal membrane stores (Fan et al., 1993; Goshima et al., 1997; Zhou and Cohan, 2001). However, retraction bulbs that have been observed *in vivo* appear to enlarge their membranes (Hill et al., 2001; Silver and Miller, 2004; Coleman, 2005) suggesting that *in vitro* studies only vaguely reflect the physiological situations to study retraction bulbs. Recently, a cell culture model that produces voluminous axonal tips reminiscent to retraction bulbs has been established using a proteoglycan-laminin gradient (Tom et al., 2004; Steinmetz et al., 2005).

Therefore, to analyze the underlying mechanisms of the non-regenerating retraction bulbs, it is necessary to work with *in vivo* models. This knowledge would shed light on the reasons of the regeneration failure in the CNS and might propose new therapeutic strategies to treat SCI.

1.4 Model of SCI

Unfortunately, attempts to treat SCI have not yet yielded a successful intervention. One reason for this is the difficultly of working with the CNS tissue which is highly complicated and protected by bones and other tissues. This protection makes the CNS tissue difficult to access. Hence, many complicated experimental procedures are used to study in the CNS, which make it difficult to conclude. For instance, to assess the regeneration of the CNS axons, injured axons should be traced either genetically or with a tracer dye by injecting it into the cell bodies. Afterwards, the animals should be killed and traced tissue should be processed to be imaged. At the end, it is extremely difficult to confirm that the target axons have been successfully cut at the beginning of the experiments (Steward et al., 2003). As a result, spared axons can be misinterpreted as regenerated axons.

The spinal cord can be transected, contused or compressed to produce an injury. Each way of injury has its own advantages and disadvantages. For instance, in contusion models, which are produced using an impactor instrument, e.g. NYU or Ohio, the lesion can be produced at the same severity (Young, 2002). This type of injury is more similar to SCI cases in humans. Hence, these models are more often used to test candidate molecules and their effects on the behavior recovery of the animals. However, it is very hard to predict the epicenter of the lesion in these models. Another disadvantage is that many axons may be left spared which would make it difficult to study axonal regeneration. On the other hand, in transection or partial transection models, the epicenter can be accurately predicted. Therefore, transection models are more often used to study axonal regeneration. It is noteworthy to mention that even in the complete transection models, some axons might be left intact in the ventral part of the spinal cord (You et al., 2003).

After injuring the axons in the spinal cord, it is necessary to trace these axons to study axonal regeneration. The anterograde tracing of descending and retrograde tracing of ascending axons were the commonly used methods for assessing the course of regenerating axons around and through a lesion site. However, to visualize the traced axons, it is necessary to sacrifice the animal and section the spinal cord, therefore, transection of the axons cannot be visualized *per se*. Besides, tracing techniques always carries the possibility of unspecific labeling of the spared axons which can be misinterpreted as regenerated axons.

Another important aspect of SCI models is the type of axonal tracks to be studied. Corticospinal track (CST) axons are commonly used in regeneration studies (Joosten, 1997). However, they are widely distributed through a cross section of the spinal cord of rodents which makes it difficult to be targeted accurately. In particular, in hemi-section injury models, CST axons, present in the lateral and ventral funiculi of the white matter, can be easily left spared (Steward et al., 2003). Hence, to lesion all CST axons a complete injury has to be performed. However, since the CST track mostly contains descending axons, it is a good model system to assess functional regeneration by behavioral analysis e.g. Basso-Beattie-Bresnahan locomotor rating scale (B.B.B) (Basso et al., 1995). The ascending DRG neurons, however, are confined to the dorsal columns and end in the dorsal column nuclei of the medulla. Furthermore, these axons can be readily traced by injecting the tracer into the DRG which reside in the periphery giving minimal chance of unspecific tracing (Chong et al., 1996; Chong et al., 1999). It is relatively easy to detect the spared axons of DRG neurons during regeneration studies. Existence of the labeled axons in the dorsal column nuclei show that there are spared axons since the sprouting of the injured axons, several centimeters up to the medulla, is highly unlikely. Thus, DRG neurons are more reliable for studying axonal regeneration in the spinal cord.

Taken together, contusion and compression injury models are excellent for studying functional regeneration, but complete transection injuries are the best for assessing axonal regeneration. CST tracks are more suitable for studying the functional recovery while DRG tracks are more

reliable for assessing axonal regeneration. To study axonal regeneration in the injured spinal cord, it is necessary to trace the axons. *In vivo* imaging of transgenic mice is a reliable way which ensures the transection of the axons at the time of injury and allows visualization of the same axons over time. However, it is not yet possible with *in vivo* imaging to image the deep CNS structures and to perform long term imaging experiments.

1.5 *In vivo* imaging to study SCI

After CNS injury, damaged axons undergo several cellular and molecular alterations to re-adopt within the traumatic tissue. The responses of injured axons can be followed as morphological changes e.g. Wallerian degeneration of distal and proximal parts of the injured axons. To study the degeneration and regeneration of the axons after injury, the pathological tissues were sectioned and stained by tracing techniques or immunohistochemistry. These methods are valuable tools to test repair strategies like promoting regrowth of damaged axons, repairing damaged myelin and stimulating growth of intact fibers (Schwab, 2002). However, important shortcomings of these methods are: 1) the necessity to sacrifice the animals in order to observe the lesion which limits the analysis to static time points, 2) it is difficult to distinguish regenerated axons from spared axons (Steward et al., 2003). *In vivo* imaging, a direct observation of the injured axons, has been recently developed to overcome such problems (Lichtman and Fraser, 2001). It has been already used in many fields of neurobiology and has provided valuable insights (Johnson et al., 1999; Becker and Penkert, 2000; Pan et al., 2003; Kerschensteiner et al., 2005). For instance, it has been used to follow the neuromuscular synapse in amphibians (Herrera et al., 1990; Chen et al., 1991; Balice-Gordon, 1997) and in mammals (Wigston, 1989; Hill and Robbins, 1991; Langenfeld-Oster et al., 1993). Recently, it has been also used to study the regeneration and degeneration of axons in the CNS and PNS (Pan et al., 2003; Kerschensteiner et al., 2005; Erturk et al., 2007). During the *in vivo* imaging of GFP expressing transgenic mice, the axons are observed before injury, some minutes after injury (to confirm the transection of the target axons) and some days after injury (to visualize the regeneration of the same axons that have been confirmed to be severed) (Kerschensteiner et al., 2005).

The *in vivo* imaging of the nervous system is based on three essential components: 1) a transgenic mice line expressing GFP or GFP variants (XFPs) in a subset of neurons or other cells (e.g. astrocytes, microglia etc.); 2) the use of proper surgery which is performed without any non-specific lesion at the accurate position; 3) a wide-field conventional fluorescent or multi-photon imaging microscopy system. The transgenic mice lines (thy1-XFP) produced by Feng et al. are suitable for *in vivo* imaging of axons in the CNS (Feng et al., 2000) for several reasons. First, they express fluorescent proteins only in neurons under the control of the neuron specific promoter, *thy1*. Second, sparse labeling of the sensory neurons allows the visualization of individual axons in the dorsal columns. Third, these mice are healthy without any visible phenotypic abnormality, they are fertile, and can survive for a period of time similar to the wild type mice. Finally, the existence of different lines expressing one of CFP, GFP, YFP and RFP allows the generation of the multi transgenic mice by crossing these lines among themselves to study axon-axon interaction in a better resolution or with the other transgenics to study the role/dynamics of this particular protein in the nervous system. For instance, a thy1-CFP line can be crossed with an actin-YFP line to study the role of the actin cytoskeleton in axon degeneration/regeneration. A surgery procedure, called laminectomy, is necessary to make the superficially running sensory axons accessible to image the dorsal column axons. The details of the surgery are explained in the material and methods section and a similar procedure has been described by Misgeld and colleagues (Misgeld et al., 2007).

However, there are certain limitations of *in vivo* imaging microscopy which makes it not applicable for all studies. The main limitation is the depth of the imaging which is restricted to the surface of the tissue in case of wide-field microscopy and to about 500 µm (max up to 1000 µm with certain adaptations) in the case of multi-photon microscopy (Helmchen and Denk, 2005). However, due to the natural position of the CNS, deep tissue imaging is required to study the neuropathology of the neurodegenerative diseases that are affecting the buried CNS structures such as those affected in Parkinson's disease. Besides, the movement of anesthesized animals due to breathing or spontaneous muscles contractions creates imaging artifacts. This difficulty is more evident during deep tissue imaging with multi-photon

microscopy which requires a fixed imaging filed during its long scan. To circumvent this problem, the animals can be intubated and suspended as mentioned above. Alternatively, Helmchen and colleagues developed a miniature head-mounted 2-photon microscope which can obtain images from freely moving animals (Helmchen et al., 2001). On the other hand, it is almost impossible to image the same spinal cord longer than a week due to accumulation of the migrating fibroblasts, astrocytes and other injury related cells on top of the lesion site that makes the lesion area opaque.

A better understanding of regeneration in the PNS should shed light on why it is so poor in the CNS. After transection of a peripheral axon the distal segment, which is disconnected from the soma, undergoes Wallerian degeneration. In a few hours, the axonal segment extending from the proximal cut end starts to regenerate and presumably reaches and reinnervates the original target within a few weeks (Fu and Gordon, 1997; Pan et al., 2003). To study peripheral axonal regeneration *in vivo* Pan and colleagues have developed the transcutaneous live imaging technique after depilation of the leg hairs (Pan et al., 2003). Using this method they showed that the effects of neurotoxic and neuroprotective reagents on axonal regeneration can be studied on live animals. However, transcutaneous imaging bears some limitations. For instance, the poor resolution through the skin usually is insufficient to image morphology of the growth cones. Therefore, we developed a new *in vivo* imaging technique by exposing the sciatic nerve with surgery to obtain higher resolution images and applied the reagents directly onto the nerve after injury (the technical details are explained in Materials and Methods). Using this technique, we studied the details of the regeneration in the PNS, i.e. growth cone morphology, regeneration of the axons and the effects of microtubule modifying drugs on growth cone morphology and axonal regeneration (Erturk et al., 2007).

2 Materials and Methods

2.1 Mice

We used GFP-M and YFP-H transgenic mice (8-16 weeks, 15-30 grams) expressing GFP/YFP under the control of the neuron specific *Thy-1* promoter (Feng et al., 2000). All animal experiments were performed in accordance with the animal handling laws of the government (Regierung von Oberbayern, No: 209.1/211-2531-115/02).

2.2 Laminectomy and Unilateral Dorsal Column Lesion

The mice were anesthetized with a mixture of midazolam (Dormicum, 2 mg/kg), medetomidine (Domitor, 0.15 mg/kg), and fentanyl (0.05 mg/kg) injected intraperitoneally. The fentanyl mixture which keeps animal 3-6 hours under anesthesia with a single shot. Animals can be even boosted for a second time to image over 8-10 hours. The desired lamina were removed by laminectomy to expose the dorsal columns where the axons of the sciatic nerve project crosswise to join axons positioned in the midline. The laminectomy was completed in accordance with the following procedure:

The upper skin was opened at the top-middle of the mouse about 1.5-2 cm with a scalpel. The left and right sides of the flanking vertebra (from just near the vertebra) and also towards little forward and back were cut. While cutting, laterally on both sides very close to the vertebra were scraped without changing position of the knife. With the small scissor, the muscle and fat tissue on top and sides of the vertebra were removed. The tissue between T12 and L1 was also cleaned to go into the vertebra with a scissors from back to forward direction. In addition, a roungers was used to remove the muscles between the target and neighboring vertebra which would allow a clear entry point for spring scissors to cut the target vertebra from the edges. The head of the small scissors was placed through the left side of opening to cut at once.

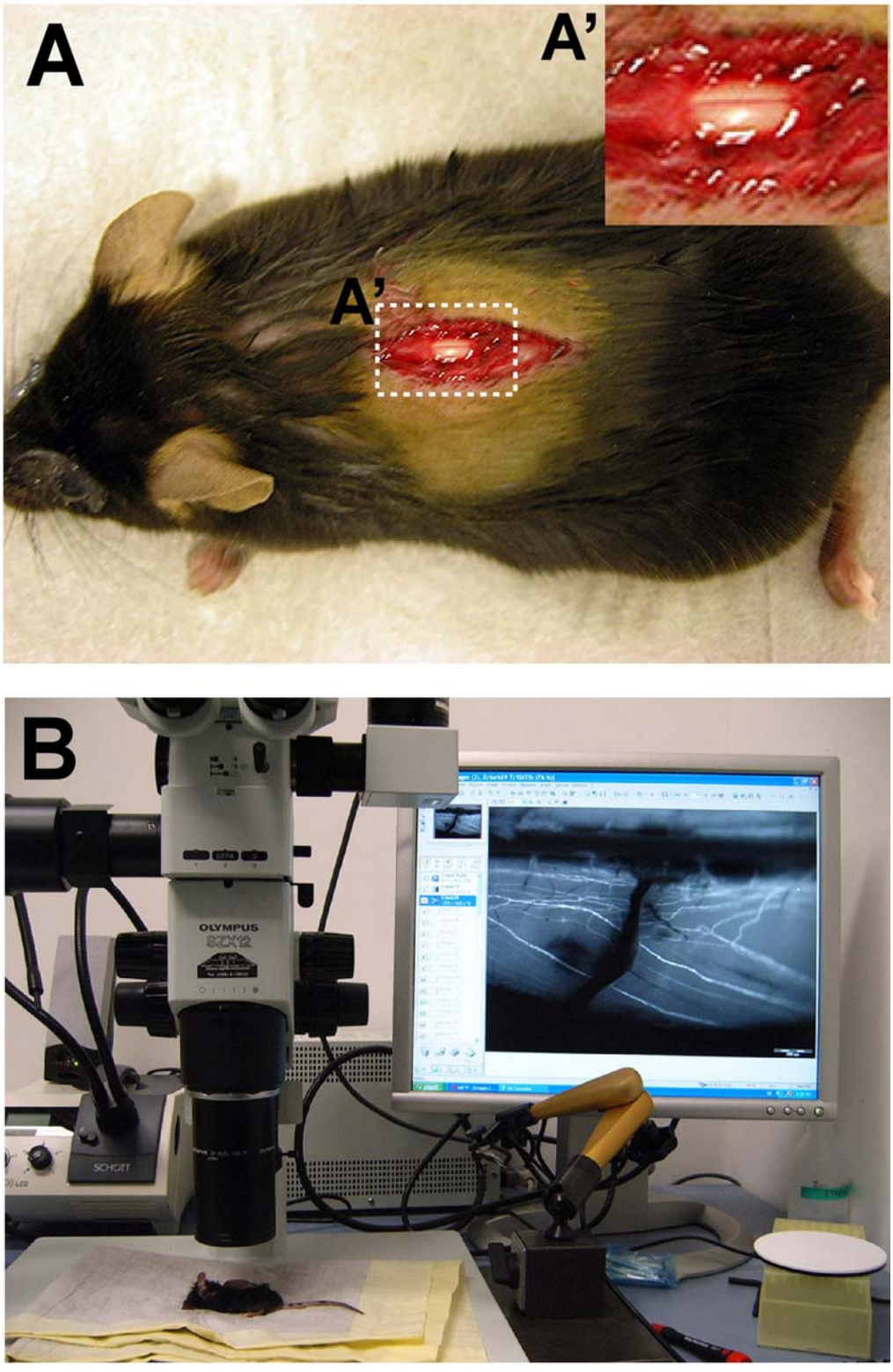

Figure 5. *In vivo* imaging setup.

(A) A laminectomy is view. After the laminectomy the spinal cord should look clean without any bleeding or bruised area (A'). (B) Overview of the binocular *in vivo* imaging system. Anesthesized animal is placed under the objective for imaging. After imaging completed, the skin is closed and animal is placed onto a heating pad until the next imaging within the same day. If the breathing is deep, the animal can be fixed with robotic arms or hanged with other instruments that would suspend the animal in the air.

The same to cut was performed at right side. The T12 was removed by lifting with a forceps and the spinal cord was exposed. If the bones are not cut enough laterally, it is necessary to clean the bones on both side of the laminectomy with the same scissors or a 0.5 mm rongeurs to have the imaging area widest. The next step is removing the dura matter. To get stronger signal during the imaging and also to apply some drugs on spinal cord, the dura matter needs to be removed at the laminectomy site. The best way to remove the dura matter was to use thick forceps to grab the dura matter from a far point to the imaging area and thin forceps to tear up the dura matter towards the sides. Since CSF will leak out after removal of dura matter, it was necessary to apply pre-warmed saline or CSF replacement (Misgeld et al., 2007). This is the most dedicate step. Any non-specific injury to spinal cord should be avoided. One thin and one think forceps were used to remove the dura. The dura matter must be grabbed at a point that is far enough from your target axons to avoid at least injuring the area of interest. After removing dura, it was the time to check if there was any non-specific injury. The anesthized and spinal cord exposed animal was placed under the microscope and checked. Waiting half an hour and checking the non-specific injury will make it sure that there was not any injury because it takes about 30 min to see the first degeneration of the axons. The skin was kept wet and closed meantime. A spinal cord with a successful laminectomy should look clean without any non-specific injury (Fig. 5A).

Afterward the laminectomy, fine irridectomy scissors (FST) was used to transect the dorsal columns unilaterally. To transect the axons as desired, the hand with the scissors should be supported to be able to cut straight and without changing the position. Just by touching the tip of the scissors, a cut on the surface of the spinal cord was performed. The cut should be as

possible as superficial to injure only the axons that are visible under the fluorescent microscope. After the laminectomy, the skin was closed with the wound clips between the imaging sessions to protect the laminectomy site from drying and outside pressure. One to two hours after imaging session, the animals were woken up by subcutaneous injection of a mixture of flumazenil (Antisedan, 0.2 mg/kg), atipamezole (Anexate, 0.75 mg/kg), and naloxone (Narcanti, 0.12 mg/kg). The animals were kept on a heating pad for the following 24 hours. Post surgical animal care was done as follows: the bladders were expressed everyday twice; antibiotics (10 µl of 7.5% Borgal solution [Hoechst Russel Vet]) were given subcutaneously once daily and buprenorphine (0.15mg/kg) once every 12 hours after surgery, in total 3 times.

2.3 *In vivo* Imaging of Dorsal Column Axons

We used an Olympus SZX-12 fluorescent stereomicroscope equipped with 1x Plan Apochromat objective and 1.6x Plan Fluorite objective (Olympus), (Fig. 1B). A ColorView II camera integrated to the microscope was used to capture images through Analysis FIVE software (Soft Imaging System). Imaging was performed as follows:

In general, after exposing the spinal cord, the animal was placed under the objective without any suspension and fast series of images were captured (Fig. 5B). Using suspensions (holding the vertebra at the each site of laminectomy, lifting the animal up and keeping it in the air with some supports e.g. robotic arms) would mostly eliminate the movement of breathing and allow a better imaging but it may cause additional damage during contact with the intact vertebra. Alternatively, one can intubate the animals to decrease the breathing movements to very low magnitudes which would allow sharper imaging in a shorter time. Indeed, the animals should be suspended or intubated to be imaged by multi-photon laser scanning microscopy as we did during the 2-photon experiments. In the continuous imaging mode of software, the lesion area was previewed. First, the focus was adjusted at lower magnifications. The GFP labeled axons were visualized as white signal in the screen (due to the black and white camera). A preview snapshot was taken at 50-100 µsec. exposure and resolution at highest 1024 with 1x binning.

To have better real time capture, one can increase the binning but this time the resolution has to be lowered. After adjusting the region of interest and focus a series images (between 25-50 images) were taken. The best image of the series was chosen for illustration. It is usually good to take the same area with different magnifications. Here, for practical reasons, we used fluorescent binocular microscope. However, to image the CNS structures located in deep tissues, a multi-photon microscope is required.

2.4 Sciatic Nerve Lesion and Peripheral Nerve Live Imaging

The mice were anesthetized as described. The sciatic nerve was exposed around 2.5 cm far from the DRG cell bodies by a small incision and crushed with forceps for ten seconds. The incision to expose the sciatic nerve should be performed without touching and stretching the nerve. The axons of the stretched nerve would look wavy rather than straight. In between the imaging sessions, the incision was filled with a physiological solution to keep the temperature and osmotic balance constant with the incision being closed between imaging sessions. Otherwise, the axons would be under stress and will not grow. During the imaging, the blood vessels were used as landmarks; specifically, the vessels perpendicular to the axons are good orientation marks. The lesion was performed close to such vertical vessels to use them as reference points. Sometimes, the sciatic nerve was found to be turned around after lesion or between imaging sessions especially if the animal was woken up. If the same area was not visible, the sciatic nerve was turned around to get the same region previously investigated. Usually, the muscles around the nerve were stretched with needle retractors to reposition the nerve and touching the nerve was avoided. For imaging, the binocular dissecting microscope was used which provided flexibility and required less time than using a conventional fluorescent or multi-photon microscope. When a drug was tested, the sciatic nerve was lesioned with forceps that have small sharp teeth to make holes in the surrounding basal lamina for a better penetration. After imaging sessions, the anesthesia was reversed and the animals were transferred to a heating pad for the following 24 hours. To get higher resolution images and to stain the sciatic nerve, the animals were perfused at the desired time points for the confocal microscopy. The basal lamina was removed for a better antibody penetration.

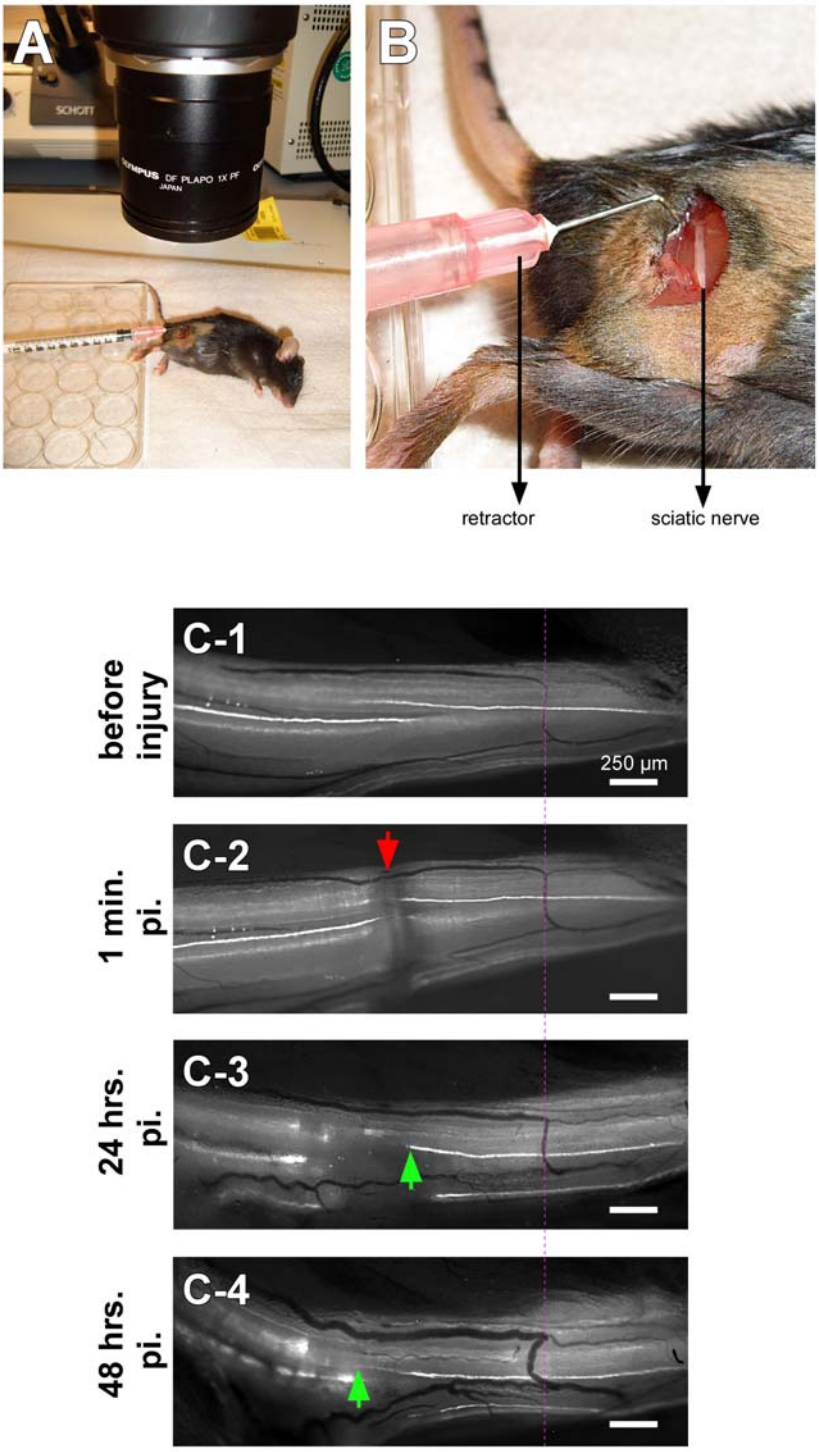

Figure 6. *In vivo* imaging of sciatic nerve axons before and after lesion.

(A-B) After exposing the sciatic nerve, the animal is placed under the microscope as shown in (A). To keep the sciatic nerve exposed during the imaging, a retractor is used to pull the muscle and skin without touching and stretching the sciatic nerve. It is important to position the sciatic nerve at a certain level of height and keep it straight (B). (C) *In vivo* imaging of sciatic nerve before injury (C-1); 1 min after injury to confirm the transection of

the axon (red arrow in C-2); 24 hours (C-3) and 48 hours (C-4) after injury to follow the regeneration of the injured axon. Here, substances, e.g. drugs can be added to study their effect on the growth cone morphology and its regeneration. The green arrows in (C-3 and C-4) mark the growth cone of this GFP positive axon to follow its extension. The images are aligned according to the same landmark, the dashed purple line which identifies the same vertical vessel.

2.5 Perfusion and Whole Tissue Dissection for Tracing

Animals were sacrificed and perfused at the defined time points. In brief, animals were anesthetized with 5-7% chloral hydrate solution (prepared in saline) and perfused intracardially with 0.1M phosphate buffer solution (PBS) at a speed of 3 ml/min for 5-10 minutes immediately followed by 4% paraformaldehyde (PFA) in PBS for 30-45 minutes. To confirm that the injured axons were really coming from the sciatic nerves, we dissected the spinal cords with the sciatic nerves without disrupting. Under the fluorescent binocular microscope, the exposed sciatic nerve axons were followed from periphery to into spinal cord, until the injury site. For whole tissue imaging with a confocal microscope, the tissues were post-fixed in 4% PFA at 4^0C overnight. The following day, the tissues were washed in PBS for 1 hour before mounting. The tissues were mounted without any sectioning onto super-frost glass slides with an aqua-based mounting media. For immunostainings and EM, the spinal cord or sciatic nerve lesion sites were carefully dissected and post fixed in 4% PFA (at room temperature for 30 minutes for immunostainings, at 4^0C overnight for morphology analysis). The tissues were incubated in 15% sucrose at room temperature for 4 hours and in 30% sucrose overnight. The tissues were embedded in OCT (Tissue-Tek) and sectioned longitudinally by a cryostat (Leica CM 3050) at 10 µm. For size quantifications, we made either thick cryostat sections (40 µm) or whole mounts for confocal observation.

2.6 Nocodazole Treatment of Peripheral Axons *in vivo*

Sciatic nerve lesion was performed as described in section 2.4. After 24 hours animals were re-anesthetized and 10 µl of 330 µM of nocodazole (Sigma-Aldrich, diluted in 5% DMSO in PBS), or 5% DMSO alone was applied onto the lesion site with a pipette. The injury site was closed and animals were perfused 24 hours after nocodazole or DMSO application for staining and

imaging. For assessing peripheral axon growth, the animals were re-anesthetized 1-2 days after lesioning and nocodazole, taxol (10 µl of 1 µM) or DMSO was applied in the same manner. The animals were either observed for 6 hours and then sacrificed or reimaged 24 hours later depending on the experimental protocol.

2.7 Taxol Treatment of Central Axons *in vivo*

After removing the laminae at T11/12 level, a small unilateral lesion was applied with vannas spring scissors (FST) by transecting only the superficial axons of the dorsal columns. We imaged the injury site before and after lesion by acquiring serial images. The animals were kept on a heating pad during the imaging session. 10 µl of 1 µM taxol (Sigma-Aldrich, diluted in Saline) or saline as control was applied onto the lesion site each hour starting immediately after lesioning. The lesion sites were visualized by *in vivo* imaging as described. The animals' anesthesia was boosted after 3 hours. At the end of the observation period animals were perfused and prepared for the confocal imaging as described.

2.8 Immunohistochemistry

The primary antibodies used were anti-Glu-tubulin (rabbit) 1:500 dilution (Chemicon) anti-Tyr-tubulin (rat) 1:500 (abcam) and anti-golgin-160 (rabbit) 1:200 (a gift from Dr. Francis Barr). Tissue sections were washed with PBS twice for 10 minutes, then incubated with blocking solution containing 10% goat serum and 0.3-0.5% Triton X-100 in PBS at room temperature for 1 hour, washed with PBS, and incubated with primary antibody (in blocking solution with 5% goat serum) at 4^0C overnight. If the thicker tissue sections (more than 20 µm) or the whole spinal cord was intended to be stained, the incubation time was 2-3 days at room temperature. The sections were washed with PBS and incubated with the following secondary antibodies: Alexa 568 anti-rabbit and Alexa 633 anti-rat (Molecular Probes). The sections were mounted with water based mounting medium (Polysciences Inc, Warrington, PA).

2.9 Confocal Imaging

We acquired confocal images with a Leica SP2 confocal microscope system in sequential scanning mode. Oil immersed 20x, 40x, and 63x Leica confocal objectives were used. Usually 2 frame average was used to improve the signal contrast over background. For noisy images, 2 frame and 2 line averaging was used together. The initial analysis of images stacks were done with the Leica software. For 3D analysis and to confirm the colocalization, I used Amira 4.1. (Mercury Systems) software.

2.10 Electron Microscopy

Animals were perfused as described above by using Lewis Shute fixative (Lewis and Shute, 1969). The tissue was dissected without drying and post fixed in Lewis Shute fixative and then in Osmium tetroxide. Afterwards, the tissue was dehydrated and embedded in araldite, cut by an ultramicrotome (LKB) at 50 nm and post stained with leadcitrate and uranylacetate by an ultrastainer (LKB). EM images of the sections were acquired using a Zeiss EM 10 electron microscope.

2.11 DRG Neurons Culture and Nocodazole Application

DRG cultures from female Sprague-Dawley rats (200-250 gr) were prepared as follows. One day before DRG isolation, poly-lysine coated slides were prepared. The poly-lysine was dissolved in Borate Buffer at a concentration of 1 mg/ml and filtered through a 0.22µ syringe. In the sterile hood, the 8 well slide was opened and 0.5 ml of the poly-lysine solution was added per well. The lid was closed and the slides were left at room temperature overnight. The next morning, the poly-lysine was aspirated off and each well was washed 3 times with sterile water. The wells were filled with 0.4 ml of growth medium (F-12 with additives or Neuro Basal with B-27 and antibiotics). The slides were placed in the 37 degrees 5% CO2 incubator and allowed equilibration for a few hours. HBSS ((HEPES Buffered Saline) with 10mM HEPES (Add 5ml of 1M HEPES, pH 7.2 to 500ml of HBSS from GIBCO)) was filled into 60 mm petridishes and placed on ice. The dissection instruments were sterilized by dipping in a beaker filled with 70% ethanol for

15 min. The instruments were placed on a 100 mm petridish and allowed to be air dried completely.

The rat was killed in the CO_2 chamber (to do so, ethanol was sprayed on the dry ice in the thermacol box and 5 layers of paper towels were placed on the dry ice after spraying). The rat was placed on the paper towel and the lid of the box was closed for 5 minutes. The rat was taken and placed on the surgery table with the ventral side up. Usually, we punctured in between the ribs on the left and right sides (the lungs) with an 18 gauge needle to ensure complete euthanasia. The animal was turned over on the dorsal side and the back was washed with ethanol. Using a scalpel, a long cut was made along the backbone from a little below the neck to almost down to the tail. Using the scalpel, the outer skin on the left and right sides from the inner layer of skin covering the peritoneal cavity was exposed. The streak of whitish connective tissue was located on the high region at the level of the hind limb and a horizontal deep cut was performed on either side to locate and expose the prominent white sciatic nerve. 2 deep longitudinal cuts were made to close the spinal column on either side from the cervical region down to the tail region. A horizontal cut was made at the cervical cut that connects the 2 longitudinal cuts. The tissue was hold at this point with the pliers and ripped so that it comes off as a long piece and exposes the vertebral column. The sciatic nerve was exposed and traced its course upwards by removing tissue with the pliers and bone cutting scissors till the hip bone was encountered.

Here the sciatic nerve disappears below the hip bone. The bone was cut using the rongeurs. To do this, one side of the scissors was inserted under the bone and cut, twist it outwards and widen the rongeurs as much as possible. The tissue was cleaned and the bone was removed to expose the sciatic nerve till it branches into two and expose further till both branches would be traced until the point where they seem to disappear into the L4 and L5 of the vertebral column. The connective tissue encasing the nerves was removed with forceps to free it from the surrounding tissue. Do the same for the left and right sides till the 4 branches would be

exposed. The nerve tissue was kept wet by spraying with sterile saline from a syringe from time to time. The spines on the vertebral column from the cervical to the caudal region were cut away using the scissors. Holding the scissors horizontally, a snip was made into the bone of the vertebral column an inch below the L4 and L5 where the sciatic nerve branches went into the spinal cord. The white spinal cord tissue was identified and then the scissors was inserted between the bony and the spinal cord was covered. The bone was cut on the left and right sides. The bone was lifted off gently upwards, making sure that the spinal cord was intact. The tissue and bits of bone was removed to clear away and locate the point where the 2 branches of the sciatic nerve meet the spinal cord. The DRG will be seen as slightly swollen bulbs at this point. The upper branch (L4) of the sciatic nerve was cut about half cm below the DRG (called the peripheral branch) and using the forceps scissors the nerve from the connective tissue freed. Continue snipping until you cross the DRG and reach a few millimeters above it (called the central branch). The nerve was cut at this point and the DRG with the peripheral and central branches were transferred into the HBSS containing petridish. The same was repeated for the lower branch (the L5 DRG) and then similarly for the right side.

Once all the 4 DRGs were obtained, the tissue was cleaned under the dissection microscope using fresh forceps and scalpel blade. To do this, the nerve was hold with the forceps and the thick peripheral branch was cut close to the swollen bulb/shell like structure (which is the DRG) with a scalpel. Using the forceps the sheath of connective tissue was removed by cutting it and peeling it off like a sock. Then the whitish central branch was cut (looks like a bunch of 2-3 thinner nerves), close to the DRG. The DRGs were transferred the cleaned up in another petridish, they were minced with the scalpel (4-5 minces per DRG) and transferred to a 15 ml falcon tube filled with HBSS. Once they settle to the bottom, the HBSS was removed with a pipette, and 2 ml of 3% collagenase was added (a total of ~3.000 units) per 4 DRGs (per rat). They were then incubated at 35C^{o} to 36C^{o} for 90 min. The supernatant was discarded carefully with a pipette and 1 ml of Trypsin solution was added and incubated for exactly 15 min at 36C^{o}. The supernatant was discarded carefully and 10 ml of F12 medium with 5% horse serum was added to inactivate the trypsin. The tube was spinned at low speed - 600 rpm for 5 min in a

table top centrifuge at room temperature. The supernatant was discarded and the DRG tissue was resuspended in 1 ml (per 4 DRGs - from 1 rat) of NeuroBasal Medium + B27 additives. They were triturated by pipetting the tissue suspension gently with a 1 ml pipette tip (about 25 times), followed by pipetting with a 200µl tip attached to the 1 ml tip (about 15 times). After a homogenous suspension was obtained, 100 µl of the cell suspension was added to each well of the 8 well slide and incubated at 37C^{o}, 5% CO_2 for 24 - 48 hours. They were viewed under the phase microscope after 18 to 24 hours to check growth of cells. Specific neuronal cell types could be identified by staining with specific antibody markers. Tuj-1 (Covance) is a neuronal specific marker which stains the large myelinating DRG neurons very well was used.

2.12 Cerebellar Granule Neurons Culture and Taxol Application

Granule neurons were isolated from the cerebellar cortex of 9 days old rats and cultured as described (Hatten, 1985). Briefly, the cerebellar cortex was trypsinized followed by trituration in a Trypsin/DNase mix (10 mg/ml and 1 mg/ml, respectively) in Tyrode solution (CMF-PBS). The granule cells were suspended in Neurobasal medium (Gibco) complemented with B-27 supplement (Invitrogen), 10% calf serum (Invitrogen), glutamine (Invitrogen) and 1 % penicillin-streptomycin (Gibco), and purified by preplating the cell suspension on poly-D-lysine (Sigma) coated dishes. The cells were plated at 2.5 x 106 / well in 8 well chamber slides (Lab-Tek system, Nunc) coated with 1 mg/ml poly-D-lysine alone or together with myelin as outgrowth inhibitory substrate. The myelin substrate was prepared as described (Neumann et al., 2002) and 1 µg of protein was dried on the poly-D-lysine pre-coated dishes per well overnight. 18 hours post-plating cells were fixed with 4% paraformaldehyde and immunostained with the beta III tubulin neuronal marker (TuJ1, Covance). The longest neurite per neuron was measured in duplicates on an average of 500 cells per condition and the results were expressed as percentage of neurite exhibiting more than 60 µm length. Each experiment was repeated at least three times.

2.13 Size, Distance and Length Quantifications, Image Processing and Data Evaluation

The size of retraction bulbs and growth cones was quantified as follows: the maximum diameter of the retraction bulb and growth cone at the tip of the axon was measured and divided by the diameter of the cylindrical shaft of the axon.

The retraction distance of taxol and saline-treated axons to the lesion site was quantified as follows: The lesion site was outlined from the *in vivo* binocular images. We then measured the distance of the axonal tips to the proximal edge of the lesion.

To measure neurite length in dorsal root ganglia neurons we took pictures from each well (80 cells per well in average) using a confocal microscope and a 10x objective. We then analyzed the data using Amira 4.1. The mean length has been calculated by measuring the total number of pixels in the images from which the pixels of the cell bodies have been subtracted and divided with the average pixel number per µm of the axons and the total number of cell bodies in the image (Total length per neuron = total number of pixels (only axons) / pixel numbers per µm / number of neurons).

We quantified the length of the crossing sprouts of regenerating axons as follows: A vertical line was drawn at epicenter of the lesion site which was outlined from the *in vivo* binocular images. The total length of the axon was quantified from the tip of the axon until the vertical line using Analysis FIVE software (Soft Imaging System). Simply, the sprouts of the regenerating axon were traced with the lines thoughtout their trajectories and the length of the individual sprout was measured. There are usually several regenerating sprouts depending on number percentage of GFP labeled axons. Therefore, usually the longest three sprouts were quantified and added up to get the total length of the regeneration.

Angle deviations, numbers of vesicle and mitochondria, size of end structures and distance to the lesion site were quantified with Analysis FIVE software. The images were assembled with Photoshop (Adobe) and Canvas (ACD Systems). The cartoons were drawn with Illustrator (Adobe). For the 3D reconstructions, the quantification of vesicle volumes and the total length of DRG neurons after *in vitro* nocodazole treatment were measured using Amira 4.1 (Mercury Computer Systems). The statistical analysis was performed with Excel (Microsoft) and statistical significance ($P < 0.05$) was calculated using the two-tailed, unpaired t-test.

3 Results

3.1 Characterization of retraction bulbs compared to growth cones

3.1.1 Morphological changes of growth cones and retraction bulbs

As indicated above, the peripheral axonal branches of the DRG neurons run in the PNS where they generate growth cones and regrow after nerve injury (Fig. 7A). In contrast, the central axonal branches coursing in the dorsal columns of the spinal cord do not regrow upon damage, and the lesioned proximal axonal terminals form retraction bulbs (Fig. 7A). To analyze the differences between retraction bulbs and growth cones *in vivo*, we again used the transgenic mice expressing GFP in a small subset of neurons, allowing a clear visualization of individual axons (Fig. 7B-K; Fig. 7) (Feng et al., 2000; Kerschensteiner et al., 2005). We induced growth cone formation by lesioning the sciatic nerve, which contains the peripheral axonal branches from the lumbar 4 and 5 DRG neurons (Fig. 7A-E; Fig. 7C-E). Retraction bulb formation, on the other hand, was induced by lesioning the dorsal columns at the thoracic 8 and 9 level (Fig. 7A, F-K; Fig. 7F-H).

Peripherally axotomized DRG neurons *in vivo* generated a slim growth cone that remained morphologically constant over time (Fig. 8B-E). While growth cones of DRG neurons in cell culture have filopodia (Fig. 9) they rarely show such structures *in vivo*. The maximal width of the *in vivo* growth cones was comparable to the diameter of the axonal shaft: The growth cone (tip) / shaft ratio was 1.31 ± 0.14 at day 1 (Fig. 8B, C; n=113 growth cones), 1.51 ± 0.15 at day 4 (n=48 growth cones) and 1.20 ± 0.20 one week after sciatic lesion (Fig. 8D, E; n=21 growth cones), (average ± s.d.; n≥ 7 mice for each time point (Fig. 8L). Later time points were difficult to visualize because of the high velocity of axonal regeneration in the PNS.

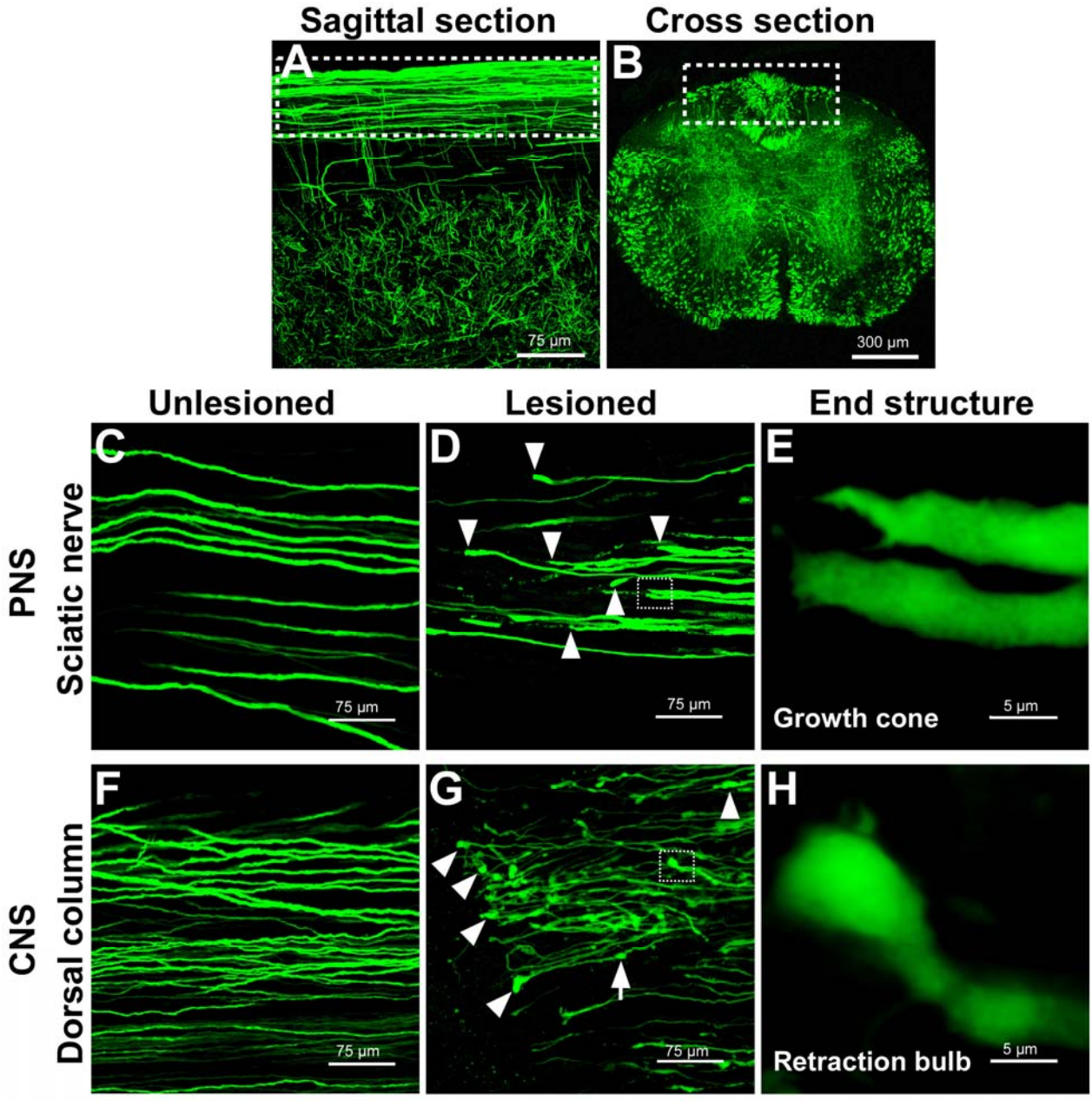

Figure 7. End-structures of PNS and CNS axons following lesion.

(A, B) Saggital section (A) and cross section (B) through the thoracic spinal cord, showing the GFP positive axons in the dorsal columns from a GFP-M transgenic mouse. The dotted rectangles frame the central axonal branches of primary sensory neurons which localize superficially within the dorsal column of the spinal cord. These axons were targeted for lesioning in this study. (C-E) Horizontal section of the sciatic nerve showing PNS axons: unlesioned (C) and 2 days after sciatic nerve lesion (D). White arrowheads in (D) show the growth cones formed at the proximal

tip of the cut peripheral axonal branches. (E) higher magnification of the marked area in (D). (F-H) Horizontal section of the dorsal column showing CNS axons: unlesioned (F) and 2 days after dorsal column lesion (G). Arrowheads in (G) show the retraction bulbs formed at the proximal tips of the lesioned central axonal branches. The arrow in (G) marks a swelling observed on the axon shaft of a lesioned neuron. (H) higher magnification of the marked area in (G).

After axotomizing the central axonal branches, retraction bulbs formed at the proximal tips. These bulbs were typically round or oval with a much larger diameter than their axons and lacked any kind of extensions (Fig. 8F-K). Retraction bulbs increased about three times in size from 1 day to 5 weeks post injury (Fig. 8F-K, L). The retraction bulb (tip) / axonal shaft ratio was 4.09 ± 0.73 at one day (Fig. 8F, G; n=109 retraction bulbs), 8.49 ± 0.51 one week (Fig. 8H, I; n=111 retraction bulbs) and 11.79 ± 0.49 five weeks post injury (Fig. 8J, K; n=92 retraction bulbs), (average ± s.d.; n≥ 8 mice for each time point [Fig. 8L]). In contrast to the slim growth cones that were continuous with the peripheral axonal shafts, the surface area of bulbous structures increased over time (Fig. 8M). Some of the axons formed smaller bulbs on their shafts in addition to the bigger terminal bulbs (arrow in Fig. 8G, Fig. 8I, K). We next aimed to address the underlying intracellular differences that could cause the formation of retraction bulbs and stalling of axons.

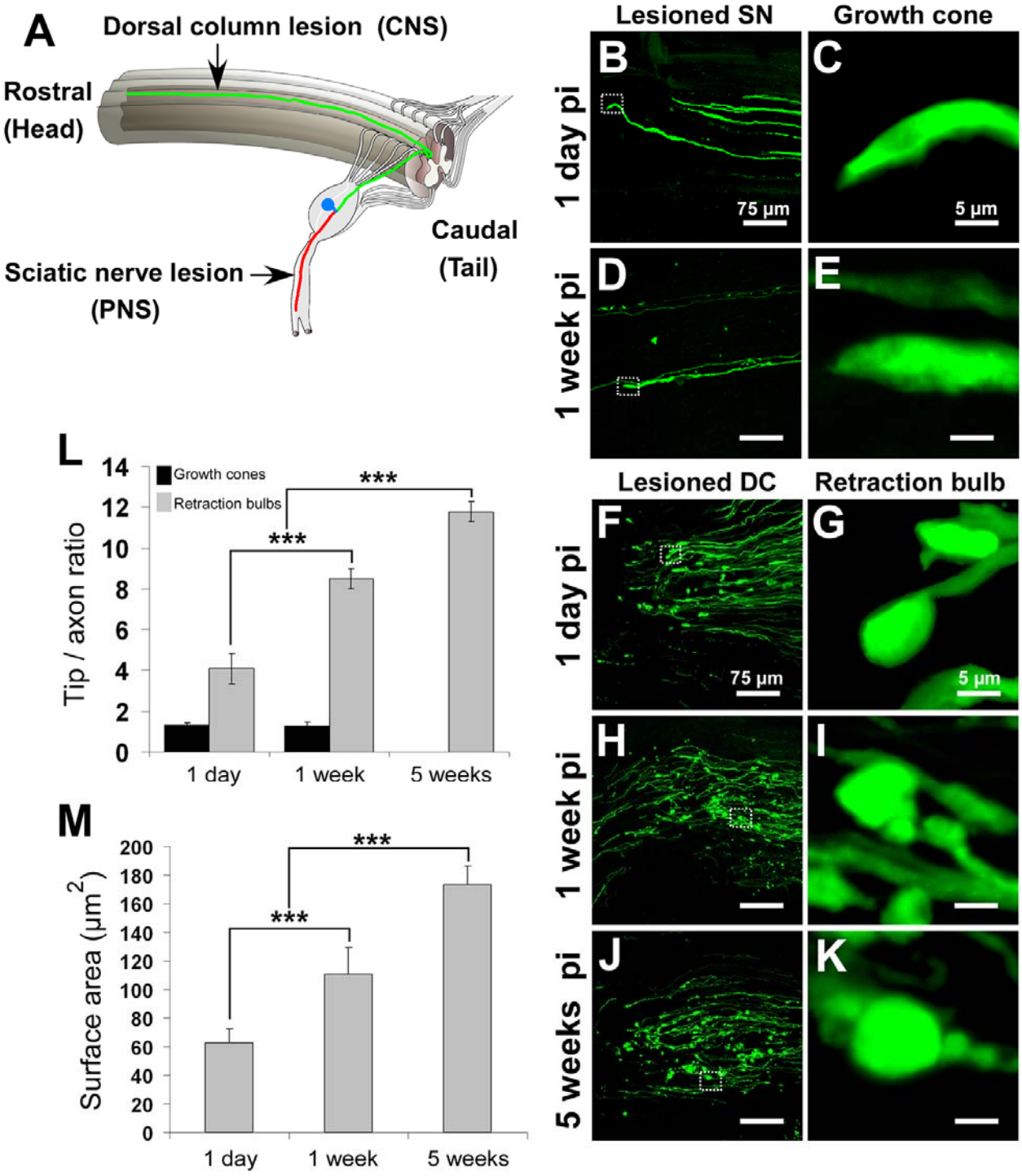

Figure 8. Retraction bulbs, but not growth cones, increase in size over time.

GFP-M mice were anesthetized, the sciatic nerve or the dorsal columns was injured, the mice were then sacrificed at various post injury times, and the tissue was fixed and analyzed by confocal microscopy. (A) Drawing of the spinal cord depicting the DRG neurons and their axons in the spinal cord and sciatic nerve. A representative DRG

neuron is highlighted; the cell body residing in the dorsal root is shown in blue, the central branch of the axon in green and the peripheral branch in red. The site of dorsal column transection to lesion the central axonal branches and the site of sciatic nerve crush to lesion the peripheral axonal branches are indicated by black arrows. (B-E) Growth cones at 1 day (B) and 1 week (D) after sciatic nerve crush; higher magnifications of (B) and (D) are shown in (C) and (E), respectively. (F-K) Retraction bulbs at 1 day (F), 1 week (H) and 5 weeks (J) after dorsal column lesion; higher magnifications of marked areas in (F, H, J) are shown in (G), (I) and (K), respectively. Note that some of the axons possess smaller swellings on the shaft in addition to the big terminal bulbs (I and K). (L) Size comparison of growth cones and retraction bulbs by tip / axonal shaft ratio. While the sizes of retraction bulbs increase, the sizes of growth cones remain constant over time. (M) Absolute size increase of retraction bulbs over time analyzed by surface area quantification.

All values are average ± s.d. *** indicates $P < 0.001$ in (L) and (M). pi: post injury.

The scale bars represent: 75 µm (B, D, F, H, J), 5 µm (C, E, G, I, K).

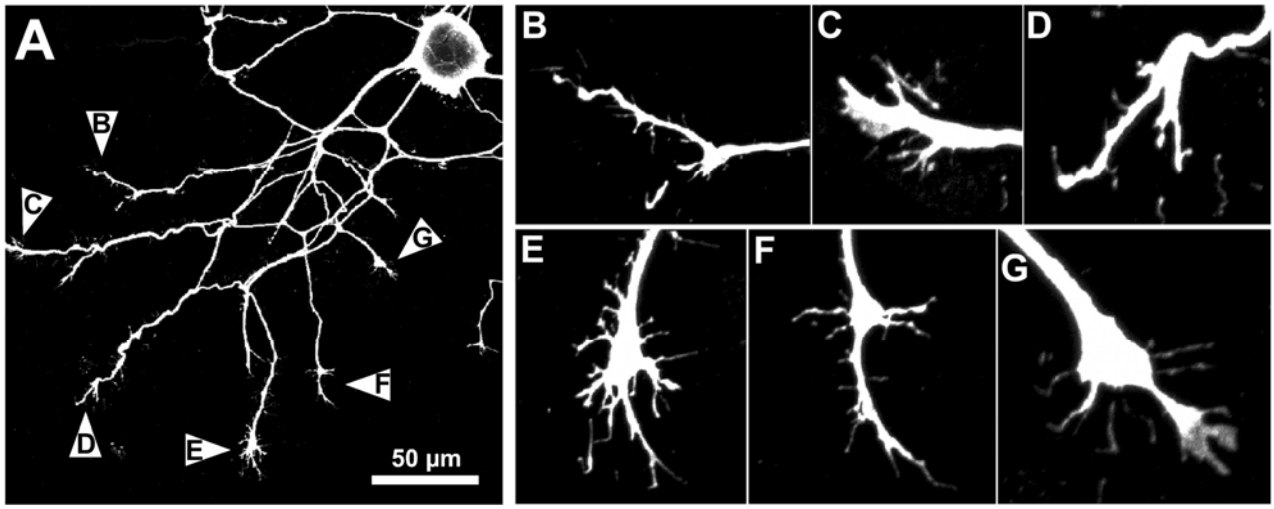

Figure 9. Typical appearance of growth cones of DRG Neurons in culture.

(A) Dissociated DRG neurons were prepared as described (Neumann et al., 2002), cultured on laminin and stained with the TuJ1 antibody (red). The axonal tips contain growth cones. (B-G) Higher magnifications of the axonal tips indicated in (A). The growth cones have several filopodia. Some of the growth cones are spread out on the substrate (C, E and G) and have a fan-like morphology in contrast to their *in vivo* counterparts that have a more stream-lined shape. The scale bar represents: 50 µm in (A).

3.1.2 Retraction bulbs contain mitochondria and trans-Golgi-Network (TGN)-derived vesicles

Sustained axonal growth requires various intracellular activities, e.g. transport of vesicles and cytoskeletal dynamics that need a high energy supply from mitochondria (Morris and Hollenbeck, 1993). Using electron microscopy, we analyzed the mitochondrial morphology and density in growth cones and retraction bulbs at various time points. The mitochondria of the retraction bulbs (Fig. 10C, D) were indistinguishable from the mitochondria of growth cones (Fig. 10A, B) and did not show characteristics of degenerating mitochondria that typically contain swollen membranes and loss of cristae (Kong and Xu, 1998). Mitochondrial density in retraction bulbs at 4 days, 2 weeks and 5 weeks post injury (3.63 ± 0.61, 3.9 ± 0.62, 4.75 ± 0.66 [mitochondria / µm2] respectively, average ± s.e.m.; n≥7 retraction bulbs per time point) was significantly higher ($P < 0.05$, Fig. 10M) than in growth cones (1.76 ± 0.47, average ± s.e.m.; n=8 growth cones).

To investigate whether lack of membrane traffic underlies both retraction bulb formation and axonal stalling after CNS injury we assessed post-Golgi trafficking by co-immunostaining GFP-labeled growth cones and retraction bulbs using the *trans*-Golgi-derived vesicle marker golgin-160 (Misumi et al., 1997). Post-Golgi vesicles accumulated both in the growth cones (Fig. 10E-H) and retraction bulbs (Fig. 10I-L). Similar results were obtained by electron microscopy (Fig. 10A, B and Fig. 10C, D; indicated by arrows). The density of smooth, small-sized vesicles was significantly higher in the retraction bulbs at 4 days, 2 weeks and 5 weeks post injury than in the growth cones ($P < 0.05$; Fig. 10N; 24.6 ± 3.86, 35.7 ± 6.54, 51.17 ± 6.52 [vesicles / µm2]; average ± s.e.m, respectively for retraction bulbs; 12.15 ± 2.5; n≥ 7 retraction bulbs per time point and n=8 growth cones). Additionally, vesicle density in the retraction bulbs significantly increased over time ($P < 0.01$; from 1 day to 5 weeks post injury in Fig. 10N).

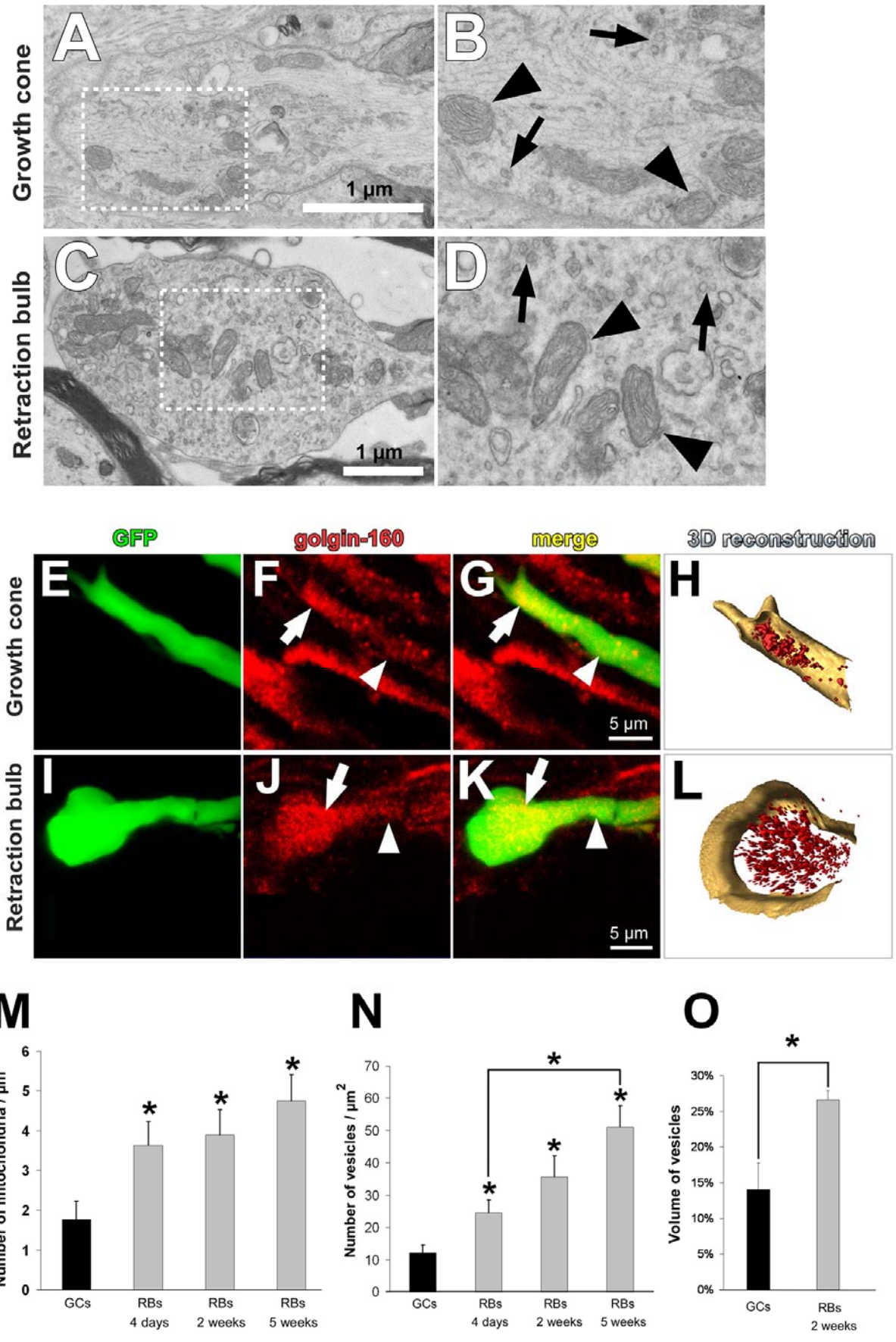
Growth cone
Retraction bulb
A
B
C
D
1 µm
1 µm
GFP
golgin-160
merge
3D reconstruction
E
F
G
H
I
J
K
L
5 µm
5 µm
M
N
O
Number of mitochondria / µm2
Number of vesicles / µm2
Volume of vesicles
GCs
RBs 4 days
RBs 2 weeks
RBs 5 weeks
RBs 2 weeks
0
1
2
3
4
5
6
10
20
30
40
50
60
70
0%
5%
10%
15%
20%
25%
30%
*

Figure 10. Retraction bulbs contain mitochondria and *trans*-Golgi-Network (TGN)-derived vesicles.
(A-D) Electron microscopy (EM) was used to analyze the morphology and quantity of vesicles and mitochondria. Electron micrographs showing a growth cone 2 days after sciatic nerve crush (A) and a retraction bulb 4 days after dorsal column lesion (C). Accumulation of mitochondria and vesicles is observed in the end structures. (B, D) higher magnification of the areas marked in (A) and (C), respectively. Black arrows show some of the vesicles and black arrowheads indicate some of the mitochondria in the end structures. (E-L) Localization of vesicles shown by immunofluorescent labeling with anti-golgin-160 antibody, specific for TGN-derived vesicles. (E, I) GFP positive end structures (green); (F, J) labeled vesicles (red); (G, K) overlay of GFP and golgin-160 signal. White arrows in (F, G, J, K) indicate the vesicles that accumulate in the end structures, and white arrowheads indicate vesicles in the axon shaft; (H, L) 3D reconstruction of the confocal images in (G, K) respectively. The red particles in (H, L) are vesicles; the outline of the end structures is partially depicted in shaded beige. (M-O) Concentration of mitochondria (M) and vesicles (N) in the growth cones at 2 days and in retraction bulbs at various time points post injury as calculated from electron micrographs. (O) concentration of vesicles in the growth cones at 2 days and retraction bulbs at 2 weeks derived from 3D volumetric quantifications. The volume of vesicles in the end structures is shown in percentages. GCs: Growth Cones and RBs: Retraction Bulbs. * in (M-O) indicates $P < 0.05$ between retraction bulbs at that time point and growth cones at 2 days pi.

Thus, it appears that vesicles are accumulating over time in the retraction bulbs. We quantified the vesicle densities in the end structures also on 3D images obtained upon reconstruction of confocal stacks and found similar results to the quantifications on the EM images (Fig. 10H, L, O; 26.6% ± 1.3 vesicles/vol. in retraction bulbs at 2 weeks and 14.1% ± 3.7 vesicles/vol. in growth cones; average ± s.d. of the total volume of the end structure; n=4 3D images per condition). Taken together, we could not find any apparent deficiencies in energy supply or membrane trafficking that hampers axon extension after SCI.

3.1.3 Retraction bulbs contain disorganized microtubules

Microtubules play a key role in axonal growth and guidance (Yamada et al., 1970; Forscher and Smith, 1988; Suter et al., 1998; Suter and Forscher, 1998; Dent et al., 1999; Dent and Gertler, 2003). They form the backbone of the axonal shafts and core domain of growth cones giving stability to those structures and enabling organelle transport (Hirokawa and Takemura, 2005). In addition, the dynamic microtubules protrude through the peripheral regions of growth cones enabling axon elongation (Kabir et al., 2001). We therefore investigated whether the

microtubular array differs in non-growing retraction bulbs and regenerating growth cones. To assess the integrity of microtubules, we co-immunostained GFP labeled axonal shafts, growth cones and retraction bulbs for detyrosinated tubulin using an anti-glu-tubulin antibody and tyrosinated tubulin using an anti-Tyr antibody as markers for stable and dynamic microtubules, respectively (Westermann and Weber, 2003). We found that detyrosinated (stable) microtubules were tightly bundled and parallel aligned in the growth cones and their axonal shaft (Fig. 11A-D; n=21 growth cones). The parallel microtubule arrays were observed all over the growth cone (arrowheads in Fig. 11D). Tyrosinated (dynamic) microtubules also showed a bundling that reaches to the tips of the growth cones (Fig. 12E-H; n=12 growth cones) similar to what has been demonstrated in cultured neurons (Schaefer et al., 2002; Dent and Gertler, 2003). In contrast, stable microtubules were highly disorganized in retraction bulbs (Fig. 11E-H; n=19 retraction bulbs). While some regions contained accumulation of stable microtubules (white arrow in Fig. 11F), other regions were devoid of microtubule filaments (white arrowhead in Fig. 11F). The orientation of different microtubules was highly heterogeneous (yellow arrows in Fig. 11F). For instance, none of the microtubules that are indicated with yellow arrowheads in the 3D reconstruction (Fig. 11H) were parallel to each other. Interestingly, dynamic microtubules were also found in retraction bulbs albeit seemingly to a smaller extent than in the growth cones (Fig. 12A-D; n=7 retraction bulbs), suggesting that the microtubules are still dynamic and can integrate new tubulin dimers. However, these dynamic microtubules in retraction bulbs were disordered (yellow arrows in Fig. 12C). Moreover, dynamic microtubules were almost absent from the tips of retraction bulbs (white arrowhead in Fig. 12C), but accumulated in the more central domain (white arrow in Fig. 12C). These results suggest that the mislocalization of dynamic microtubules in the non-growing bulbs could account for axon stalling.

We further quantified the deviation of microtubules from the axonal axis by analyzing electron micrographs of axonal terminals. In unlesioned controls, the microtubules aligned in parallel to the axonal axis: 99% of the microtubules deviated less than 30° from the axonal axis (a representative image is shown in Fig. 11I, the microtubules of the same image were traced with

black lines for clearer visualization in Fig. 11J; a higher magnification of the marked area, showing the angle of deviation, is presented in Fig. 11K, [n=7 axonal shafts]). In growth cones, 97.0% of the microtubules deviated less than 30° from the axonal axis, similar to the unlesioned controls (Fig. 11L-N, [n=8 growth cones]). In retraction bulbs, only 51% of the microtubules deviated less than 30° from the axonal axis; instead, 35% of the microtubules deviated between 30° and 60° and 13% more than 60° from the axonal axis (Fig. 11O-R [n=9 retraction bulbs]). These results show that microtubules in retraction bulbs are disorganized and dispersed compared to unlesioned axons and growth cones ($P < 0.001$; the quantification of the data is shown in Fig. 11S).

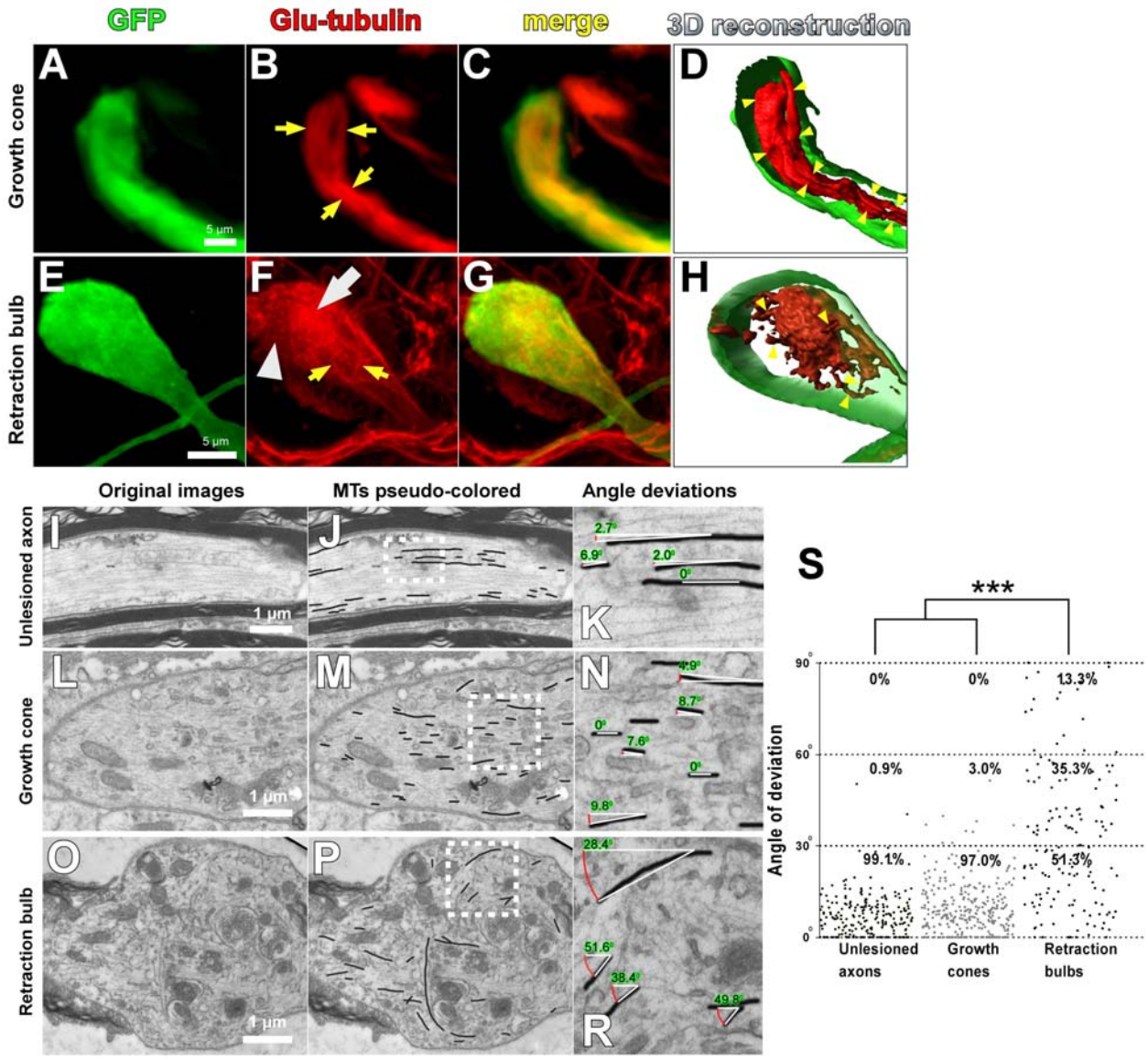

Figure 11. Retraction bulbs have dispersed and disorganized microtubules.

(A-H) Immunostaining of axonal end structures with anti-Glu-tubulin antibody, recognizing the detyrosinated α-tubulin subunits, which are already assembled into microtubules, to visualize the organization of microtubules. (A-D), growth cones possess tightly bundled microtubules parallel to the axonal axis. GFP positive growth cone (green) (A), anti-Glu-tubulin staining (red) (B), merge (C) and 3D reconstruction (D). The arrows in (B) and arrowheads in (D) point to some of the parallel microtubule bundles. (E-H), retraction bulbs have highly dispersed and disorganized microtubules. GFP positive retraction bulb (green) (E), anti-Glu-tubulin staining (red) (F), merge (G) and 3D reconstruction (H). The arrows in (F) and arrowheads in (H) indicate dispersed microtubules that are highly deviated. In (F), the white arrow indicates regions where microtubules are densely accumulated and the

white arrowhead indicates regions without microtubules. (I-R) Electron micrographs of retraction bulbs and growth cones were analyzed to quantify the angle of deviation of microtubules. Unlesioned central axons were also quantified as a control. A representative unlesioned CNS axon (I), growth cone (L) and retraction bulb (O) are shown. (J, M, P) the microtubules in the images (I,L,O) were manually traced in black to visualize the overall microtubule organization in the axonal structures. (K, N, R) higher magnifications of the marked areas in (J, M and P) respectively. (S) Quantifications of the microtubule deviation from the axonal axis. Each dot represents a single microtubule filament (at least 7 electron micrographs were analyzed and pooled for each condition). The microtubules are significantly more vertical in the retraction bulbs compared to both growth cones and unlesioned central axons. *** indicates $P < 0.001$.

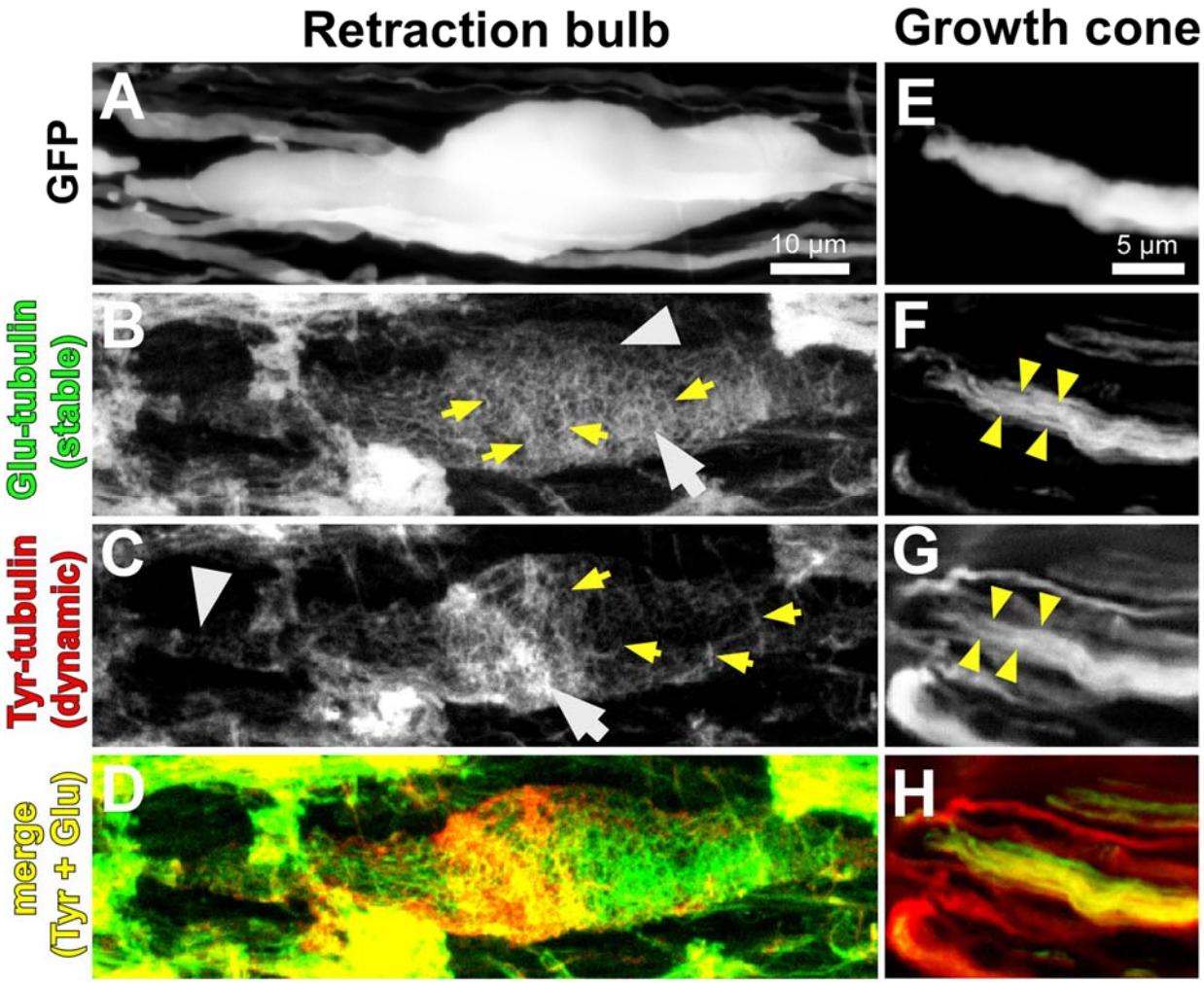

Figure 12. Retraction bulbs have dispersed and disorganized stable and dynamic microtubules.

Growth cones and retraction bulbs were fixed and stained with an anti-Glu-tubulin antibody, which reveals relatively old microtubules, and an anti-Tyr-tubulin antibody, which show relatively newly polymerized

microtubules. (A-D) In retraction bulb tyrosinated microtubules (C) show a dispersed and disorganized distribution similar to de-tyrosinated microtubules (B). However, distribution of tyrosinated and de-tyrosinated microtubules differed within retraction bulbs. Whereas de-tyrosinated microtubules are present within most of the regions (B), tyrosinated microtubules show more restricted localizations (C) and do not enrich at the axonal tip. In (B) and (C), the yellow arrows point some of the highly deviated microtubules; the white arrowheads point the regions with few microtubule filaments and the white arrows show the regions of microtubule accumulations. (D) is the merge of de-tyrosinated (B) and tyrosinated tubulin channels (C). (E-H) In growth cones tyrosinated microtubules (G) also align in parallel bundles within growth cones and show a similar distribution as de-tyrosinated microtubules (F). The yellow arrowheads in (F) and (G) show some of the microtubules which are organized in parallel bundles. (H) is the merge image of de-tyrosinated (F) and tyrosinated tubulin channels (G).

3.1.4 Microtubule destabilization converts a growth cone into a retraction-bulb-like structure and halts axonal growth *in vivo*

Our observation of disorganized microtubules in retraction bulbs led us to examine whether destabilization of microtubules in a growth cone would be sufficient to transform it into a retraction bulb. To address this point, we injured the sciatic nerve of GFP-M mice to obtain regenerating growth cones, as before, and applied 10 µl of the microtubule disrupting drug nocodazole (330 µM) to the site of the lesioned sciatic nerve one day later. Upon examination of the sciatic nerve 24 hours after nocodazole treatment, we found that 42.3% ± 13.2% of the axons (average ± s.d.; n=165 axons from 11 mice) had transformed their growth cones into a bulb (Fig. 13D-F). Application of DMSO, which served as a negative control, did not cause bulb formation (Fig. 13A-C). The tip / axonal shaft ratio of nocodazole-induced bulbs (4.25 ± 0.56, average ± s.d.; n=70 from 12 mice) was significantly higher than in both lesioned, untreated (1.45 ± 0.13, average ± s.d.; n=53 from 8 mice) and lesioned, DMSO-treated (1.64 ± 0.46, average ± s.d.; n=62 from 12 mice) controls (Fig. 13G; $p < 0.001$ for both). These nocodazole-induced peripheral bulbs showed a similar size increase to the retraction bulbs seen in the CNS one day after SCI (4.09 ± 0.73; Fig. 13F, G, L). When we analyzed the nocodazole-induced peripheral bulbs, we found a dispersed microtubule organization, similar to that in retraction

bulbs of the CNS (Fig. 13H-K; compare to Fig. 11E-H). Lower concentrations of nocodazole did not cause bulb formation (10µl of 3.3µM or 33 µM nocodazole; Fig. 14A-J).

To assess the growth capacity of the nocodazole-induced peripheral bulbs, we performed *in vivo* imaging and followed the advance of injured peripheral axonal endings (Fig. 13L-O). Two days after sciatic nerve injury the lesion sites containing the growth cones were treated either with nocodazole or vehicle (DMSO). We imaged axons at the time of treatment and 6 hours later and measured their extension. Nocodazole treatment (10 µl 330 µM) significantly ($P < 0.05$) inhibited the growth of axons compared to control treatment (control: green arrowheads in Fig. 13L, M; nocodazole: red arrowheads in Fig. 13N, O). All control animals showed axonal growth of 20-100 µm within the observation period. In contrast, nocodazole treated animals showed very little axonal regrowth: only 2 out 7 animals extended their axons up to 10 µm whereas the other nocodazole-treated animals did not elongate their axons during the observation period (Fig. 13P). Lower concentrations of nocodazole did not show any growth inhibitory effect (10µl of 3.3µM or 33 µM nocodazole; Fig. 14K-P).

Taken together, our results demonstrate that destabilization of microtubules *in vivo* is sufficient to generate retraction-bulb-like structures from a growth cone, as judged by morphological, cytoskeletal and growth criteria.

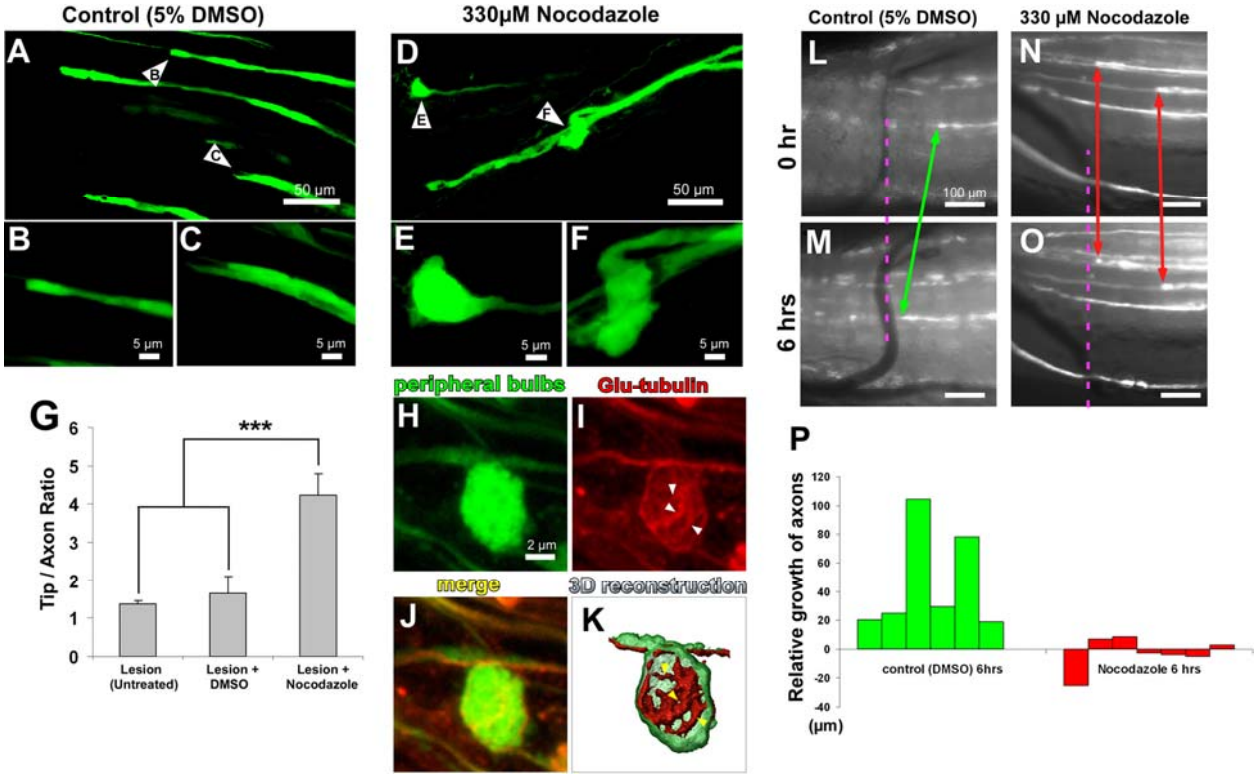

Figure 13. Nocodazole application converts a growth cone into a retraction-bulb-like structure and restricts axonal growth *in vivo*.

(A-K) One day after sciatic nerve injury, GFP-M mice were re-anesthetized and their sciatic nerves exposed. The exposed sciatic nerves were treated with 10 µl of either 330 µM nocodazole (D-F; H-K) or 5% DMSO as control (A-C). The effects on the morphology and the cytoskeletal structure were assessed 24 hours after the treatment. (A) The morphology of the growth cones does not change under control conditions. Growth cones treated with 5% DMSO resemble untreated growth cones. (B), (C) show higher magnifications of the growth cones marked with arrowheads in (A). (D) After treatment with nocodazole the axons form bulbs at their tips instead of growth cones. (E), (F), higher magnifications of the peripheral bulbs marked with arrowheads in (D). (G) Quantification of peripheral bulb sizes. The axon / tip ratio of the peripheral bulbs is significantly higher than that of either DMSO-treated growth cones or untreated growth cones (*** indicates $P < 0.001$). All values are average ± s.d. (H-K) The nocodazole-treated peripheral bulb (H) immunostained with an anti-Glu-tubulin antibody (I) to assess the underlying microtubule organization. The white arrowheads in the merged image (J) and yellow arrowheads in 3D reconstruction (K) point to some of the microtubules which are dispersed in a similar way as observed in retraction bulbs (compare with Fig. 3E-H). (L-O) 2 days after sciatic nerve injury, the lesion site was re-exposed and binocular images were captured before the treatments. Immediately after the imaging, 10 µl of 330 µM nocodazole (after N) or 5% DMSO (after L) were applied. The position of the axonal tips followed over 6 hours. The nocodazole-treated axonal tip in (N) remains at its position 6 hours post-treatment (O). The tip of this axon is marked by red

arrowheads in (N, O). The DMSO-treated growth cone extends during the time of imaging (L, M). The tip of this axon is followed by the green arrowheads in (L, M). The images are aligned with the purple-dashed lines with respect to the landmarks, the vertical vessels, which remain at the same position during imaging. (P) Quantification of the relative growth of axon terminals after nocodazole and DMSO treatments. Only the axons which were clearly visible at each imaging time have been considered and averaged for each animal. Each green bar represents one control and each red bar represents one nocodazole-treated animal. The scale bars represent: 100 μm in (L-O).

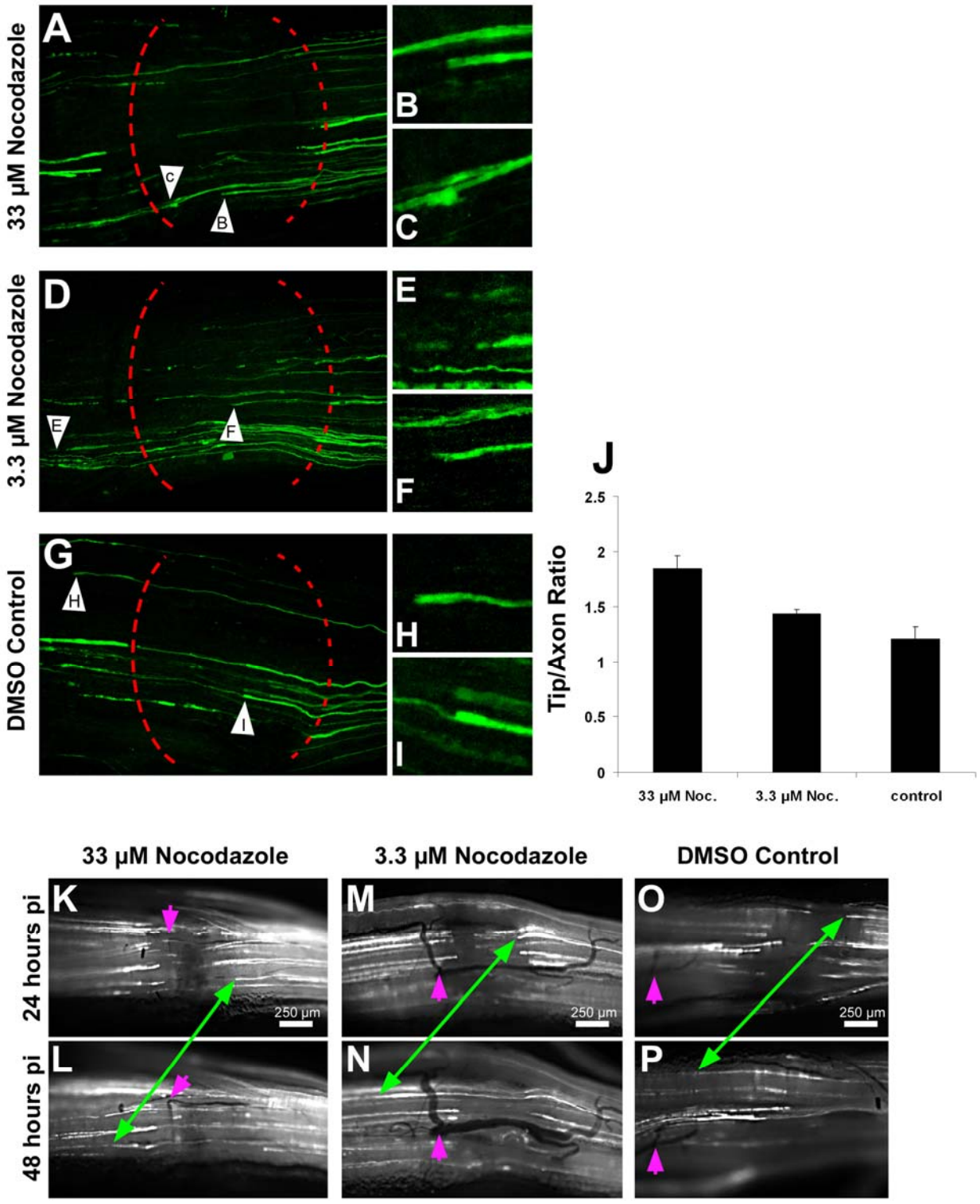

Figure 14. Low concentrations of nocodazole neither caused retraction bulb formation nor inhibited the growth of injured peripheral axons.

(A-I) In addition to 330 µM nocodazole, we also tested the effects of 33 µM and 3.3 µM concentrations of nocodazole on growth cones. 24 hours post sciatic nerve injury, the mice were re-anesthetized and their sciatic nerves exposed. We treated the injured sciatic nerve with 10 µl of 33 µM nocodazole (A), 3.3 µM nocodazole (D) or 0.5% DMSO (G). Unlike 330 µM nocodazole, 33 µM and 3.3 µM nocodazole do not cause formation of big bulbous axon terminals at the axons terminals. (B, C), (E, F) and (H, I) are higher magnifications of the marked axon terminals in (A), (D) and (G) respectively. The red brackets in (A, D and G) show the injury sites which were determined by delimitating the deformed tissue. In both relatively low doses of nocodazole treatments, many axons regenerate and grow beyond the crush site, as do the ones in the control (6 out of 6 animals for 33 µM nocodazole and 5 out of 5 animals 3.3 µM nocodazole). (J) The axon / tip ratio quantification of axon terminals after treatments. Application of 33 µM nocodazole has a weak effect on the morphology of axon terminals (1.84 ± 0.12, average ± s.d.; n=43 from 6 mice); 3.3 µM Nocodazole does not show any significant change of the size of axon terminals (1.44 ± 0.04, average ± s.d.; n=29 from 5 mice) compared to control (1.21 ± 0.11, average ± s.d.; n=31 from 5 mice). (K-P) *In vivo* live imaging shows that low doses of nocodazole treatments do not inhibit the growth of peripheral axons. The tips of the axons from 24 hours to 48 hours are followed by the green arrowheads in 33 µM nocodazole (K, L), 3.3 µM nocodazole (M, N) or control (O, P). The images are aligned with the purple arrows with respect to the landmarks, the vertical vessels, which remained at the same position during imaging. In all cases, the peripheral axons are able to grow a distance of about 0.5 to 1 mm within 24 hours of observation.

3.1.5 Microtubule destabilization induces the formation of bulbous axon terminals and restricts axon outgrowth in cell culture

To address if nocodazole-induced axonal stalling and morphological changes of the growth cones function cell autonomously, we attempted to generate retraction-bulb-like structures in isolated DRG neurons in cell culture. DRG neurons were dissected and cultured as described before (Neumann et al., 2002). One day after plating, when DRG neurons formed several axons with growth cones at their tips, they were treated with various concentrations of nocodazole for another day. Whereas only a minor fraction of control neurons had tips with a bulbous, club-like morphology, nocodazole-treated neurons had significantly more bulbous endings (Fig. 15A-J; 9.6 ± 2.3 % in controls, 29.1 ± 4.4 % in 75 nM nocodazole, 41.1 ± 8.2 % in 250 nM nocodazole, $P < 0.001$; average ± s.d.; data derived from 3 independent cultures per condition). Similar to the retraction bulbs formed after SCI, nocodazole-induced bulbous endings possessed

disorganized stable and dynamic microtubules compared to the growth cones (Fig. 15 K, L; Fig. 16).

The growth of the nocodazole-treated axons was significantly ($P < 0.01$) inhibited compared to controls. The total length of the axons per DRG neuron two days in culture (treated from 24 hours to 48 hours) was 2849 ± 46 µm in controls, but reduced to 2132 ± 138 µm in 75 nM nocodazole and 1555 ± 142 µm in 250 nM nocodazole (Fig. 15M-P; average ± s.e.m.; data derived from 3 independent cultures per condition). After nocodazole treatments, the total number of cells did not change (data not shown). Thus, destabilization of microtubules is sufficient to cause formation of bulbous endings reminiscent of retraction-bulb-like structures by their morphology, microtubule structure and growth ability.

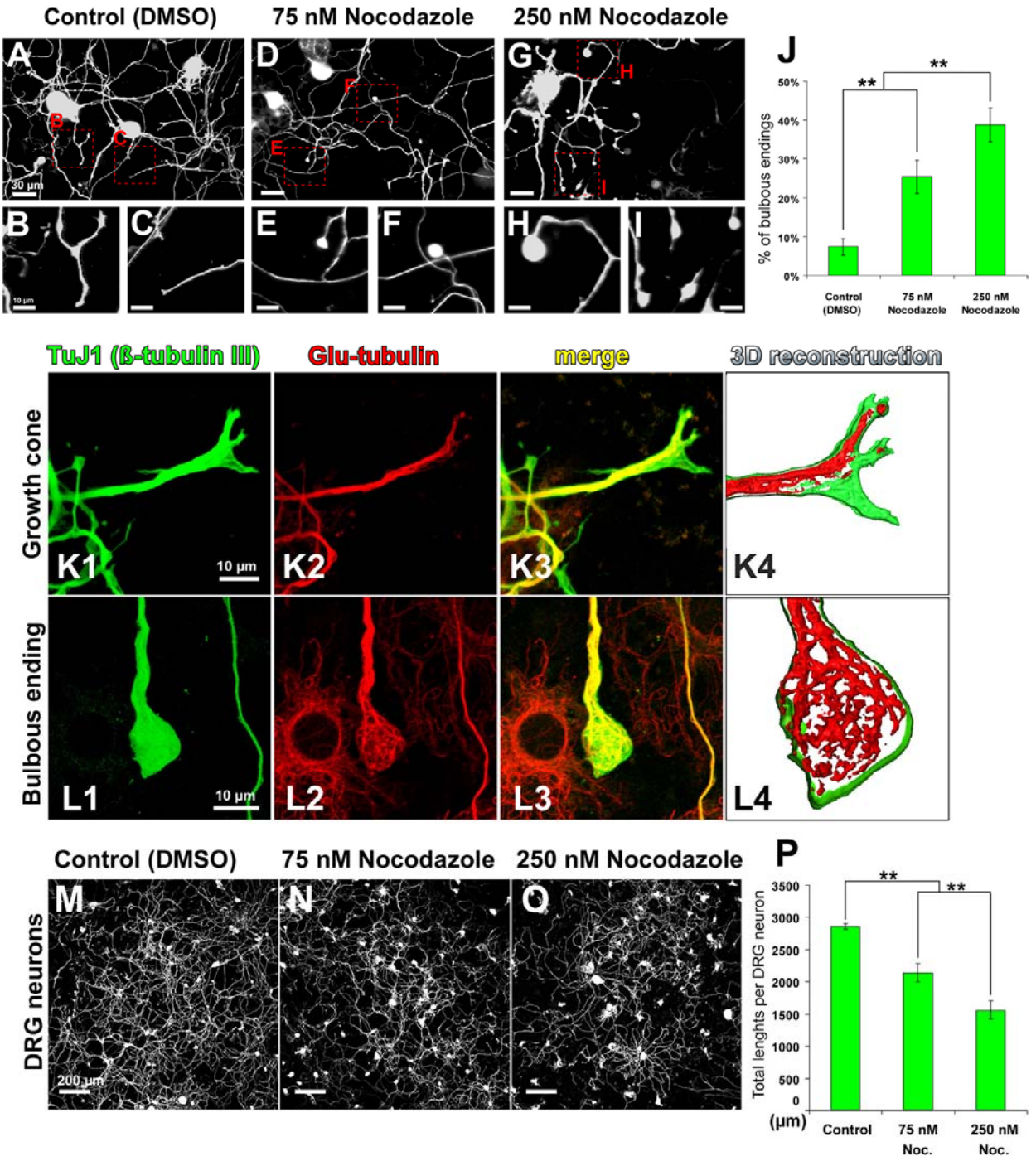

Figure 15. Nocodazole application converts the axon terminals into retraction-bulb-like swellings and inhibits axonal growth *in vitro*.

(A-I) DRG neurons from adult rats were cultured on laminin for 48 hours. From 24 hours to 48 hours the neurons were incubated either with 0.33% DMSO (control) (A) 75 nM nocodazole (D) or 250 nM nocodazole (G). (B) and (C), higher magnifications from (A) showing *in vitro* DRG growth cones. (E) and (F), (H) and (I) higher magnifications

from (D) and (G) respectively, showing the retraction-bulb-like swellings *in vitro* after nocodazole treatments. (J) Quantification of the retraction bulbs formed at the axonal endings in percentages. 75 nM and 250 nM nocodazole treatments induces significantly more bulbous endings than control treatments ($P < 0.05$). (K, L) The microtubule organization of the control and 250 nM nocodazole-treated axonal endings, which were identified by immunostaining with a general neuronal tubulin antibody recognizing class III β-tubulin (TuJ1) and with anti-Glu-tubulin antibody. Similar to *in vivo* growth cones, *in vitro* growth cones possess bundled microtubules (K1-K4). In contrast, the nocodazole-induced bulbous axon terminals contain disorganized microtubules similar to their *in vivo* counterparts (L1-L4). (M-P) The growth of the axons after treatments were analyzed by calculating the total length of the axons per DRG neuron. TuJ1 stained neurons were imaged by confocal microscopy under identical conditions and quantified. (M) Control, (N) 75 nM nocodazole, (O) 250 nM nocodazole-treated DRG neurons. (P) Quantification of the average total length of the axons per DRG neuron. There is a significant decrease in the length of nocodazole-treated DRG axons compared to controls. ** indicates $P < 0.05$. The scale bars represent: 30 µm in (A, D, G), 10 m in (B, C, E, F, H, I), 200 µm in (M-O).

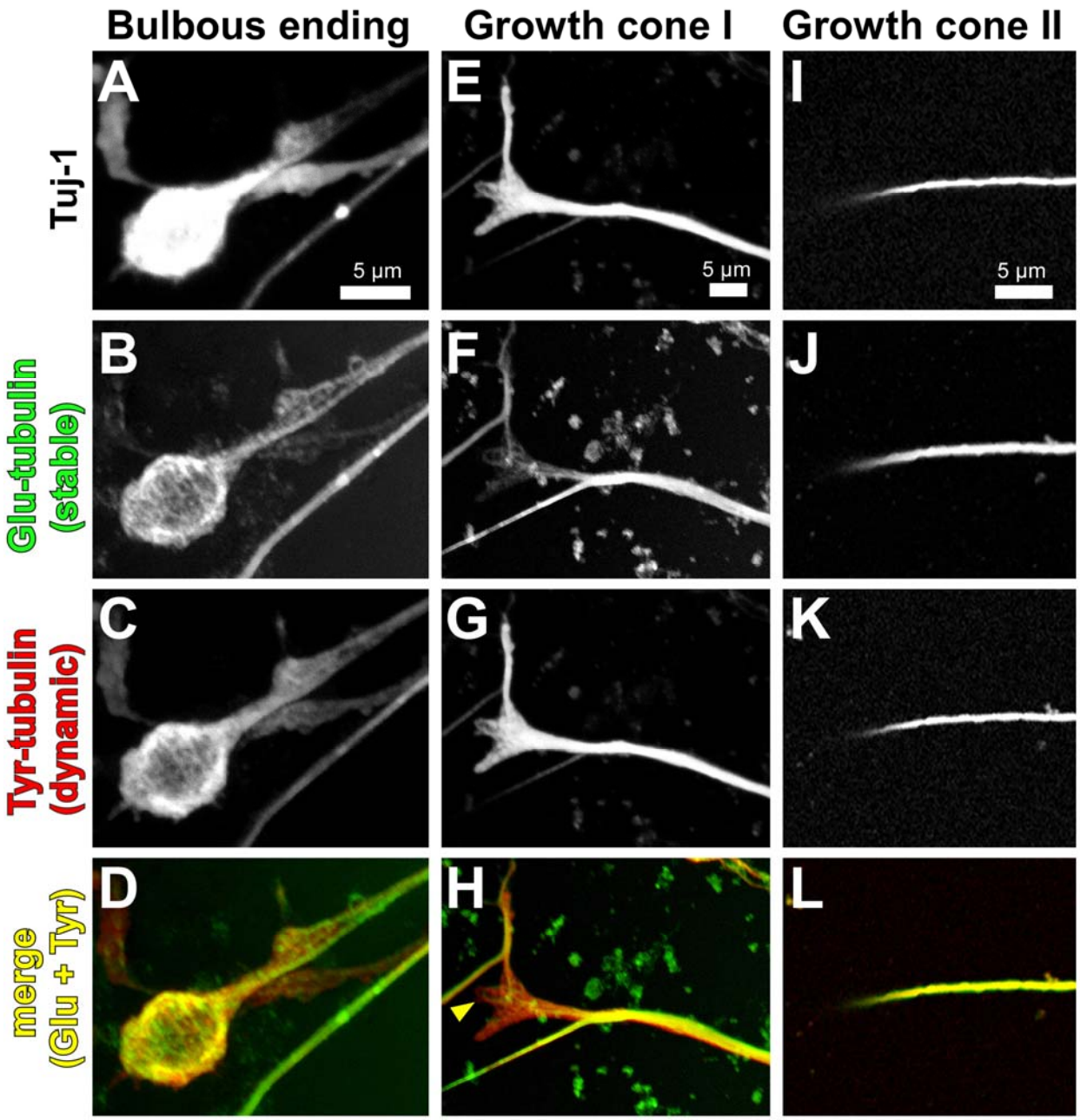

Figure 16. Co-immuno-staining of *in vitro* growth cones and nocodazole induced bulbous ending with tyrosinated and de-tyrosinated tubulin antibodies.

(A-D) A bulbous axon terminal **(A)** stained with both anti-Glu-tubulin antibody **(B)** and anti-tyrosinated-tubulin antibody **(C)**. Tyrosinated microtubules are disorganized and dispersed in bulbous endings similar to de-tyrosinated microtubules. **(E-H)** An expanded growth cone **(E)** stained with both with anti-Glu-tubulin antibody **(F)** and anti-Tyr-tubulin antibody **(G)**. **(H)** is the merge image of stable **(F)** and dynamic microtubules **(G)** in this growth cone. Tyrosinated microtubules also align in parallel bundles within axonal shafts similar to de-tyrosinated microtubules.

However, they extend into peripheral region of the growth cone. **(I-L)** A slim growth cone **(I)** stained with both anti-Glu-tubulin antibody **(J)** and anti-Tyr-tubulin antibody **(K)** antibodies and their merge is shown in **(L)**. Notably, dynamic and stable microtubules are tightly bundled and extended to the tip of the growth cone indicating that this is a fast growing growth cone similar to the ones seen *in vivo* at the injured peripheral axons of DGR neurons (see also Fig. 11B,C).

3.1.6 Microtubule stabilization interferes with the formation of retraction bulbs

Since microtubule destabilization appears to be crucial element in the generation of retraction bulbs we wondered whether microtubule stabilization would be sufficient to prevent the formation of retraction bulbs after CNS injury. To this end we applied taxol, a microtubule stabilizing drug, to the injured spinal cord and assessed the alteration of the axonal stumps' terminals by *in vivo* imaging. We performed a small unilateral lesion in the dorsal columns of GFP-M mice at the T12 level (Fig. 17A and B) and the injury sites were bathed in either the microtubule stabilizing drug taxol or in vehicle (saline). We then continuously observed the behavior of the axons during the subsequent 6 hours, using a binocular microscope (Kerschensteiner et al., 2005; Misgeld and Kerschensteiner, 2006) (Fig. 17C and D). In control conditions, we started to observe formation of apparent retraction bulbs one hour after injury (Fig. 17D). At 6 hours post injury already 71.3 ± 9.1 % of the axons (average ± s.d.; n=18 mice) formed retraction bulbs at their tips (Fig. 17D, F, M). However, when 1 µM taxol was repetitively applied (10 µl per hour), starting immediately after the injury, only 22.8 ± 13.1 % (average ± s.d.; n=11 mice) of the axons developed bulbs (defined by a tip / axon ratio > 2) in the first 6 hours (Fig. 17C, E, M). In addition, the size of the axon terminals formed after taxol treatment was smaller (Fig. 17G-I; tip / axon ratio: 2.53 ± 0.54 [average ± s.d.] for the 5 biggest retraction bulbs per animal) than the retraction bulbs of control treatment (Fig. 17J-L; 4.14 ± 0.44 [average ± s.d.]; n=11 mice for each condition; $P < 0.001$). The microtubules of taxol-treated axonal endings were bundled and aligned in parallel to the axonal axis resembling the cytoskeletal structure of *in vivo* growth cones (Fig. 17N-R, compare to Fig. 11A-D). Interestingly, some axons of taxol-treated animals also showed decreased acute axonal degeneration (Kerschensteiner et al., 2005) and Wallerian degeneration as shown by the reduced axonal retraction from the lesion site. In 6 out of 11 taxol-treated animals the proximal axonal stumps

were as close as 25 µm to the injury site 6 hours after injury (red arrow in Fig. 17E) whereas only 1 out of 11 controls showed such minimal retraction (compare Fig. 17E and F). These results suggest that stabilization of microtubules prevents the formation of retraction bulbs and interferes with axonal retraction after CNS lesioning. To test whether the effect of taxol is specific for inhibiting degeneration of central axonal branch or whether it can change the growth of the peripheral branch after injury, we applied the same concentration of taxol onto the regenerating axons after a sciatic nerve lesion. We observed that 1 µM taxol application did not significantly alter the growth speed of the axons compared to controls. The average growth of the axons was 572 ± 277 µm in the taxol treated group (Fig. 18A, B, E) and 511 ± 276 µm in the DMSO treated group (Fig. 18C, D, E) within 24 hours after treatment (average ± s.d., n≥7 mice per group). Thus, these suggest that taxol at the concentration used interferes with the growth restraint inflicted on axons but does not change the general growth rates of axons.

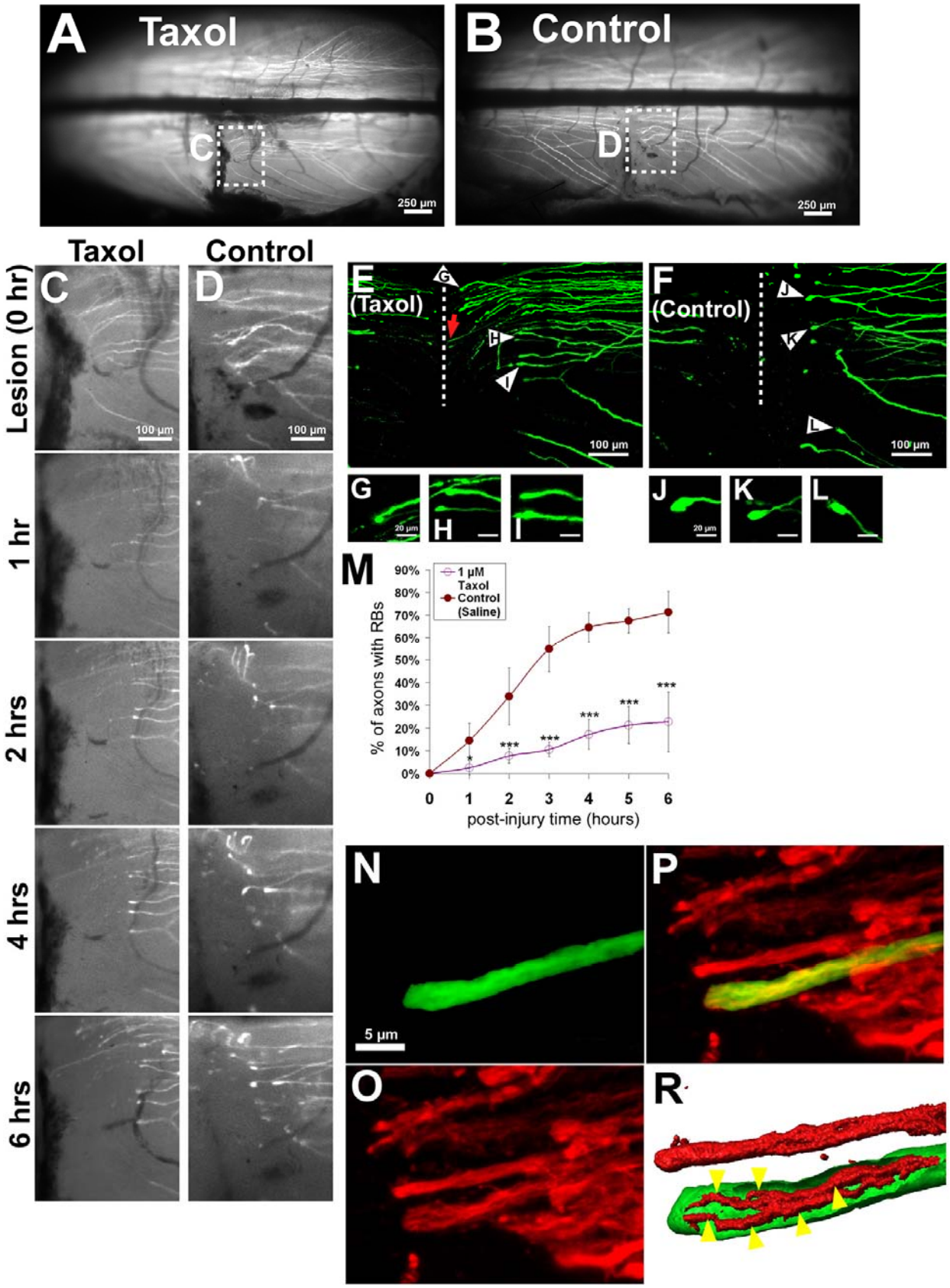

Figure 17. Taxol application interferes with the formation of retraction bulbs.

(A-D) *In vivo* imaging to identify effect of the taxol vs. control after a small lesion on dorsal column **(A, B)**. 10 µl of 1 µM taxol **(C)** or saline **(D)** was applied repetitively (once per hour) starting immediately after injury (0 hr). The lesion sites before and after injury (up to 6 hours post injury) in taxol **(C)** and saline **(D)** applications are shown from top to bottom. One hour after injury the first retraction bulbs form in control animals **(C)**, but not in the taxol appliedanimals **(D)**. Although most of the axons form retraction bulbs after 6 hours in the control only a minority of taxol-treated animals show axons forming retraction bulbs (compare also the 6 hour time point of **(C)** and **(D)**). **(E, F)** Confocal image of the lesion sites at 6 hours after injury from the same animals shown in **(C)** and **(D)**, respectively. The dotted lines indicate the injury sites. The red arrow in **(E)** indicates an axon which is within a few micrometer proximity of the lesion site. **(G-L)** Higher magnifications of the axon terminals indicated in **(E)** and **(F)** (the biggest ones from the samples); **(G-I)** the taxol-treated, **(J-L)** the control-treated axon terminals. Note that the sizes of the taxol-treated axonal endings are smaller than the retraction bulbs in controls. **(M)** The percentage of axons with retraction bulbs in taxol-treated (white circles; n= 11 animals) compared to saline (control) treated animals (dark circles; n=18 animals). From 1 hour post injury on, there are significantly less bulbs in taxol-treated animals (*$P < 0.05$, *** $P < 0.001$). **(N-R)** The Glu-tubulin antibody was used to identify microtubule structure of taxol-treated central axon terminals. GFP positive axon in green **(N)**, the anti-Glu-tubulin antibody staining in red **(O)**, the merge image **(P)** and the 3D reconstruction of the presented sample **(R)** are shown. Note that the microtubules are highly parallel to the axonal axis and mostly bundled as it is seen in the growth cones. The yellow arrowheads in **(R)** focus on some of the microtubule aligned in parallel bundles. The scale bars represent: 20 µm in **(G-L)**.

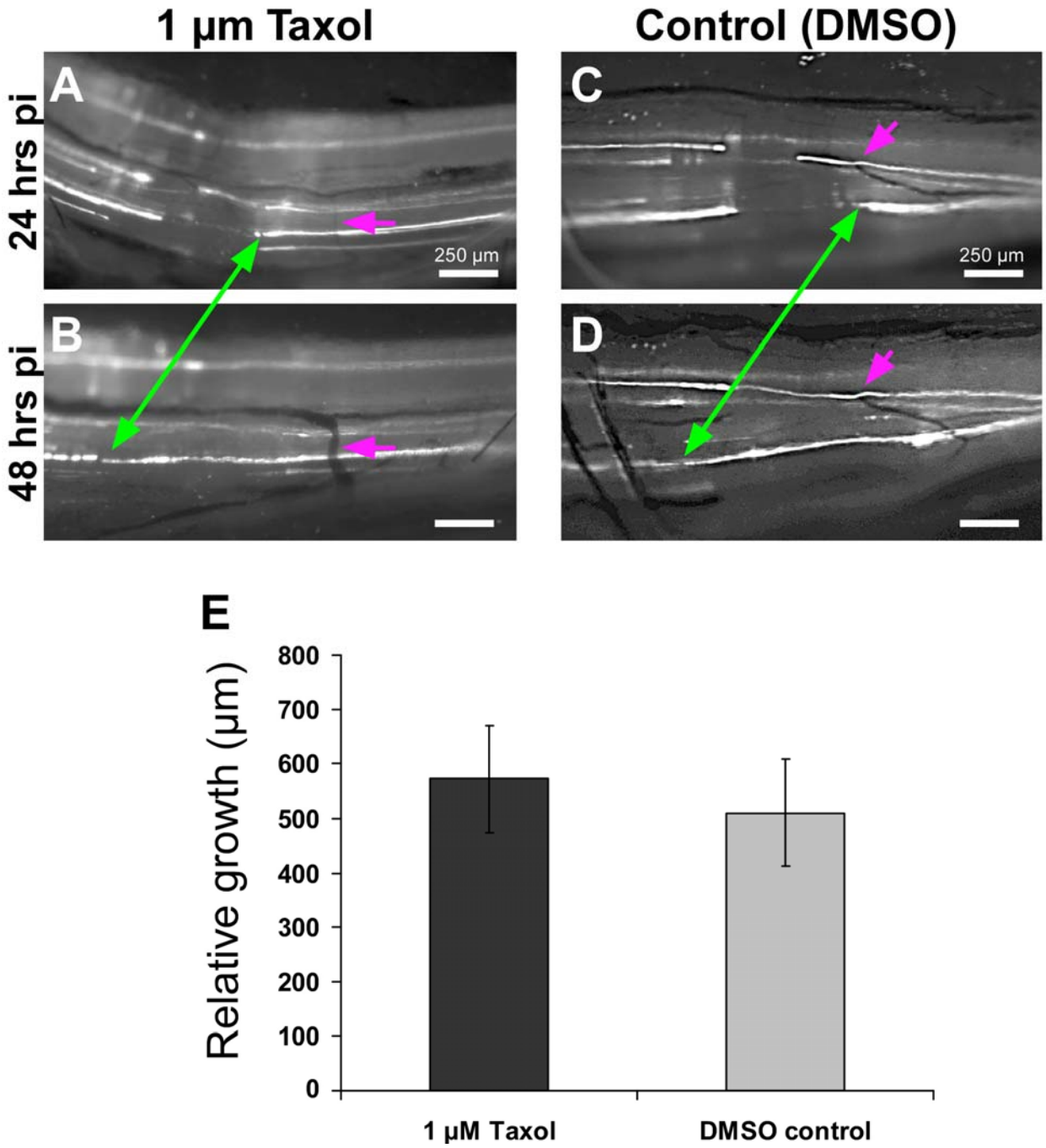

Figure 18. Taxol treatment does not alter the growth capacity of the peripheral axons.

In vivo imaging of injured sciatic nerve axons from 24 hours to 48 hours post-injury times after taxol or control treatments. **(A-D)** 24 hours after the sciatic nerve injury, the mice were re-anesthetized and their sciatic nerves treated once with 10 µl of 1 µM taxol or DMSO control. Then we observed the growth of the axons from 24 to 48 hours post injury times for taxol **(A, B)** and control treatments **(C, D)**. Taxol treatment does not affect the growth ability of the injured peripheral axons. The tips of the axons followed by the green arrowheads and the images are

aligned with the purple-dashed lines with respect to the landmarks. **(E)** The quantification of axonal regeneration after the treatments. The axons grow 572 ± 277 µm (average ± s.d.; n= 8 mice) in taxol conditions and 510 ± 276 µm (average ± s.d.; n= 7 mice) in controls.

3.1.7 Microtubule stabilization enhances the growth capacity of neurons cultured on myelin

We further investigated whether taxol application could enhance axonal growth of neurons cultured on an inhibitory substrate. Cultured DRG neurons contain axons that resemble peripheral axonal branches according to their growth rates (Smith and Skene, 1997). We therefore decided to use CNS neurons to study growth of axons on inhibitory substrates. Dissociated cerebellar granule neurons (CGNs) were plated on poly-lysine or CNS myelin (Niederost et al., 1999) and treated with taxol or vehicle. When granule neurons were cultured on poly-lysine, 42.9 ± 4.1 % of neurons formed long neurites within 18 hours (Fig. 19A, B, I). In contrast, myelin inhibited the formation of long neurites: only 7.4 ± 2.6 % of neurons were able to form a process longer than 60 µm (Fig. 19E, F, I). Remarkably, in the presence of taxol (10 nM), a significant amount of neurons plated on myelin showed enhanced axonal growth; 29.9 ± 2.35 % of the cells contained neurites longer than 60 µm ($P < 0.001$; Fig. 19G, H, I). Notably, taxol application did not change the growth capacity of CGNs when they were plated on poly-lysine: 40.4% ± 3.3% of neurons had processes longer than 60 µm (Fig. 19C, D, I; average ± s.d $n \geq 3$ independent experiments per condition). These results show that stabilization of microtubules in culture increases the growth ability of neurons in the presence of an inhibitory environment.

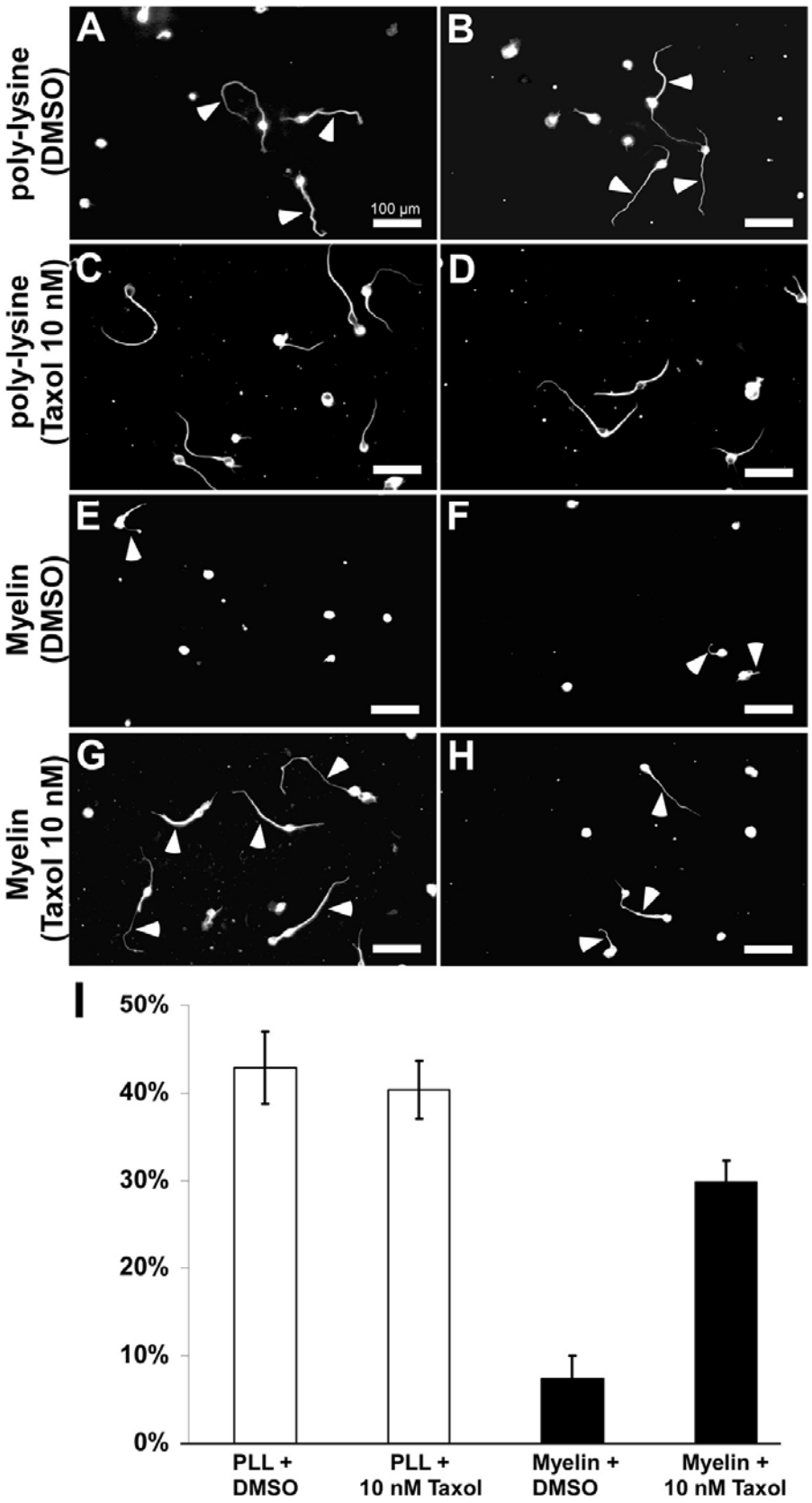

Figure 19. Taxol treatment increases the growth capacity of neurons in culture.

Cerebellar granule neurons (CGNs) were cultured either on poly-lysine (A-D) or on an inhibitory substrate (myelin), **(E-H)**. **(A, B)** Most of the CGNs cultured on poly-lysine form long axons (42.9% ± 4.1% of the cells had processes longer than 60 µm) within a short time (18 hours). **(C, D)** Treatment of CGNs cultured on poly-lysine does not change the growth capacity of these neurons (40.4% ± 3.3% of the cells had processes longer than 60 µm). **(E, F)** CGNs cultured on myelin show reduced axonal growth: only 7.5% ± 2.67 of the cells have processes longer than 60 µm. **(G, H)** Treatment of CGNs with 10 nM taxol largely rescues the formation of long axons on an inhibitory myelin substrate, resulting in 29.9% ± 2.35 of CGNs with axons longer than 60 µm. **(I)** The percentage of the neurites which are longer than 60 µm is plotted for each condition. *** indicates $P < 0.001$. The scale bars represent: 100 µm (A-H). The data is shown as average ± s.d., n≥ 3 independent experiments per condition.

3.1.8 Retraction bulbs contain disorganized actin cytoskeleton

How the actin filaments are organized in the retraction bulbs? Our EM microscopy observations suggested that both neurofilaments and actin filaments within the retraction bulbs are disorganized similar to the microtubules. To reveal the actin organization in the retraction bulbs, we performed rhodamine phalloidin staining on nocodazole induced terminal bulbs in culture as well as on *in vivo* retraction bulbs. Our data showed that actin filaments are enriched in the filopodia of the *in vitro* DRG growth cones (Fig. 20A-D) but showed an irregular staining in the nocodazole induced bulbs (Fig. 20E-H). In addition, *in vivo* retraction bulbs also showed a disorganized actin filament distribution (Fig. 20I-L). These data suggest that besides the microtubules, actin filaments are also disorganized in the retraction bulbs and may play a crucial role in the formation and maintenance of the retraction bulbs after CNS injuries.

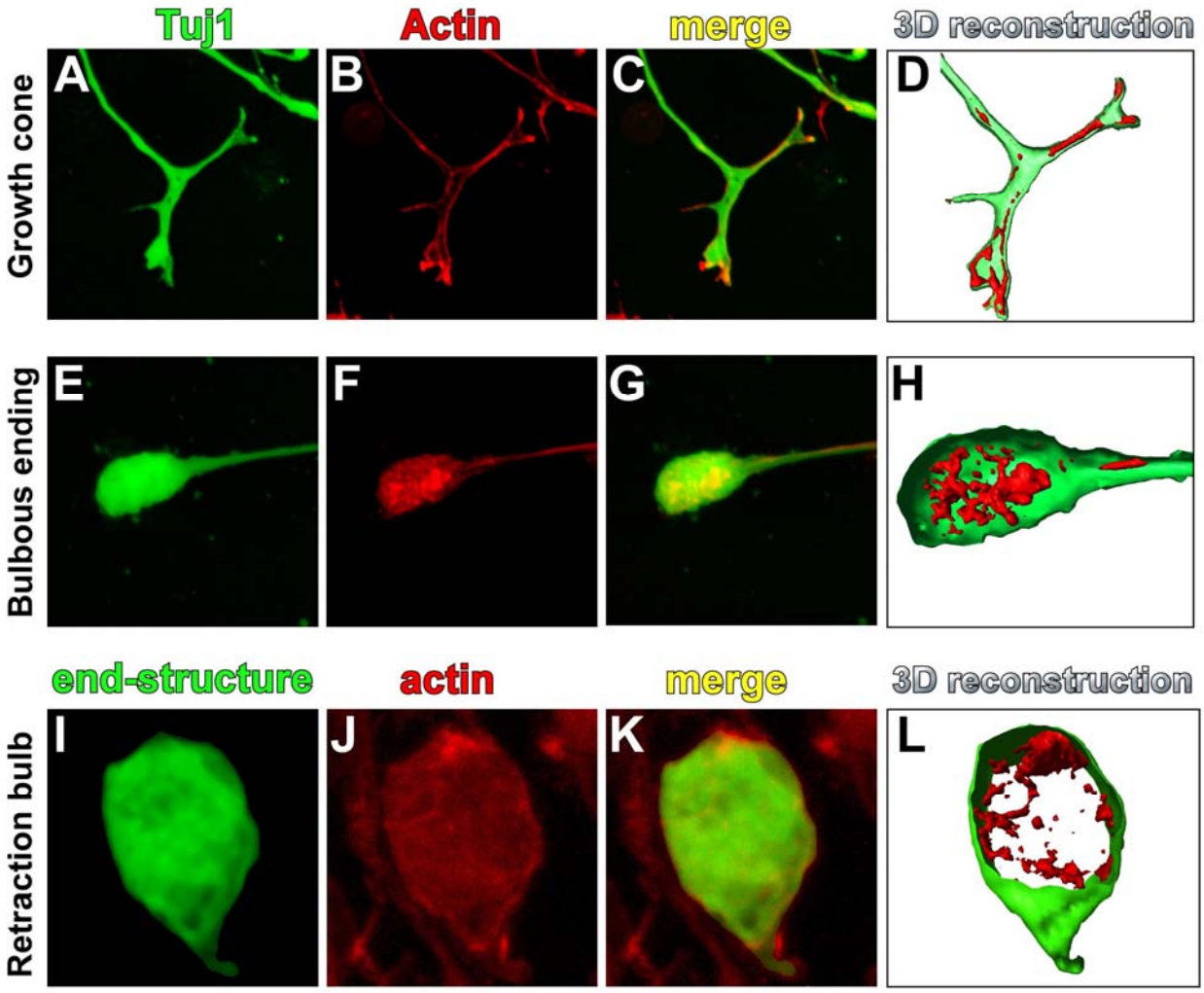

Figure 20. Actin cytoskeleton of retraction bulbs *in vitro* and *in vivo*.

The actin cytoskeleton of *in vitro* growth cones **(A-D)** and 250 nM nocodazole induced retraction bulbs from cultured DRG neurons **(E-H)** revealed by rhodamine phalloidin staining. The filopodia of the growth cones filled with dense actin filaments. However, nocodazole induced retraction bulbs have been observed to possess an irregular distribution of actin, which is mostly accumulated randomly within the bulb. **(I-L)** Rhodamine phalloidin staining of an *in vivo* retraction bulb showing the irregular distribution of the actin cytoskeleton within the bulb.

3.2 *In vivo* imaging of pre and reverse-conditioned axons

3.2.1 *In vivo* imaging of axonal degeneration and regeneration in the injured spinal cord

To study the effect of pre-conditioning lesion over time, we compared the regeneration behavior of the axons in conditioned and non-conditioned animals using *in vivo* imaging. The animals are conditioned by lesioning the sciatic nerves 1 week prior to dorsal column lesions. After performing the laminectomy (Fig. 21 A-1 and B-1), a small uni-lateral lesion was performed to transect the axons joining from lateral site to the midline (Fig. 21 A-2 and B-2). These recently joining axons show a sparse labeling due to their trajectories and therefore are better targets compared to the dense midline axons. The animals were observed at 6-7 hours post-injury (pi) to confirm the transection and retraction of the lesioned axons (Fig. 21 A-3 and B-3). Finally, we observed the animals at 48 hours pi when many regenerating sprouts already can be observed (Fig. 21 A-4 and B-4). In the control group, none of the animals could form crossing sprouts (0 out of 9 animals; Fig. 21 A-4, A-5 and Fig. 22). In average, they retracted 65 µm ± 33 µm (mean ± s.e.m.) from the lesion site. However, remarkably, most of the pre-conditioned animals were able form regenerating sprouts crossing the lesion site (6 out of 8 animals; Fig. 21 B-4, B-5 and Fig. 22) within 48 hours. The average crossing distance of the regenerating sprouts in conditioned animals was 320 µm ± 111 µm (mean ± s.e.m.). Overall, these results demonstrate that the effect of pre-conditioning lesion can be resolved as early as 48 hours post injury much earlier than previously described (Neumann and Woolf, 1999).

To confirm that the injured axons are coming from the sciatic nerves, we perfused the animals at the end of *in vivo* imaging experiments. We exposed the spinal cord and sciatic nerve by removing the vertebra and muscles. Using fluorescent microscope, the transected axons were traced back to the sciatic nerve (Fig. 23A). In addition, the tissues were dissected out and traced by lifting and following the peripheral branches until the lesion site (Fig. 23B-D).

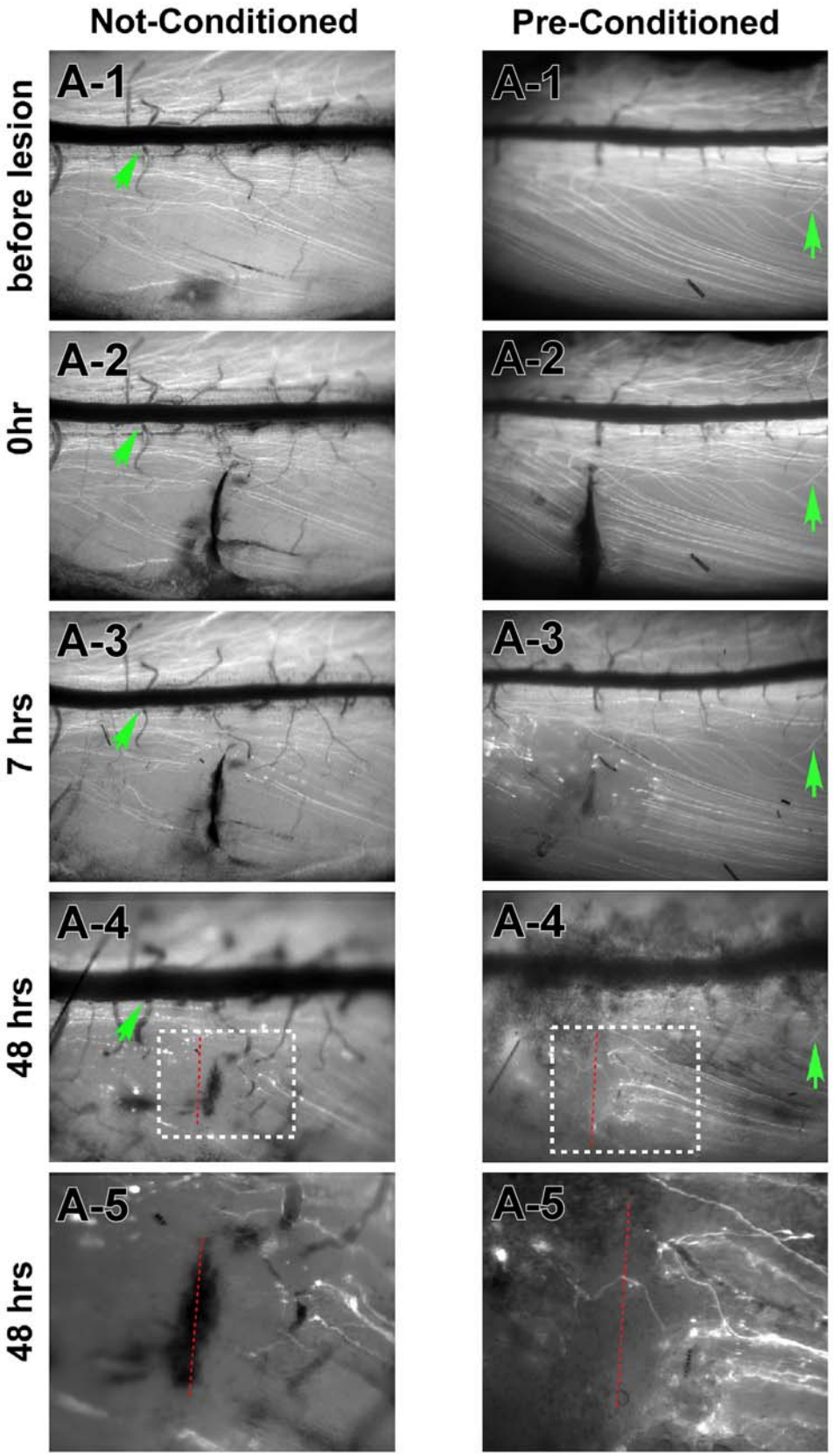
Not-Conditioned
Pre-Conditioned
before lesion
0hr
7 hrs
48 hrs
48 hrs
A-1
A-1
A-2
A-2
A-3
A-3
A-4
A-4
A-5
A-5

Figure 21. *In vivo* imaging of regenerating sprouts after pre-conditioning lesion.

(A-B) The live imaging series of an unconditioned **(A)** and a conditioned **(B)** animal. **(A-1, B1)** The spinal cord is imaged 20-30 min after laminectomy just before lesioning to confirm the absence of any non-specific injury. **(A-2, B-2)** The lesion site is imaged immediately after the lesion to confirm the transection and at 7 hours pi to detect the retraction of the transected axons **(A-3, B3)**. The animals are woken up by reverse-anesthesia until the next imaging. **(A-4, B4**) The regenerating sprouts are observed at 48 hours pi. In the unconditioned cases, although several axons formed thin regenerating sprouts which extended sometimes into lesion area, none of them was able to cross the lesion site. However, in almost all conditioned animals, the crossing sprouts were observed (**D-4**, yellow arrow). **(A-5, B-5)** are higher magnifications of the marked areas in **(A-4, B-4)** respectively. The images are aligned vertically according to land marks, the vertical vessels, which are indicated by green arrows. The red dashed lines indicate the lesion sites.

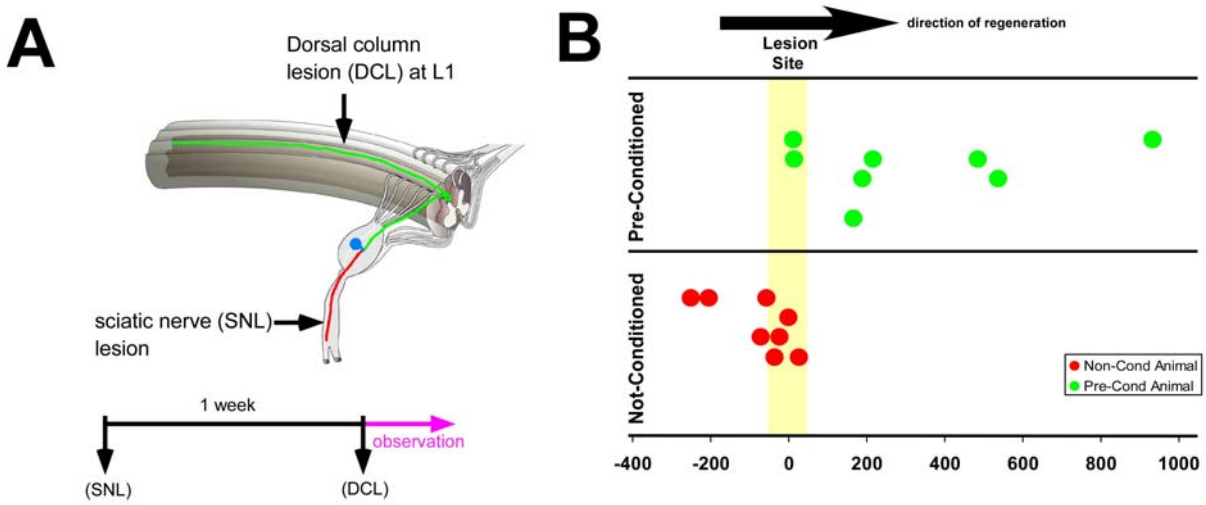

Figure 22. Quantification of regenerating pre-conditioning sprouts.

(**A**) The plan for the preconditioning lesion. The sciatic nerve is transected one week prior to central lesion. In unconditioned group, only the central lesion is performed. (**B**) The quantification of the sprout lengths with respect to epicenter of the lesion. In almost all of the pre-conditioned animals, we observed the sprouts crossing the lesion site (green dots), whereas none of the non-conditioned animals showed crossing sprouts (red dots). The light yellow division in the graph which is positioned from -50 µm to +50 µm marks the lesion site (average 100 µm) that is quantified from the binocular images.

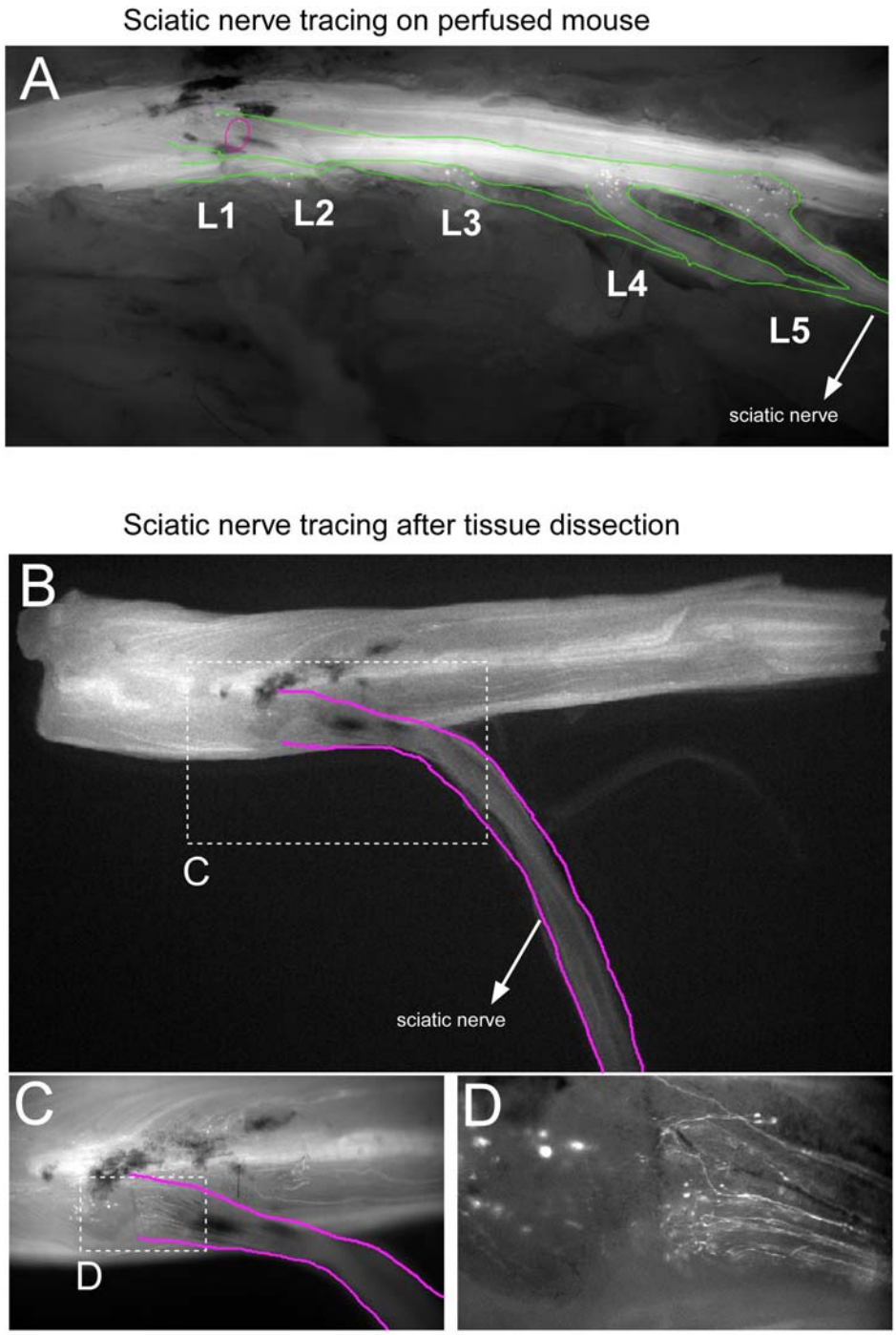

Figure 23. ***In vivo*** **tissue tracing of the sciatic nerve axons.**

At the end of the imaging sessions, we used two methods to confirm that the targeted axons are coming from the sciatic nerves: First, **(A)** after perfusing the animal, all the spinal cord along the lumbar level and sciatic nerve were exposed. The central extensions of the sciatic nerve are followed by a fluorescent microscope on the perfused animal (the green borders in **(A)**). The lesioned axons (purple circle) were readily traceable back to the sciatic nerve (L4 and L5). Second, **(B-D)** the spinal cord with the sciatic nerve was dissected and the lesion site was traced from

the sciatic nerve to the lesion site under the fluorescent microscope. **(C)** is the marked area in **(B)** indicating the entry of sciatic nerve into dorsal columns. **(D)** is the marked area in **(C)** showing the transected central axons which are coming from the sciatic nerve.

3.2.2 *In vivo* imaging of conditioned and unconditioned axons on the same animal

The effect of the pre-conditioning lesion on axonal regeneration highly depends on the surgical procedure, the age/type of the individual animal, imaging procedure, post-operative care and tissue processing after sacrificing the animal. Therefore, most of the *in vivo* regeneration experiments could not be accurately compared due to the possible artifacts caused by these variable steps. Sensory axons entering spinal cord keep their lateral positions without crossing the midline. This clear separation between the right and left sides allowed us to image both conditioned and not conditioned axons on the same animal. The sciatic nerve on the left side but not the right side of the animal was conditioned. 1 week after conditioning lesion, one small unilateral lesion on the conditioned (ipsi-lateral) and another one on the unconditioned (contra-lateral) side were performed (Fig. 24B). Retraction and degeneration of the axons were confirmed a few hours after lesioning (Fig. 24C). When we investigated the regenerating sprouts 48 hours post injury, we observed many regenerating sprouts in the conditioned side (Fig. 24D and F) whereas fewer sprouts in unconditioned side (Fig. 24D and E). In most of the conditioned sides, we were able to detect crossing axons (6 out of 7 animals). The average distance of regeneration from the epicenter of the lesion was 371 µm ± 212 µm (Fig. 24G; green circles). However, in those animals, none of the unconditioned sides could form crossing sprouts. The average retraction in unconditioned side was 39 µm ± 60 µm (Fig. 24G; red circles). Subsequently, we checked the lesion sites 8 days after injury when most of the remnants of degenerating distal axons cleared off and observed a more drastic difference. Whereas unconditioned sides possess some sprouts a few hundred micrometers in length around the lesion site (the red arrows in Fig. 24H), the conditioned sides contain many sprouts elongating several millimeters rostral to the lesion site (the white arrows in Fig. 24H). Taken together, these results demonstrate that the boosting effect of pre-conditioning lesion on axons can be observed on the same animal with its control.

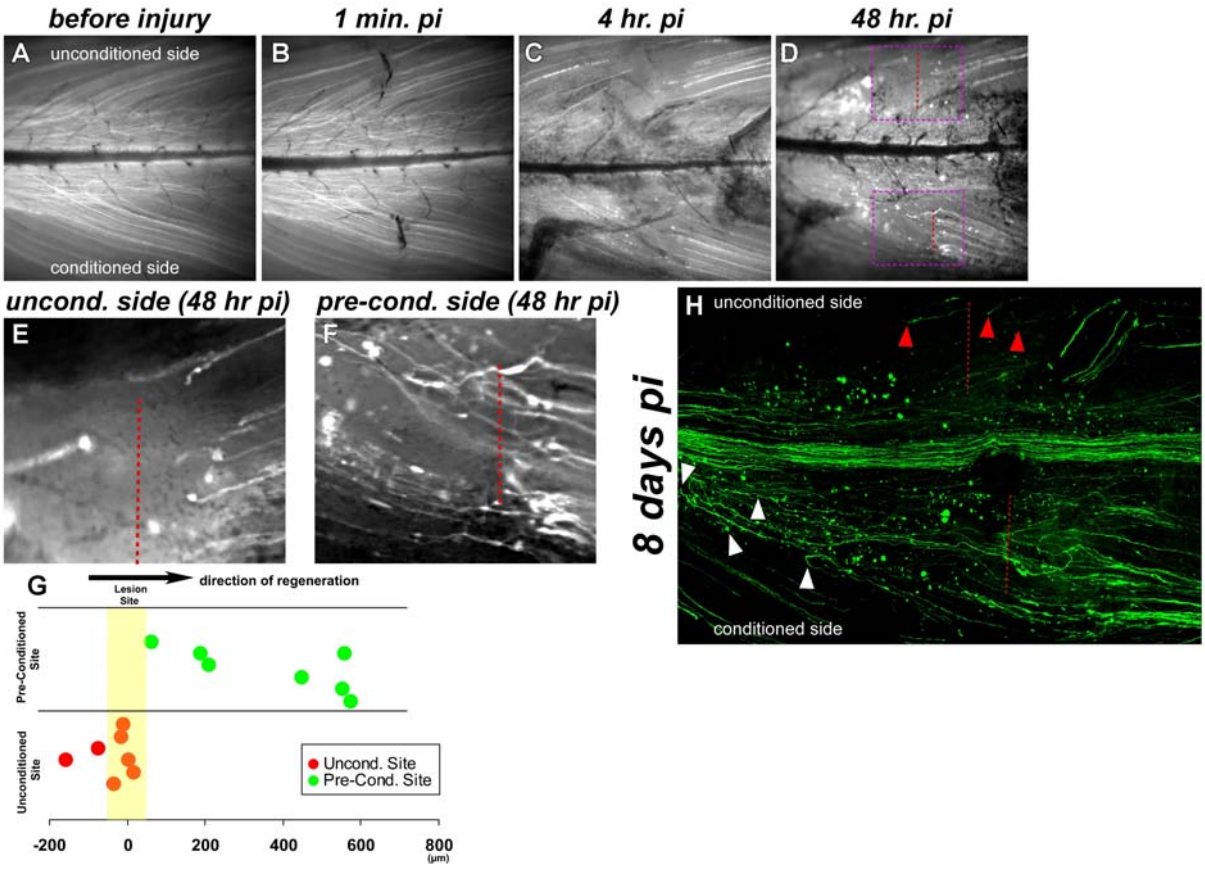

Figure 24. *In vivo* imaging of pre-conditioned and unconditioned (control) on the same animal.

1 week prior to central lesion, the left side of the animal was received peripheral lesioning to condition the DRG neurons. The peripheral lesion performed by putting knots (two single at the same point) and cutting the nerve rostral to the knot. **(A)** A delicate laminectomy at L1 level is performed to expose the central axons coming from sciatic nerves. This is the level where the sciatic nerve axons follow a trajectory from lateral side to the midline, therefore, they are crosswise and more sparsely localized. **(B)** The lateral axons coming from the sciatic nerves were lesion by a small transection. The lesions were applied more or less at the same x axis for a better comparison. **(C)** An image was taken a few hours post injury to confirm the transection and retraction of the axons. **(D-F)** Regeneration of the axons was observed at 48 hours post injury. The existence of several sprouts both behind and beyond the lesion sites on the conditioned side **(E)** compared to unconditioned side **(F)** were readily noticeable.**(E)** and **(F)** are the higher magnifications of the marked areas (purple rectangles) in **(D)**. The red dashed lines in **(D-F)** indicate the lesion site based on the measurements with respect to the lateral blood vessels. **(G)** Almost all of the pre-conditioned sides (6 out 7 animals) were able form sprouts crossing the lesion sites but none of the control sides. Some of the sprouts were able extend as long as 600 μm within 48 hours. **(H)** At 8 days post injury, the same animal was perfused and imaged with a confocal microscope to demonstrate the drastic difference between conditioned and unconditioned sides of the same animals. On the conditioned side, there are

axons elongating several millimeters caudally (white arrow heads) whereas only a few sprouts could go beyond the lesion site for about a few hundred micrometers on the unconditioned side (red arrow heads). The red dashed lines indicate the lesion sites.

3.2.3 Crossing axons possess slim growth cones

As shown above, the injured CNS axons form retraction bulbs, the characteristics of regeneration failure in the CNS (Silver and Miller, 2004). When we analyze the axon terminals of the sprouts after pre-conditioning lesion, we observed that most of the crossing sprouts possessed slim growth cones (94% ± 12%, average ± s.d.; n= 9 animals; Fig. 25E and the white arrowheads in Fig. 25F) significantly more than the axon terminals remaining behind the lesion site (23% ± 13%, average ± s.d.; n= 12 animals; Fig. 25E and the red arrowheads in Fig. 25G). These results demonstrate that the conditioning lesion modulate the intrinsic growth capacity of axons to form growth cones which can elongate long distances and cross the lesion sites.

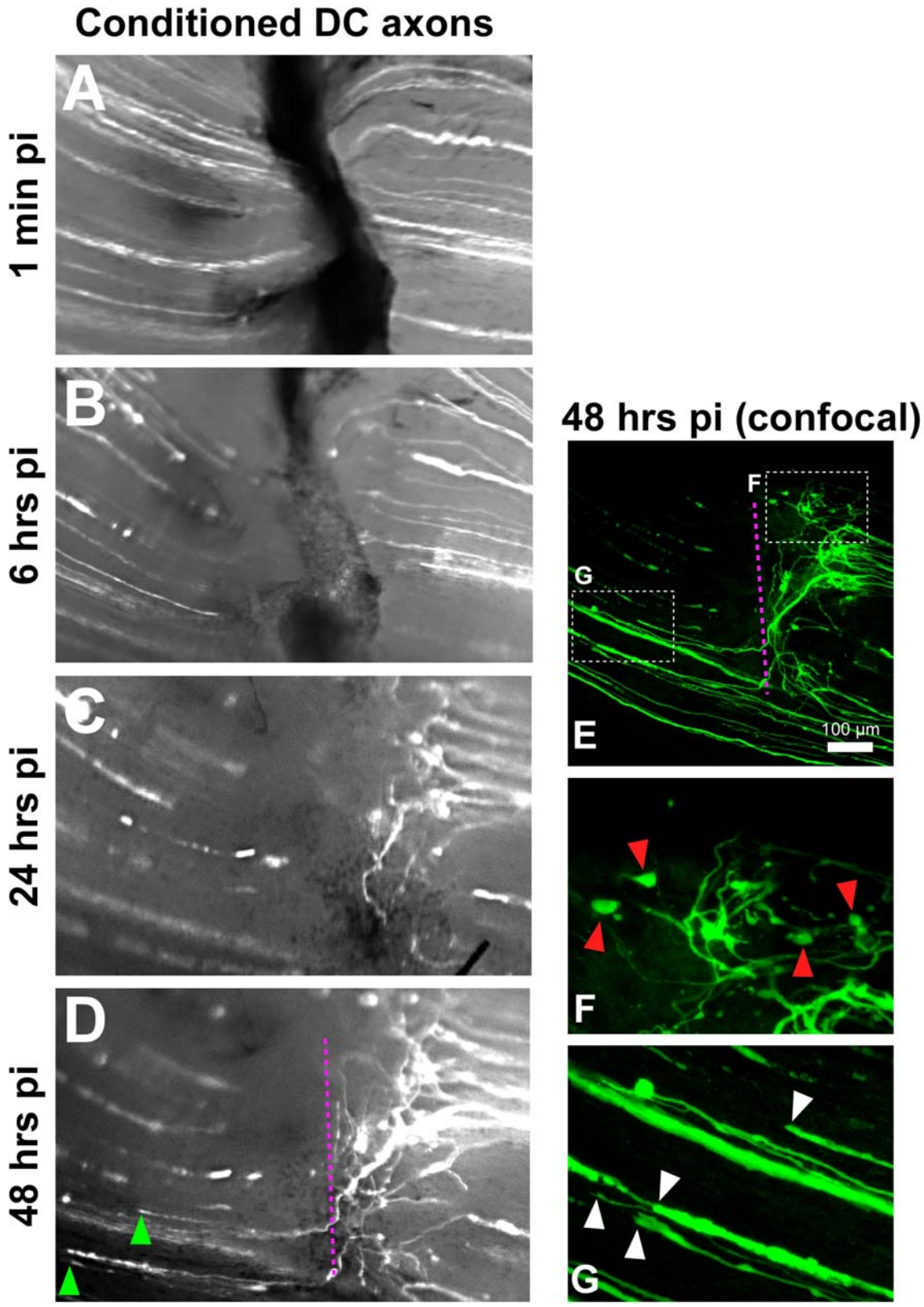

Figure 25. Regenerating sprouts possess growth cones.

In vivo imaging shows that the crossing sprouts mostly have growth cones. **(A-D)** The central axonal branches of conditioned neurons transected at L1 level **(A)**. 6 hours post-injury, transection and retraction of the axons were confirmed **(B).** The same area was imaged 24 hours post injury. There are already several sprouts at 24 hours post-injury possess slim growth cones (green arrowheads) similar to those seen in the PNS *in vivo*. **(E-G)** After *in vivo* imaging at 48 hours, the animals were perfused and the sprout terminals investigated in detail. **(E)** is the confocal image of the area shown in **(D)**. The axonal endings, which remained behind the lesion site had mostly retraction bulbs (redarrowheads in **(F)**). Conversely, the crossing sprout terminals possessed growth cones (white arrowheads in **(G)**).

3.2.4 Reverse-conditioned axons carry the potentials to cross the lesion site

Although pre-conditioning increases the regeneration of CNS neurons, it has not any clinical relevance since it is a pre-injury manipulation. Potentially a more clinically relevant approach is a post-injury intervention i.e. lesioning the peripheral branches is performed after SCI has occurred called “reverse-conditioning”. Unfortunately, many studies on reverse-conditioning showed the failure of this approach in boosting regeneration of injured CNS axons (Richardson and Issa, 1984; Neumann and Woolf, 1999). However, recent studies in our laboratory showed that after a reverse-conditioning, the DRG neurons up-regulate the regeneration associated genes (RAGs) and show an enhanced growth potential both on permissive and inhibitory substrates similar to pre-conditioning (Ylera et al. submitted). This suggests that possible axonal regeneration after a reverse-conditioning lesion might be blocked by inhibitory scar tissue rather than the lack of intrinsic growth competence of axons. To test whether a glial scar is responsible for the failure of regeneration after reverse-conditioning, we followed two different procedures which resulted in complete absence or minimal formation of the glial scar. First, performing a second central lesion on the reverse-conditioned axons caudal to the first lesion and follow the regeneration of the reverse-conditioned neurons through a fresh lesion using *in vivo* imaging; second, we performed a 2-photon laser injury to transect only one labeled axon and followed its regeneration after reverse-conditioning.

The first approach has been performed as follows: a dorsal column hemisection was performed to transect all the dorsal column axons at T8 level. 2 weeks post-injury, reverse-conditioning

was induced by lesioning the sciatic nerve. 1 week after the sciatic nerve lesion, the reverse-conditioned axons transected caudal to first injury at L1 (Fig. 26A) and live imaging was performed to follow the regeneration of these cut axons through the fresh lesion site (Fig. 26B-F). 5-7 hours post injury, the lesion sites were re-imaged to confirm the transection and retraction of these axons (Fig. 26D). Remarkably, when we observed the lesion sites again at 48 hours post-injury, in 4 out of 6 animals we found the crossing axons (Fig. 26E, F, and G). The average crossing distance was 168 µm ± 60 µm (mean ± s.e.m.; n= 6 animals, the data presented in Fig. 26G with the re-print of the pre-conditioned and unconditioned results for comparison). These results show that reverse-conditioned axons are able to cross the lesion site through a fresh lesion.

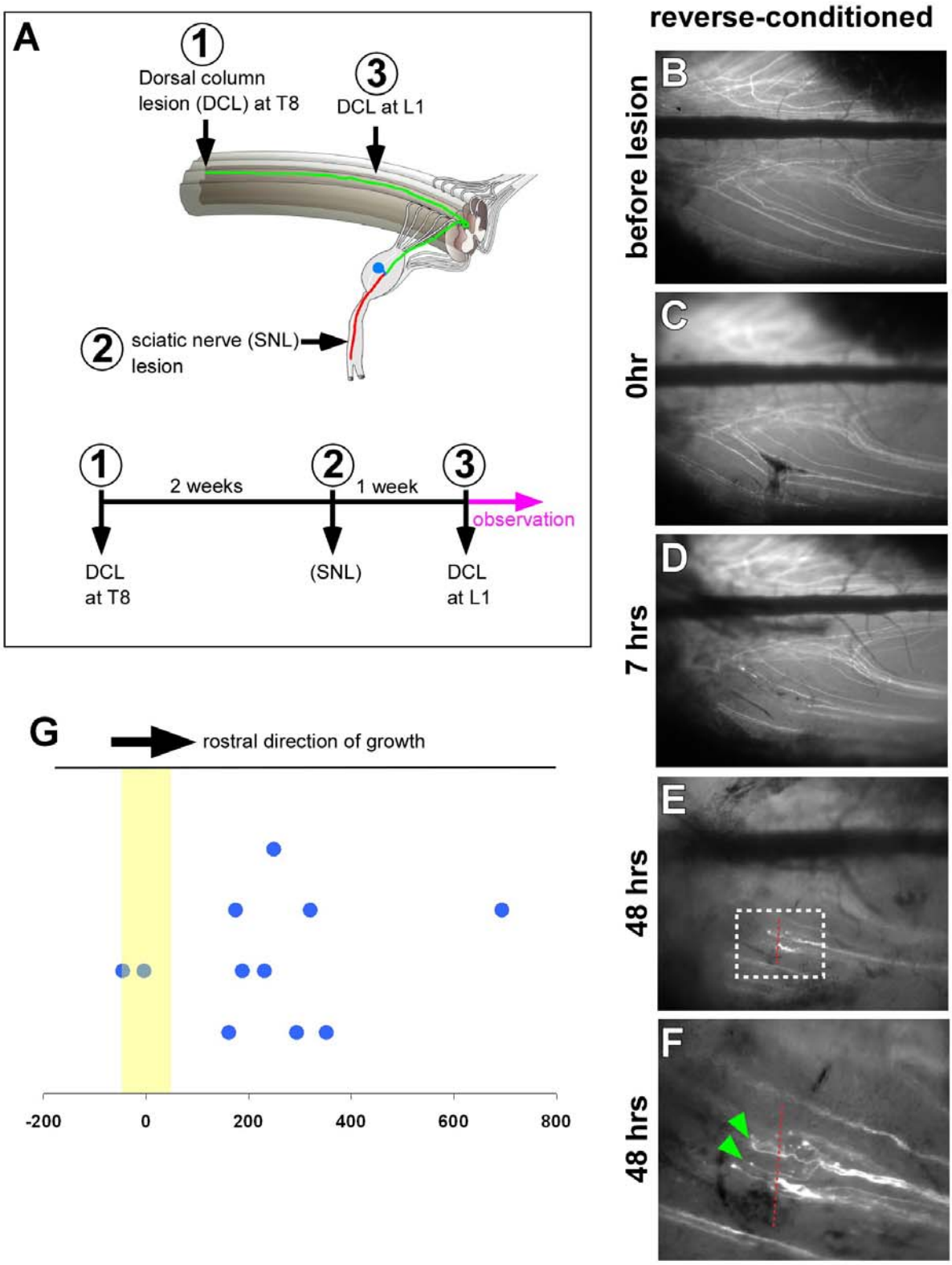
A
1
Dorsal column lesion (DCL) at T8
3
DCL at L1
2
sciatic nerve (SNL) lesion
1
2 weeks
2
1 week
3
observation
DCL at T8
(SNL)
DCL at L1
reverse-conditioned
B
before lesion
C
0hr
D
7 hrs
E
48 hrs
F
48 hrs
G
rostral direction of growth
-200
0
200
400
600
800

Figure 26. Reverse-conditioned axons cross the fresh lesion site devoid of the glial scar.

A dorsal column hemisection was performed at T8 to transect all the axons in the dorsal columns. 2 weeks post lesion, the animals were reverse-conditioned by lesioning the sciatic nerves. The third lesion was made at L1 to transect the axons of reversed-conditioned DRG neurons and live imaging was performed to follow the fate of these conditioned axons through a fresh glial scar. **(A)** The plan for the reverse-conditioning lesion. The first lesion is performed at T8 to transect all the dorsal column axons. 2 weeks after the T8 injury, the sciatic nerve is lesioned to condition the axons. 1 week after the sciatic nerve lesion, a new dorsal column lesion is performed at L1. The growth behavior of the axons at the third lesion side (L1) is observed. **(B)** The target axons at L1 before the second lesion. **(C)** A small unilateral lesion was performed to cut these conditioned axons. **(D)** The transection and retraction of the axons were confirmed 5-7 hours post injury. **(E)** The same lesion site was observed at 48 hours to check the regeneration of the reverse-conditioned axons through the fresh lesion. **(F)** Is the higher magnification of the marked are in **(E)**. After reverse-conditioning, several sprouts have formed. The crossing sprouts (the red arrowheads in **(F)**) have been observed within 48 hours. **(G)** Shows the data of reverse-conditoned animals. The red dashed lines in **(E)** and **(F)** indicate the lesion site. The live images from **(B)** to **(E)** were aligned according to the same landmark (the right-purple line through the vertical vessel). The left purple line goes through the cut site in live images from **(B)** to **(E)**.

In the second approach, we tested reversed-conditioning effect in the absence of the glial scar. We used the 2-photon laser to transect single axon in the spinal cord and avoid formation of a glial scar. 3 days after the 2-photon lesion a conditioning lesion was performed. As negative control, we 2-photon lesioned contra-lateral site of the same animal and left it unconditioned. As positive control, pre-conditioned axons were 2-photon lesioned and followed over days (Fig. 27A). As expected, pre-conditioned axons started to cross the lesion site already at 3 days pi (Fig. 27D). They formed several sprouts already at 3 days pi and kept elongating these sprouts over 5 and 9 days pi (Fig. 27E and F). Remarkably, we observed that the reverse-conditioned axon also regenerated better during the initial 2 days of conditioning and showed significantly longer sprouts and more axonal regeneration within 6 days of post reverse-conditioning (Fig. 27J-K) compared to their negative control sites (Fig. 27O-P). The reverse-conditioning was performed as follows: 3 days post 2-photon injury, the spinal cord was re-exposed and imaged (Fig. 27I). At this time point, we performed the sciatic nerve lesioning for reverse-conditioning. The reverse-conditioned axon was further followed at 5 and 9 days pi (Fig. 27J and K). We observed that already 2 days after the reverse-conditioning, the axon started to form long

sprouts (green arrow in Fig. 27J) and already 6 days after, it crossed the lesion site for several micrometers (green arrow in Fig. 27K). In contrast, we observed some sprouting on the control site of the same animal (Fig. 27L-P).

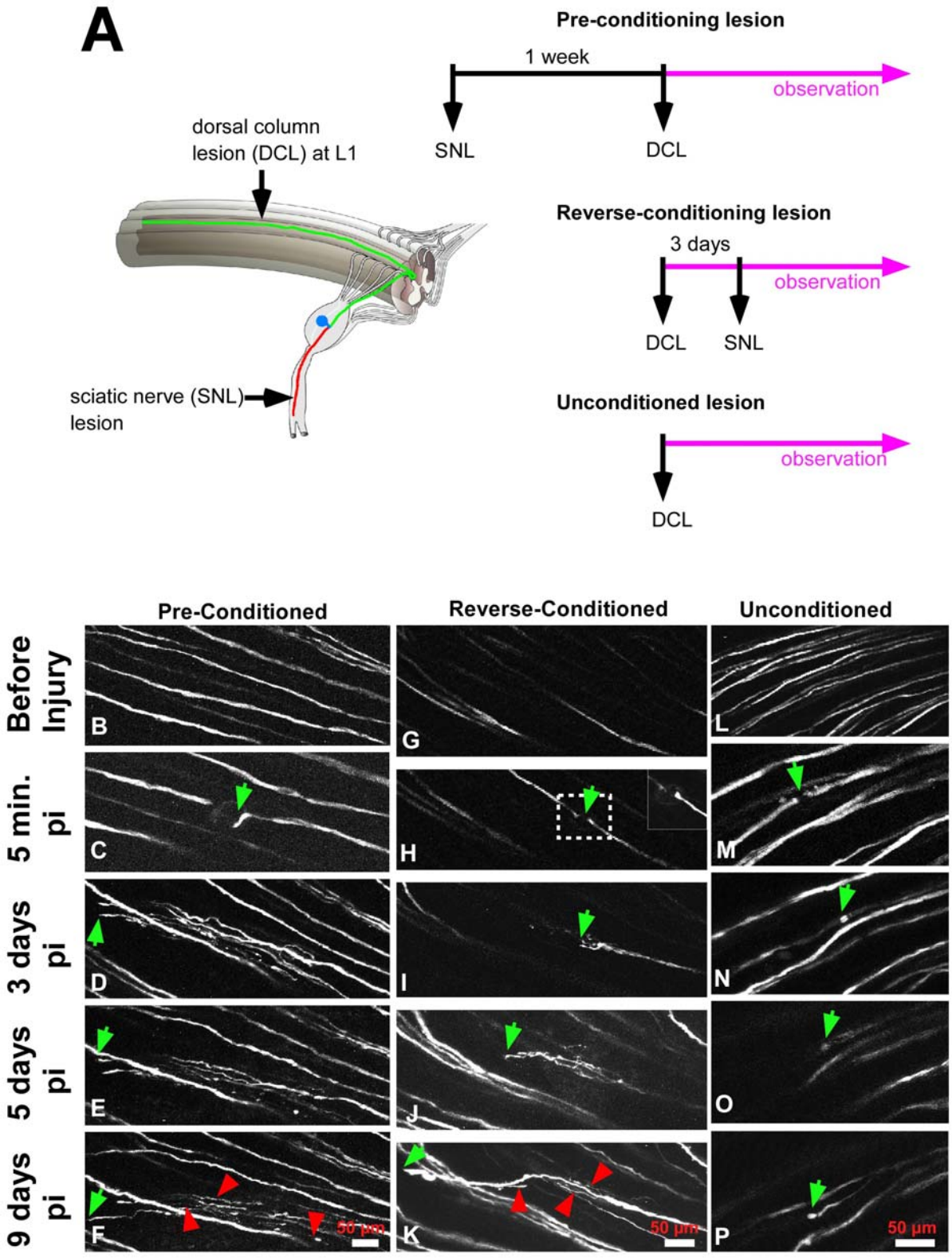

Figure 27. Two-photon lesioned axons show better regeneration when they are reverse-conditioning.

To perform a lesion that is devoid of a glial scar, we used 2-photon laser to transect the axons. The animals are either pre or reverse-conditioned. The contra-lateral sides were used as internal controls. **(A)** In pre-conditioned cases, the sciatic nerves were lesioned one week prior to the dorsal column lesion. In reverse-conditioned group, the sciatic nerves were lesioned 3 days after the dorsal column lesion. In all experimental groups, the observation started with the dorsal column lesion. A pre-conditioned **(B-F)**, a reverse-conditioned **(G-K)** and an unconditioned **(L-P)** sample. The target areas before the lesions **(B, G, L)**, immediately after the laser cut **(C, H, M)**, 3 days **(D, I, N)**, 5 days **(E, J, O)** and 9 days after the lesions **(F, K, P)**. The green arrows follow the regenerating tips of the axons and the red arrowheads mark some of the regenerating sprouts in the samples. Note that in both pre and reverse-conditioned cases, the transected axon formed several regenerating sprouts and achieved to cross the lesion sites. However, the unconditioned axon showed very few sprouts and small distance regeneration. **(P)**.

This data has shown that the reverse-conditioning induces a regenerative response when the minimal lesion is performed. How big are the glial activation and the scar formation after 2-photon lesioning? To answer this question, a few days after the last imaging session, the same animals were killed and the size of the glial scar was checked by GFAP staining (Fig. 28). The staining results showed that even 14 days after the laser lesion, there is a minimal astrocytes activation which most probably was not enough to form an inhibitory barrier against regenerating axon (the white arrows in Fig. 28B, E, H). Overall, these results demonstrate that CNS axons possess intrinsic regeneration capacity even in the adulthood but this regeneration activity is blocked by the inhibitory environment mainly by the glial scar.

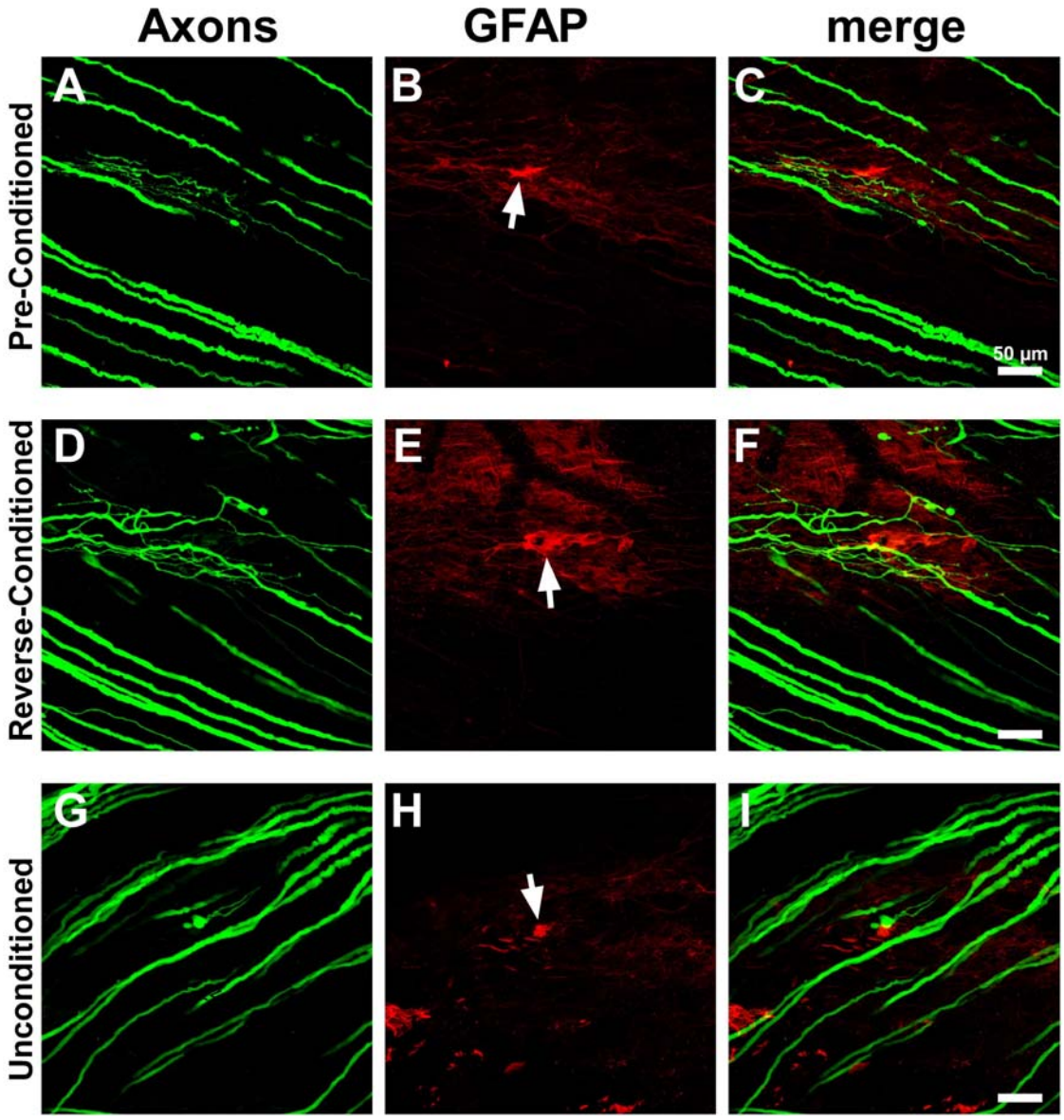

Figure 28. Two-photon lesion induces minimal glial cell response.

The same animals presented in Fig. 28 were perfused 2 weeks after 2-photon lesioning. The spinal cords were stained with GFAP antibody to reveal the astrocytes around the lesion. **(A-C)** the preconditioned, **(D-F)** reverse-conditioned and **(G-I)** unconditioned samples. The white arrows in GFAP images point the lesion epicenter. As it is clearly seen, there are only a few reactive astrocytes around the lesion.

4 Discussion

4.1 The basic intracellular events of retraction bulb formation and maintenance

Retraction bulbs are the morphological hallmarks of lesioned axons that do not regenerate (Ramon y Cajal, 1928). We have shown that one of the main features of retraction bulb formation is the loss of the microtubule organization (Figure 29). Disorganizing the microtubules of growth cones using nocodazole was sufficient to generate retraction bulbs as well as to inhibit axonal growth both *in vitro* and *in vivo*. Conversely, preventing microtubule disorganization by the microtubule stabilizing drug taxol blocks the formation of retraction bulbs. Moreover, we demonstrate that microtubule stabilization is sufficient to induce elongation of CNS axons cultured on a growth inhibitory substrate.

Formation of axonal swellings is one of the early manifestations of axonal degeneration. In our experiments, the first retraction bulbs start to form within one hour, consistent with previous observations (Kerschensteiner et al., 2005), and they possess dynamic morphologies during initial hours of injury. Subsequently, they enlarge in size over weeks.

In aiming to identify the mechanisms underlying retraction bulb formation and lack of axonal growth we assessed effects on membrane trafficking, energy supply and microtubules. Our results suggest that *trans*-Golgi derived vesicles and mitochondria reach and accumulate in the retraction bulbs indicating that they are not restricting factors of axonal regeneration after CNS injury. Indeed, ongoing membrane trafficking of stalled axons might be one cause for the expansion of the retraction bulbs over time together with endocytosis (Tom et al., 2004).

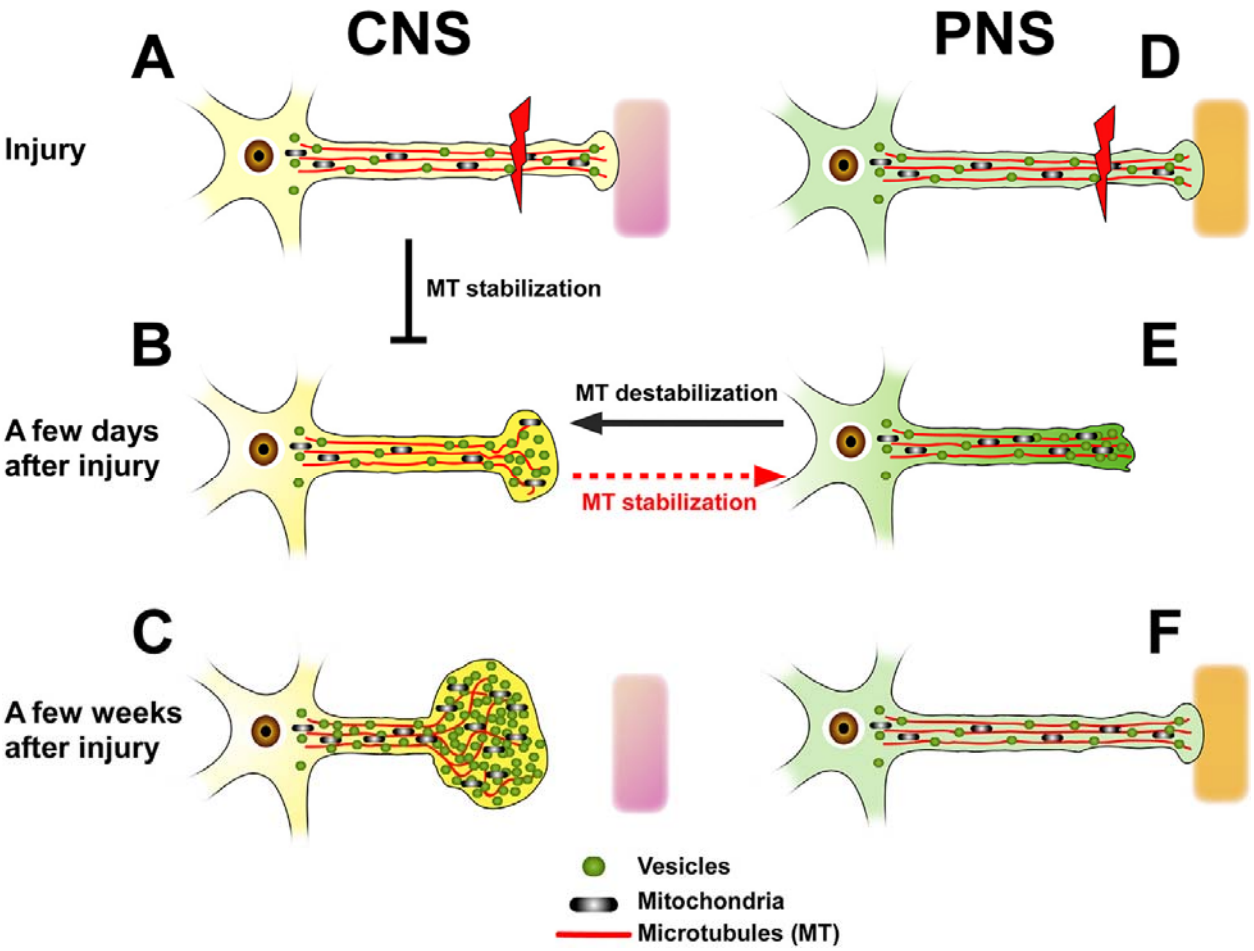

Figure 29. Model for retraction bulb formation versus growth cone mediated regeneration.

(A, D) Before injury: PNS and CNS axons are connected to their targets and are functional. An injury (red-flashes) to a CNS axon **(A)** or PNS axon **(D)** results in disconnection of the axon from the target tissue. **(B, E)** A few days after injury: The axonal part distal from the lesion site dies back (not shown). The CNS axon proximal to axotomy responds to injury by forming a retraction bulb **(B)** which is characterized by dispersed stable and dynamic microtubules and accumulated organelles including *trans*-Golgi derived vesicles and mitochondria. Stabilization of the microtubules starting immediately after injury (from **A**) inhibits the formation of retraction bulbs, and can furthermore induce axon outgrowth. The PNS axon forms a growth cone following a lesion **(E)** which efficiently uses membrane trafficking, energy and an intact cytoskeleton for elongation. Stable microtubules aligned in parallel bundles and serve as tracks for organelle transport to support the rapidly advancing growth cone, and to form the backbone of the growing axon. Dynamic microtubules reach the axonal tip. Destabilization of microtubules at this level can convert the growth cones into retraction-bulb-like structures containing dispersed microtubule organization. **(C, F)** A few weeks after injury: the retraction bulb still enlarges with the accumulation of

organelles due to a continuous membrane traffic **(C)**. In contrast, the PNS axon continues its rapid elongation until finding and connecting to the target **(F)**.

While growth cones *in vivo* have bundled and parallel aligned stable and dynamic microtubules that reach the tip, we found that retraction bulbs contain disorganized and dispersed stable and dynamic microtubules. Notably, dynamic microtubules are mislocalized in retraction bulbs. This contrasts with *in vivo* growth cones that contain bundled dynamic microtubules that extend to the axonal tips. Reorganization of dynamic microtubules is crucial to generate a pushing force against the plasma membrane (Dogterom et al., 2005). Dynamic microtubules probe the actin-rich peripheral regions of *in vitro* growth cones and continuously project into lamellipodia and filopodia showing the typical dynamic behavior of microtubules necessary for axon extension (Kabir et al., 2001; Schaefer et al., 2002). Thus, it appears that disorganized microtubules present in retraction bulbs are not able to support axon extension.

Interestingly, slowly growing or pausing growth cones *in vitro* share some similarities with retraction bulbs. For example, pausing growth cones expand their surface area and show rearrangements of their microtubules (Tanaka and Kirschner, 1991; Dent et al., 1999). Specifically, WNT-7a causes axon inhibition and the generation of enlarged mossy fiber growth cones that possess unbundled microtubules reminiscent to the microtubules in retraction bulbs (Hall et al., 2000).

4.2 Manipulating the microtubule network to convert the end-structures

Modification of microtubules with pharmacological drugs can change the direction (Buck and Zheng, 2002), morphology and elongation of the axons (Pan et al., 2003). Our findings demonstrate that microtubule destabilization using nocodazole is sufficient to produce retraction-bulb-like structures from growth cones and to block axonal growth both in culture and *in vivo* after peripheral injury.

We also demonstrate that stabilization of microtubules using taxol after CNS injury inhibits dispersion of the microtubules preventing retraction bulb formation and axonal degeneration. One way to interpret these results is that taxol could inhibit microtubule catastrophe events that occur after CNS injury, probably caused by a rapid intra-axonal accumulation of Calcium (Balentine and Spector, 1977) . Interestingly, pharmacological inhibition of calpains, a group of proteases which cleaves the major proteins including cytoskeletal proteins (George et al., 1995) also has a neuroprotective effect in the optic nerve (Araujo Couto et al., 2004) and in DRG neurons (Kerschensteiner et al., 2005).

In addition, we show that taxol treatment increases the growth ability of cultured post-natal CGNs when plated on CNS myelin, which is an established cell culture assay that resembles some aspects of the inhibitory environment of the injured spinal cord. Interestingly, taxol treated neurons do not show enhanced growth when plated on poly-lysine, suggesting that taxol enables axons to overcome growth restraint rather than enhancing their general growth potential. Consistent with this interpretation, we demonstrate that taxol treated injured peripheral axons of DRG neurons do not change their growth rate.

Taken together, our *in vitro* and *in vivo* findings present promising insights to study the therapeutical potentials of microtubule stabilization in SCI. It is important to stress that microtubules need to be dynamic to support axon extension. Indeed, low concentrations of taxol do not block microtubule dynamics, but suppress the rate and extent of microtubule shrinkage, yet, still allow polymerization (Derry et al., 1995). In contrast, high concentrations of taxol suppress microtubule dynamics, and thereby axon elongation (Schwamborn and Puschel, 2004) ,and cause toxicity for cells which would imbalance the recovering tissue. Hence, a proper range of drug and delivering methods should be investigated for assessing the effect of taxol on axonal regeneration *in vivo*.

4.3 Putative signaling mechanisms underlying microtubule disorganization

Peripheral and central injuries trigger axonal responses that are dependent on distinct extrinsic factors present in the CNS and PNS. Microtubules are regulated by external signals during axon elongation and guidance (Suter et al., 1998; Buck and Zheng, 2002; Dent and Gertler, 2003). In fact, the known inhibitory cues present in the CNS myelin and the glial scar including MAG, Nogo, OMgP and Versican converge downstream of their receptors onto signaling pathways of the Rho GTPases (Dubreuil et al., 2003; Fournier et al., 2003; Schweigreiter et al., 2004; Sivasankaran et al., 2004), which, besides the actin cytoskeleton, also affect microtubule stability and dynamics (Etienne-Manneville, 2004; Mimura et al., 2006). This suggests that extracellular inhibitory molecules could also induce changes in the dynamics and morphology of the axonal tip by affecting microtubule organization. Indeed, a recent report from Yamashita and colleagues showed that MAG inhibits microtubule assembly and axon outgrowth in postnatal cerebellar granule neurons via Rho kinase activation(Etienne-Manneville, 2004; Mimura et al., 2006) . Interestingly, they identified Collapsin Response Mediator Protein-2 (CRMP-2), a microtubule associated protein, as a target for microtubule disassembly both *in vitro* and *in vivo* after SCI.

In addition to externally triggered responses induced by inhibitory factors, there are intrinsic determinants that confer growth competence. Lesioning the peripheral axonal branches of DRG neurons causes expression of a distinct set of genes, termed regeneration associated genes, which are not upregulated upon central lesioning (Ylera and Bradke, 2006). Interestingly, those sets of genes contain direct and indirect regulators of microtubule polymerization and stabilization including tubulin isoforms, microtubule associated proteins (MAPs) and Arginase I (Miller et al., 1989; Moskowitz and Oblinger, 1995; Cai et al., 2001; Bosse et al., 2006), which may enhance the rapid regrowth of lesioned PNS axons. Notably, it has been demonstrated that interfering with the expression of microtubule binding proteins inhibits neurite outgrowth (Caceres et al., 1992). Taken together, our work establishes microtubules aside from the actin cytoskeleton as a major intracellular regulator of growth restraint after CNS lesioning.

4.4 *In vivo* imaging

To study developmental events in their natural environment, there are two types of imaging: the “static” imaging (collecting data from different animals of related experiments, for example, observing degeneration of axons on animals at different injury time points) or “dynamic” approach (collecting data from one animal, for example, observing the degeneration/regeneration of injured axons over time). Dynamic imaging on the living organism is technically more challenging but provides more accurate data by following the key events over time (Lichtman and Fraser, 2001). *In vivo* imaging has been applied at several neuropathologies including trauma, degeneration, ischaemia, inflammation and seizures and provided extremely valuable insights (Misgeld and Kerschensteiner, 2006). For example, after labeling the vessels by intravenous injection of fluorescent dextran-conjugates, neurovasculature of the CNS can be studied in neurodegenerative diseases like ischaemic stroke (Villringer et al., 1994). In our imaging model, it is also possible to study the alterations in neurovasculature since the blood vessels of spinal cord are readily visible (see Fig. 21).

However, there are several complications of this technique due to surgery and imaging procedures which can cause interpretive pitfalls. For example, the usage of anesthetics that avoid this pitfall, one may need to use different anesthetics and compare the results. Besides, unintended alterations that might be induced during the surgical access and imaging sessions (infections, tissue displacements, phototoxicity etc.) should be carefully watched. To screen the candidate molecules of axonal regeneration, reagent and control treated animals should be tested exactly under the same conditions. Similarly, to eliminate these kinds of problems, we studied pre-conditioning effect on the same animal with its control by performing a double sided injury (Fig. 24). Observation of regeneration in the conditioned but unconditioned axons on the same animal confirms the effect of this manipulation independent of surgical and imaging artifacts.

In vivo imaging is a powerful technique 1) to observe the pathology of lesioned axons on living animals, 2) to investigate therapeutic approaches including drug applications and transplantation studies. In future, improvements in both transgenic and imaging technologies will open new avenues for researchers to apply *in vivo* imaging in neuroscience. For instance, recent microscopy techniques which can image several millimeters deep in tissue e.g. selective plane illumination microscopy (SPIM) (Huisken et al., 2004) or even the whole mouse brain in fixed tissues (Dodt et al., 2007) are promising advances indicating that the whole CNS structures will be imaged in near future on live animals. In parallel, the emergence of the new transgenics in which different cellular structures are labeled e.g. mitochondria and synaptic proteins (Misgeld and Kerschensteiner, 2006), makes it possible to study those cellular events within the nervous system. Creation of multi-transgenics expressing different fluorescent proteins tagged to different targets will be a fascinating tool to study development and pathology of the nervous system.

Overall, our *in vivo* imaging results provide an essential knowledge to screen the effect of the putative regeneration promoting molecules within short time. For instance, the effect of cAMP which was shown to induce regeneration would be studied by *in vivo* imaging in comparison to pre-conditioning. If the pre-conditioning lesion is inducing its effect via cAMP pathway, one would expect to see the same amount of regeneration within 48 hours after the injury in cAMP treated animals.

4.5 Pre-conditioning lesion

Failure of CNS axons to regenerate has been attributed to both extrinsic inhibitory molecules present in the scarred tissue and poor intrinsic response of neurons which fails to activate regeneration associated mechanisms. Denaturalization of extrinsic inhibitory molecules either by antibodies or enzymes increased the regeneration of the CNS axons confirming the growth inhibitory effects of these factors (Schwab and Bartholdi, 1996; Chen et al., 2000; Moon et al., 2001; Bradbury et al., 2002; Schwab, 2004; Buchli and Schwab, 2005; Carulli et al., 2005;

Galtrey et al., 2007). Studies on CNS neurons showed that the intrinsic growth ability of the DRG neurons can be increased by performing a pre-conditioning lesion (McQuarrie et al., 1977; McQuarrie et al., 1978; Richardson and Issa, 1984; Richardson and Verge, 1987). An important feature of the pre-conditioning induced regeneration is that it allows axons to pass through the lesion site in the presence of inhibitory milieu of white matter, without a need to manipulate the inhibitory environment (Neumann and Woolf, 1999). However, rationally, injuring the peripheral axon cannot be a therapy in the clinic. Hence, the studies on the pre-conditioning showed that intraganglionic injection of membrane permeable cAMP analogues mimics the effect of the pre-conditioning lesion (Neumann et al., 2002; Qiu et al., 2002). Therefore, cAMP injection can substitute the conditioning lesioning. Similarly, the attempts to understand the cellular and molecular basis of pre-conditioning phenomenon became a useful way in identifying RAGs. It has been shown that IL6 and LIF are upregulated by Schwann cells that activate signaling pathways via gp130 receptors and JAK-STAT pathway, which in turn induce the transcription of RAGs (Cafferty et al., 2001; Zang and Cheema, 2003; Cafferty et al., 2004; Qiu et al., 2005). On the other hand, increased cAMP after a pre-conditioning lesion activates transcription of arginase gene in a PKA dependent manner (Cai et al., 2002; Qiu et al., 2002).

Using *in vivo* imaging we found that pre-conditioning enables DRG neurons to form long crossing sprouts within 48 hours post-injury which has not been observed in controls. These results demonstrate that the effect of pre-conditioning on regeneration emerges as early as 48 hours, much earlier than previously reported (Neumann and Woolf, 1999). It suggests that the regeneration associated molecules which are activated after pre-conditioning have already been transported to the central axonal branches of the neurons. Supporting this hypothesis, it has been shown that the molecules controlling the cytoskeleton dynamics and stability directly or indirectly effect the regeneration such as arginase I and microtubule associated proteins (MAPs), which have been shown to be upregulated after pre-conditioning, are transported into the central axonal branches concomitantly into the peripheral axonal branches (Miller et al., 1989; Moskowitz and Oblinger, 1995; Cai et al., 2002; Bosse et al., 2006). Alternatively or concurrently, the quick response of the axons would be due to the local translation of the

mRNAs belong to the regeneration associated proteins such as MAP1B which has been shown to localize in the growth cones of cultured hippocampal neurons (Antar et al., 2006).

4.6 Reverse-conditioning lesion

Previous studies demonstrated that lesioning the peripheral branches of DRG neurons after the central lesion (reverse/post conditioning) did not boost the regeneration of these neurons (Richardson and Verge, 1987; Neumann et al., 2002). Why the reverse-conditioning, which has a more clinical relevance as being a post-injury manipulation does not work? There are two possible reasons for the insufficiency of reverse-conditioning: 1) being unable to increase the intrinsic growth capacity; 2) being unable to overcome the inhibitory environment e.g. glial scar, which form before the possible effect of revere-conditioning appears. Our studies showed that RAGs are upregulated in reverse-conditioned DRG neurons and reverse-conditioned neurons form neurites as efficiently as pre-conditioned neurons on a substrate permissive for axonal growth and on myelin which is inhibitory to the axon outgrowth (Ylera et al; unpublished data). Therefore, the scar that formed after central lesioning seems to be a major obstacle that is causing the poor regenerative ability of reverse-conditioned neurons, since it follows a different time line of development in pre-conditioning versus reverse-conditioning. We tested this hypothesis directly and found that in the absence of a glial scar, reverse-conditioned axons can regenerate better compared to the unconditioned axons. We used a 2-photon laser which would cut the axons located under the dura matter without damaging the dura or surrounding tissue. The laser of 2-photon microscope was enough to transect the single axons by just only heating up an area as thick as the axon. When we reserve-conditioned this single transected axon, we could clearly see its regeneration in 5 days.

These data show that a mature glial scar is indeed a barrier for the regenerating axons. Supporting our results, Bhatt and colleagues showed that zebrafish, which do not form a glial scar and instead possess a permissive environment around their CNS, respond favorably to cAMP application initiated several days post injury, and regain neuronal function (Bhatt et al.,

2004). Our work is in agreement with other studies showing the role of the glial scar in blocking regeneration. For instance, in several studies the CSPGs, a major inhibitory constituent of the glial scar were targeted to eliminate their effects. Steinmetz and colleagues showed that when the sensory ganglia are pre-treatmented with zymozan to boost intrinsic growth potential in combination with ChABC modification of CSPGs to eliminate the glial scar, the axons could achieve robust regeneration (Steinmetz et al., 2005). In one another work, usage of antibodies against NG2 proteoglycan induced better regeneration of sensory axons in the spinal cord (Tan et al., 2006). When anti-NG2 treatment combined with pre-conditioning lesion which increases the intrinsic regeneration capacity, the axons could grow long distances, past the glial scar and reach into the white matter rostral to injury, indicating that a combinatorial strategy used to reduce extrinsic inhibition while intrinsic growth is increased, results in noticeable regeneration which contributes to the functional recovery of the animals. Consistently, Lu and colleagues showed that the boundaries of the glial scar at sites of chronic SCI are not impenetrable but very permissive. In this study, they demonstrated that introduction of local and diffusible permissive signals that favor regeneration can balance the inhibition regardless the glial scar (Lu et al., 2007). On the other hand, delayed administration of rolipram, which targets both intrinsic and extrinsic aspects, stimulated axonal regeneration and functional improvement even after 2 weeks after the injury (Nikulina et al., 2004). It elevates intracellular cAMP levels and thereby triggers a favorable growth promoting signaling cascade within the cell via. On the other hand it attenuates reactive gliosis and consequently formation of glial scar. All these works independently show that activation of astrocytes and extracellular matrix associated inhibitors that collectively constitute the glial scar are critical factors to be taken care of while developing new therapeutical interventions to treat the CNS injuries.

Overall, our data suggest that conditioning effect as well as mimicking its effects by stimulating signaling cascades have a clinical relevance opposite to the previous assumptions since now we demonstrated the relevance of a post-injury conditioning.

4.7 Overview and Outlook

In my thesis, I aimed to analyze a long lasting question of the neuroscience field “Why do axons in the PNS regenerate but not the axons in the CNS?” from a novel and original perspective. Although there is a relatively broad knowledge about the extrinsic inhibitory factors of axonal regeneration (Schwab and Bartholdi, 1996; Hata et al., 2006; Yiu and He, 2006), the intrinsic events causing CNS axons to stop are not well characterized. One reason may be the technical limitations which mostly are not enough to uncover the on going cellular and molecular events in complex nervous system. Therefore, I developed a new *in vivo* imaging techniques that we used to investigate regeneration and degeneration of the axons in both CNS and PNS *in vivo*. In my thesis, I worked on injured CNS axon terminals “retraction bulbs” which are the hallmarks of the stalled axons. These axonal swellings were reported almost a centaury ago by Ramon Cajal but they have remained mostly unknown. I analyzed the retraction bulbs in comparison to the growth cones and found a major difference which can be used to manipulate and convert them into growth cones. Afterwards, using the *in vivo* imaging techniques in combination with the other essential methods e.g. immunostaining, cell-culture, electron microscopy and 2-photon microscopy I studied regeneration of the axons after reverse-conditioning lesion in comparison to the pre-conditioning lesion which is known to induce axonal regeneration in the CNS.

Below, I summarize my main findings and point out some of the remaining open questions.

4.7.1 Characterization of retraction bulbs compared to growth cones

Advance of growth cones and subsequent events of the axonal elongation require membrane delivery, energy supply and cytoskeletal dynamics. These processes appear to function in the peripheral axons after lesioning. In contrast, axons coursing in the central nervous system do not regrow after injury and form retraction bulbs. While many of the components in the CNS myelin and the glial scar preventing axon growth have been identified and characterized, we still do not understand the intracellular machinery inside the axons that causes them to stop. Here, we show that retraction bulbs contain considerably disorganized microtubules blocking

axonal growth. Moreover, disrupting microtubules in growth cones transforms them into retraction-bulb-like structures and inhibits their outgrowth both *in vivo* and *in vitro*. Finally, stabilizing microtubules of injured CNS axons interferes with the formation of retraction bulbs *in vivo* and overcomes growth inhibitory effect of myelin *in vitro*. Thus, the stability and organization of microtubules play an essential role in shaping the axonal terminals of injured neurons as regenerating growth cones or stalled retraction bulbs. In conclusion, the Injured axon terminals "retraction bulbs" *in vivo* are hallmarks of regeneration failure in the injured spinal cord as well as most of the other CNS neurodegenerative disorders including traumatic brain injury, Alzheimer's disease, Parkinson's disease and multiple sclerosis (Coleman, 2005). Hence, identification of the differences inherent to formation of retraction bulbs and advancing growth cones would provide essential insights to better address the causes of regeneration failure in the CNS. We believe that our results decipher a key intracellular mechanism that determines the formation and differential growth properties of growth cones and retraction bulbs. The future challenge will be to manipulate the microtubules of retraction bulbs *in vivo* to induce regrowth of injured CNS axons. We expect that stabilization of microtubules, alone or combined with other therapeutic interventions, will be a potential approach to enhance regeneration of injured CNS axons.

Below I listed several related questions that are particularly interesting and require further study:

- We observed that vesicles and mitochondria arrive to the retraction bulbs. However, there are several questions regarding these processes which may need further investigation. For instance, we do not know whether these vesicles carry regeneration associated molecules or not. Therefore, the content of these cargos should be analyzed in detail. On the other hand, although their morphologies look healthy, it is not clear if the mitochondria within the retraction bulbs are able to produce energy. It would be necessary and interesting to study ATP production efficiency of the mitochondria in the retraction bulbs.

- We showed that the actin filaments are also disorganized in retraction bulbs. In addition, based on our EM images (data not shown), retraction bulbs seem to have a disorganized neurofilaments as well as actin filaments similar to their microtubules. However, these two cytoskeleton elements have to be further studied to elucidate their exact roles in the formation and maintenance for the retraction bulbs. Particularly, it would be interesting to study the causal relationships of actin cytoskeleton and neurofilaments on the formation of a retraction bulb. For instance, is it possible to convert a growth cone into a retraction bulb by manipulating the actin cytoskeleton or neurofilaments? It has been demonstrated that in the growth cones microtubules present at the peripheral regions of the growth cone interact with the retrogradely flowing actin filaments (Schaefer et al., 2002; Myers et al., 2006). It would be interesting to investigate such interactions in the retraction bulbs. Perhaps, the disruption of interaction of different cytoskeleton elements is one of the causes of the retraction bulb formation.

- We showed that microtubules are highly disorganized in retraction bulbs. What are the underlying molecules/signaling pathways? Could some of the microtubule associated proteins be upstream of the microtubule disorganization? To answer these questions, the presence and distribution of the microtubule associated proteins should be investigated in retraction bulbs compared to growth cones. For instance, MAP1B has been shown to concentrate in the tip of the growth cones (Black et al., 1994) and involve in regulation of microtubules in the growth cones (Ma et al., 2000; Mack et al., 2000). Interestingly, phosphorylated form of MAP1B is up-regulated in the regenerating DRG neurons (Ma et al., 2000) and play a role in the coordination of actin and microtubule cytoskeletons (Bouquet et al., 2007) indicating that microtubule organization in the growth cones of the elongating axons during both development and regeneration requires MAP1B. In addition, It has been implicated that many inhibitory pathways of axonal regeneration relay their signals on the cytoskeleton through the RhoA GTPases (Niederost et al., 2002; Silver and Miller, 2004; Hiraga et al., 2006; Gross

et al., 2007). Does RhoA pathway play also a role in the formation of retraction bulbs? If it is the pathway that is causing disorganization of cytoskeleton, would it be possible to inhibit formation of retraction bulbs by inactivating RhoA pathway?

- Interfering with the formation of retraction bulbs *in vivo* may induce axonal regeneration in long-term. Would it be possible to promote axonal regeneration by applying taxol with a intrathecal pump? At this point, it is essential to find the optimum concentration of the taxol which would inhibit the disorganization of the microtubules and formation of retraction bulbs and at the same time would allow the polymerization of the microtubules to support the growing axon.

- Other neurodegenerative diseases also form axonal swellings (Bernstein and Lichtman, 1999; Coleman, 2005). It would be interesting to apply our knowledge about the retraction bulbs into the other neurodegenerative diseases having axonal swelling as a complication. What is the level of the similarity among the axonal swellings forming after different neurodegenerative diseases? Would it be also possible to inhibit formation of axonal swellings and degeneration using taxol in the other neurodegenerative diseases?

4.7.2 *In vivo* imaging of pre and reverse-conditioned axons

Injured axons in the CNS do not regenerate or partially regenerate which mostly is not sufficient to re-establish original connections and functions. This limited regeneration can be boosted in DRG neurons by lesioning the peripheral extensions prior to the central lesion. However, it has been unclear why a post injury conditioning lesion does not induce such a positive effect. Using *in vivo* imaging, I tried to understand how a successful regeneration is achieved in pre-conditioned animals and why reverse-conditioning fails. Our data showed that pre-conditioned axons were remarkably able to cross the lesion within 48 hours post injury which was never seen in unconditioned cases. These crossing sprouts have been observed to possess growth cones unlike the sprouts which fail to cross and stop their regeneration. Interestingly, reverse-

conditioning of previously lesioned axons has also formed crossing sprouts within 48 hours post injury. This suggests that the glial scar play an important role in the inhibition of regeneration in reserves-conditioned axons. To this end, we performed a small lesion by using a 2-photon microscopy laser and observe the regeneration of the reverse-conditioned axons in minimal presence or completely absence of a glial scar. We demonstrated that when such small lesion is performed, the reverse-conditioned neurons can form long regenerating sprouts.

- Several therapeutical interventions that have been claimed to induce regeneration e.g. elimination of Nogo have not been fully reproduced by other groups (He et al., 2003; Kim et al., 2003; Zheng et al., 2003). It would be interesting to use *in vivo* imaging and study the effect of promising substances like anti-Nogo antibody in comparison to pre-conditioning lesion.

- What are the signaling pathways underlying reverse-conditioning in the absence of the glial scar? Can this effect also be initiated with some substances without performing a lesion? Could this effect be combined with therapies that aim to remove the inhibitory effect of the glial scar to induce regeneration even in the cases of big spinal cord lesions?

- The injured axons in the white matter of spinal cord mostly regenerate towards the gray matter and they were proposed to make synapses in these regions. However, the true nature of these re-wring has not been well characterized. Do these regenerating sprouts form synapses? If yes, what are the target cells?

- We showed that reverse-conditioning can induce axonal regeneration when the glial scar formation is avoided. It would be interesting to combine the reverse-conditioning effect with the substances that decreases the inhibitory effect of the glial scar such as Nogo-A antibody (Schnell and Schwab, 1990; Brosamle et al., 2000) and Chondroitinase

ABC (Krekoski et al., 2001; Bradbury et al., 2002; Morgenstern et al., 2002; Steinmetz et al., 2005).

5 References

Antar LN, Li C, Zhang H, Carroll RC, Bassell GJ (2006) Local functions for FMRP in axon growth cone motility and activity-dependent regulation of filopodia and spine synapses. Mol Cell Neurosci 32:37-48.

Araujo Couto L, Sampaio Narciso M, Hokoc JN, Blanco Martinez AM (2004) Calpain inhibitor 2 prevents axonal degeneration of opossum optic nerve fibers. J Neurosci Res 77:410-419.

Balentine JD, Spector M (1977) Calcification of axons in experimental spinal cord trauma. Ann Neurol 2:520-523.

Balice-Gordon RJ (1997) *In vivo* approaches to neuromuscular structure and function. Methods Cell Biol 52:323-348.

Bamburg JR, Bray D, Chapman K (1986) Assembly of microtubules at the tip of growing axons. Nature 321:788-790.

Basso DM, Beattie MS, Bresnahan JC (1995) A sensitive and reliable locomotor rating scale for open field testing in rats. J Neurotrauma 12:1-21.

Becker CG, Becker T (2002) Repellent guidance of regenerating optic axons by chondroitin sulfate glycosaminoglycans in zebrafish. J Neurosci 22:842-853.

Becker S, Penkert G (2000) *In vivo* visualization of the neuromuscular junction before and after autologous nerve transfer in the rat. J Reconstr Microsurg 16:111-120.

Bernstein M, Lichtman JW (1999) Axonal atrophy: the retraction reaction. Curr Opin Neurobiol 9:364-370.

Bhatt DH, Otto SJ, Depoister B, Fetcho JR (2004) Cyclic AMP-induced repair of zebrafish spinal circuits. Science 305:254-258.

Black MM, Slaughter T, Fischer I (1994) Microtubule-associated protein 1b (MAP1b) is concentrated in the distal region of growing axons. J Neurosci 14:857-870.

Bosse F, Hasenpusch-Theil K, Kury P, Muller HW (2006) Gene expression profiling reveals that peripheral nerve regeneration is a consequence of both novel injury-dependent and reactivated developmental processes. J Neurochem 96:1441-1457.

Bouquet C, Ravaille-Veron M, Propst F, Nothias F (2007) MAP1B coordinates microtubule and actin filament remodeling in adult mouse Schwann cell tips and DRG neuron growth cones. Mol Cell Neurosci.

Bradbury EJ, Moon LD, Popat RJ, King VR, Bennett GS, Patel PN, Fawcett JW, McMahon SB (2002) Chondroitinase ABC promotes functional recovery after SCI. Nature 416:636-640.

Bradke F, Dotti CG (1997) Neuronal polarity: vectorial cytoplasmic flow precedes axon formation. Neuron 19:1175-1186.

Bradke F, Dotti CG (2000) Establishment of neuronal polarity: lessons from cultured hippocampal neurons. Curr Opin Neurobiol 10:574-581.

Bray D (1970) Surface movements during the growth of single explanted neurons. Proc Natl Acad Sci U S A 65:905-910.

Bray D, Chapman K (1985) Analysis of microspike movements on the neuronal growth cone. J Neurosci 5:3204-3213.

Brosamle C, Huber AB, Fiedler M, Skerra A, Schwab ME (2000) Regeneration of lesioned corticospinal tract fibers in the adult rat induced by a recombinant, humanized IN-1 antibody fragment. J Neurosci 20:8061-8068.

Buchli AD, Schwab ME (2005) Inhibition of Nogo: a key strategy to increase regeneration, plasticity and functional recovery of the lesioned central nervous system. Ann Med 37:556-567.

Buck KB, Zheng JQ (2002) Growth cone turning induced by direct local modification of microtubule dynamics. J Neurosci 22:9358-9367.

Bulsara KR, Iskandar BJ, Villavicencio AT, Skene JH (2002) A new millenium for spinal cord regeneration: growth-associated genes. Spine 27:1946-1949.

Caceres A, Mautino J, Kosik KS (1992) Suppression of MAP2 in cultured cerebellar macroneurons inhibits minor neurite formation. Neuron 9:607-618.

Cafferty WB, Gardiner NJ, Das P, Qiu J, McMahon SB, Thompson SW (2004) Conditioning injury-induced spinal axonal regeneration fails in interleukin-6 knock-out mice. J Neurosci 24:4432-4443.

Cafferty WB, Gardiner NJ, Gavazzi I, Powell J, McMahon SB, Heath JK, Munson J, Cohen J, Thompson SW (2001) Leukemia inhibitory factor determines the growth status of injured adult sensory neurons. J Neurosci 21:7161-7170.

Cai D, Qiu J, Cao Z, McAtee M, Bregman BS, Filbin MT (2001) Neuronal cyclic AMP controls the developmental loss in ability of axons to regenerate. J Neurosci 21:4731-4739.

Cai D, Deng K, Mellado W, Lee J, Ratan RR, Filbin MT (2002) Arginase I and polyamines act downstream from cyclic AMP in overcoming inhibition of axonal growth MAG and myelin *in vitro*. Neuron 35:711-719.

Carulli D, Laabs T, Geller HM, Fawcett JW (2005) Chondroitin sulfate proteoglycans in neural development and regeneration. Curr Opin Neurobiol 15:116-120.

Chada SR, Hollenbeck PJ (2003) Mitochondrial movement and positioning in axons: the role of growth factor signaling. J Exp Biol 206:1985-1992.

Chen DF, Jhaveri S, Schneider GE (1995) Intrinsic changes in developing retinal neurons result in regenerative failure of their axons. Proc Natl Acad Sci U S A 92:7287-7291.

Chen LL, Folsom DB, Ko CP (1991) The remodeling of synaptic extracellular matrix and its dynamic relationship with nerve terminals at living frog neuromuscular junctions. J Neurosci 11:2920-2930.

Chen MS, Huber AB, van der Haar ME, Frank M, Schnell L, Spillmann AA, Christ F, Schwab ME (2000) Nogo-A is a myelin-associated neurite outgrowth inhibitor and an antigen for monoclonal antibody IN-1. Nature 403:434-439.

Chong MS, Woolf CJ, Haque NS, Anderson PN (1999) Axonal regeneration from injured dorsal roots into the spinal cord of adult rats. J Comp Neurol 410:42-54.

Chong MS, Woolf CJ, Turmaine M, Emson PC, Anderson PN (1996) Intrinsic versus extrinsic factors in determining the regeneration of the central processes of rat dorsal root ganglion neurons: the influence of a peripheral nerve graft. J Comp Neurol 370:97-104.

Coleman M (2005) Axon degeneration mechanisms: commonality amid diversity. Nat Rev Neurosci 6:889-898.

Craig AM, Wyborski RJ, Banker G (1995) Preferential addition of newly synthesized membrane protein at axonal growth cones. Nature 375:592-594.

Dai J, Sheetz MP (1995) Axon membrane flows from the growth cone to the cell body. Cell 83:693-701.

Davies SJ, Goucher DR, Doller C, Silver J (1999) Robust regeneration of adult sensory axons in degenerating white matter of the adult rat spinal cord. J Neurosci 19:5810-5822.

Dent EW, Gertler FB (2003) Cytoskeletal dynamics and transport in growth cone motility and axon guidance. Neuron 40:209-227.

Dent EW, Callaway JL, Szebenyi G, Baas PW, Kalil K (1999) Reorganization and movement of microtubules in axonal growth cones and developing interstitial branches. J Neurosci 19:8894-8908.

Derry WB, Wilson L, Jordan MA (1995) Substoichiometric binding of taxol suppresses microtubule dynamics. Biochemistry 34:2203-2211.

Dodt HU, Leischner U, Schierloh A, Jahrling N, Mauch CP, Deininger K, Deussing JM, Eder M, Zieglgansberger W, Becker K (2007) Ultramicroscopy: three-dimensional visualization of neuronal networks in the whole mouse brain. Nat Methods 4:331-336.

Dogterom M, Kerssemakers JW, Romet-Lemonne G, Janson ME (2005) Force generation by dynamic microtubules. Curr Opin Cell Biol 17:67-74.

Dubreuil CI, Winton MJ, McKerracher L (2003) Rho activation patterns after SCI and the role of activated Rho in apoptosis in the central nervous system. J Cell Biol 162:233-243.

Erturk A, Hellal F, Enes J, Bradke F (2007) Disorganized microtubules underlie the formation of retraction bulbs and the failure of axonal regeneration. J Neurosci 27:9169-9180.

Etienne-Manneville S (2004) Actin and microtubules in cell motility: which one is in control? Traffic 5:470-477.

Fan J, Mansfield SG, Redmond T, Gordon-Weeks PR, Raper JA (1993) The organization of F-actin and microtubules in growth cones exposed to a brain-derived collapsing factor. J Cell Biol 121:867-878.

Faulkner JR, Herrmann JE, Woo MJ, Tansey KE, Doan NB, Sofroniew MV (2004) Reactive astrocytes protect tissue and preserve function after SCI. J Neurosci 24:2143-2155.

Feng G, Mellor RH, Bernstein M, Keller-Peck C, Nguyen QT, Wallace M, Nerbonne JM, Lichtman JW, Sanes JR (2000) Imaging neuronal subsets in transgenic mice expressing multiple spectral variants of GFP. Neuron 28:41-51.

Ferretti P, Zhang F, O'Neill P (2003) Changes in spinal cord regenerative ability through phylogenesis and development: lessons to be learnt. Dev Dyn 226:245-256.

Filbin MT (2003) Myelin-associated inhibitors of axonal regeneration in the adult mammalian CNS. Nat Rev Neurosci 4:703-713.

Filbin MT (2006) How inflammation promotes regeneration. Nat Neurosci 9:715-717.

Forscher P, Smith SJ (1988) Actions of cytochalasins on the organization of actin filaments and microtubules in a neuronal growth cone. J Cell Biol 107:1505-1516.

Fournier AE, Takizawa BT, Strittmatter SM (2003) Rho kinase inhibition enhances axonal regeneration in the injured CNS. J Neurosci 23:1416-1423.

Fournier AE, GrandPre T, Gould G, Wang X, Strittmatter SM (2002) Nogo and the Nogo-66 receptor. Prog Brain Res 137:361-369.

Fu SY, Gordon T (1997) The cellular and molecular basis of peripheral nerve regeneration. Mol Neurobiol 14:67-116.

Gallo V, Bertolotto A (1990) Extracellular matrix of cultured glial cells: selective expression of chondroitin 4-sulfate by type-2 astrocytes and their progenitors. Exp Cell Res 187:211-223.

Gallo V, Bertolotto A, Levi G (1987) The proteoglycan chondroitin sulfate is present in a subpopulation of cultured astrocytes and in their precursors. Dev Biol 123:282-285.

Galtrey CM, Asher RA, Nothias F, Fawcett JW (2007) Promoting plasticity in the spinal cord with chondroitinase improves functional recovery after peripheral nerve repair. Brain 130:926-939.

Gao Y, Deng K, Hou J, Bryson JB, Barco A, Nikulina E, Spencer T, Mellado W, Kandel ER, Filbin MT (2004) Activated CREB is sufficient to overcome inhibitors in myelin and promote spinal axonal regeneration *in vivo*. Neuron 44:609-621.

George EB, Glass JD, Griffin JW (1995) Axotomy-induced axonal degeneration is mediated by calcium influx through ion-specific channels. J Neurosci 15:6445-6452.

Goldberg JL (2004) Intrinsic neuronal regulation of axon and dendrite growth. Curr Opin Neurobiol 14:551-557.

Goldberg JL, Klassen MP, Hua Y, Barres BA (2002) Amacrine-signaled loss of intrinsic axon growth ability by retinal ganglion cells. Science 296:1860-1864.

Goshima Y, Kawakami T, Hori H, Sugiyama Y, Takasawa S, Hashimoto Y, Kagoshima-Maezono M, Takenaka T, Misu Y, Strittmatter SM (1997) A novel action of collapsin: collapsin-1 increases antero- and retrograde axoplasmic transport independently of growth cone collapse. J Neurobiol 33:316-328.

Griffin JW, Price DL, Drachman DB, Morris J (1981) Incorporation of axonally transported glycoproteins into axolemma during nerve regeneration. J Cell Biol 88:205-214.

Grimpe B, Silver J (2002) The extracellular matrix in axonal regeneration. Prog Brain Res 137:333-349.

Gross RE, Mei Q, Gutekunst CA, Torre E (2007) The pivotal role of RhoA GTPase in the molecular signaling of axon growth inhibition after CNS injury and targeted therapeutic strategies. Cell Transplant 16:245-262.

Hall AC, Lucas FR, Salinas PC (2000) Axonal remodeling and synaptic differentiation in the cerebellum is regulated by WNT-7a signaling. Cell 100:525-535.

Hanz S, Perlson E, Willis D, Zheng JQ, Massarwa R, Huerta JJ, Koltzenburg M, Kohler M, van-Minnen J, Twiss JL, Fainzilber M (2003) Axoplasmic importins enable retrograde injury signaling in lesioned nerve. Neuron 40:1095-1104.

Harel NY, Strittmatter SM (2006) Can regenerating axons recapitulate developmental guidance during recovery from SCI? Nat Rev Neurosci 7:603-616.

Hata K, Kubo T, Yamaguchi A, Yamashita T (2006) Signaling mechanisms of axon growth inhibition. Drug News Perspect 19:541-547.

Hatten ME (1985) Neuronal regulation of astroglial morphology and proliferation *in vitro*. J Cell Biol 100:384-396.

He XL, Bazan JF, McDermott G, Park JB, Wang K, Tessier-Lavigne M, He Z, Garcia KC (2003) Structure of the Nogo receptor ectodomain: a recognition module implicated in myelin inhibition. Neuron 38:177-185.

Helmchen F, Denk W (2005) Deep tissue two-photon microscopy. Nat Methods 2:932-940.

Helmchen F, Fee MS, Tank DW, Denk W (2001) A miniature head-mounted two-photon microscope. high-resolution brain imaging in freely moving animals. Neuron 31:903-912.

Herrera AA, Banner LR, Nagaya N (1990) Repeated, *in vivo* observation of frog neuromuscular junctions: remodelling involves concurrent growth and retraction. J Neurocytol 19:85-99.

Hill CE, Beattie MS, Bresnahan JC (2001) Degeneration and sprouting of identified descending supraspinal axons after contusive SCI in the rat. Exp Neurol 171:153-169.

Hill RR, Robbins N (1991) Mode of enlargement of young mouse neuromuscular junctions observed repeatedly *in vivo* with visualization of pre- and postsynaptic borders. J Neurocytol 20:183-194.

Hiraga A, Kuwabara S, Doya H, Kanai K, Fujitani M, Taniguchi J, Arai K, Mori M, Hattori T, Yamashita T (2006) Rho-kinase inhibition enhances axonal regeneration after peripheral nerve injury. J Peripher Nerv Syst 11:217-224.

Hirokawa N, Takemura R (2005) Molecular motors and mechanisms of directional transport in neurons. Nat Rev Neurosci 6:201-214.

Huang DW, McKerracher L, Braun PE, David S (1999) A therapeutic vaccine approach to stimulate axonal regeneration in the adult mammalian spinal cord. Neuron 24:639-647.

Huber AB, Schwab ME (2000) Nogo-A, a potent inhibitor of neurite outgrowth and regeneration. Biol Chem 381:407-419.

Huisken J, Swoger J, Del Bene F, Wittbrodt J, Stelzer EH (2004) Optical sectioning deep inside live embryos by selective plane illumination microscopy. Science 305:1007-1009.

Jareb M, Banker G (1997) Inhibition of axonal growth by brefeldin A in hippocampal neurons in culture. J Neurosci 17:8955-8963.

Johnson-Green PC, Dow KE, Riopelle RJ (1991) Characterization of glycosaminoglycans produced by primary astrocytes *in vitro*. Glia 4:314-321.

Johnson FA, Dawson AJ, Meyer RL (1999) Activity-dependent refinement in the goldfish retinotectal system is mediated by the dynamic regulation of processes withdrawal: an *in vivo* imaging study. J Comp Neurol 406:548-562.

Jones LL, Margolis RU, Tuszynski MH (2003) The chondroitin sulfate proteoglycans neurocan, brevican, phosphacan, and versican are differentially regulated following SCI. Exp Neurol 182:399-411.

Joosten EA (1997) Corticospinal tract regrowth. Prog Neurobiol 53:1-25.

Kabir N, Schaefer AW, Nakhost A, Sossin WS, Forscher P (2001) Protein kinase C activation promotes microtubule advance in neuronal growth cones by increasing average microtubule growth lifetimes. J Cell Biol 152:1033-1044.

Katoh-Semba R, Matsuda M, Kato K, Oohira A (1995) Chondroitin sulphate proteoglycans in the rat brain: candidates for axon barriers of sensory neurons and the possible modification by laminin of their actions. Eur J Neurosci 7:613-621.

Kerschensteiner M, Schwab ME, Lichtman JW, Misgeld T (2005) *In vivo* imaging of axonal degeneration and regeneration in the injured spinal cord. Nat Med 11:572-577.

Kikuchi K, Kishino A, Konishi O, Kumagai K, Hosotani N, Saji I, Nakayama C, Kimura T (2003) *In vitro* and *in vivo* characterization of a novel semaphorin 3A inhibitor, SM-216289 or xanthofulvin. J Biol Chem 278:42985-42991.

Kim JE, Li S, GrandPre T, Qiu D, Strittmatter SM (2003) Axonal regeneration in young adult mice lacking Nogo-A/B. Neuron 38:187-199.

Krekoski CA, Neubauer D, Zuo J, Muir D (2001) Axonal regeneration into acellular nerve grafts is enhanced by degradation of chondroitin sulfate proteoglycan. J Neurosci 21:6206-6213.

Langenfeld-Oster B, Dorlochter M, Wernig A (1993) Regular and photodamage-enhanced remodelling in vitally stained frog and mouse neuromuscular junctions. J Neurocytol 22:517-530.

Lewis PR, Shute CC (1969) An electron-microscopic study of cholinesterase distribution in the rat adrenal medulla. J Microsc 89:181-193.

Li M, Shibata A, Li C, Braun PE, McKerracher L, Roder J, Kater SB, David S (1996) Myelin-associated glycoprotein inhibits neurite/axon growth and causes growth cone collapse. J Neurosci Res 46:404-414.

Li Y, Raisman G (1995) Sprouts from cut corticospinal axons persist in the presence of astrocytic scarring in long-term lesions of the adult rat spinal cord. Exp Neurol 134:102-111.

Lichtman JW, Fraser SE (2001) The neuronal naturalist: watching neurons in their native habitat. Nat Neurosci 4 Suppl:1215-1220.

Lockerbie RO, Miller VE, Pfenninger KH (1991) Regulated plasmalemmal expansion in nerve growth cones. J Cell Biol 112:1215-1227.

Lu P, Jones LL, Tuszynski MH (2007) Axonal regeneration through scars and into sites of chronic SCI. Exp Neurol 203:8-21.

Ma D, Connors T, Nothias F, Fischer I (2000) Regulation of the expression and phosphorylation of microtubule-associated protein 1B during regeneration of adult dorsal root ganglion neurons. Neuroscience 99:157-170.

Mack TG, Koester MP, Pollerberg GE (2000) The microtubule-associated protein MAP1B is involved in local stabilization of turning growth cones. Mol Cell Neurosci 15:51-65.

Margolis RK, Margolis RU (1993) Nervous tissue proteoglycans. Experientia 49:429-446.

McGee AW, Yang Y, Fischer QS, Daw NW, Strittmatter SM (2005) Experience-driven plasticity of visual cortex limited by myelin and Nogo receptor. Science 309:2222-2226.

McKeon RJ, Jurynec MJ, Buck CR (1999) The chondroitin sulfate proteoglycans neurocan and phosphacan are expressed by reactive astrocytes in the chronic CNS glial scar. J Neurosci 19:10778-10788.

McKeon RJ, Schreiber RC, Rudge JS, Silver J (1991) Reduction of neurite outgrowth in a model of glial scarring following CNS injury is correlated with the expression of inhibitory molecules on reactive astrocytes. J Neurosci 11:3398-3411.

McQuarrie IG, Grafstein B, Gershon MD (1977) Axonal regeneration in the rat sciatic nerve: effect of a conditioning lesion and of dbcAMP. Brain Res 132:443-453.

McQuarrie IG, Grafstein B, Dreyfus CF, Gershon MD (1978) Regeneration of adrenergic axons in rat sciatic nerve: effect of a conditioning lesion. Brain Res 141:21-34.

Miller FD, Tetzlaff W, Bisby MA, Fawcett JW, Milner RJ (1989) Rapid induction of the major embryonic alpha-tubulin mRNA, T alpha 1, during nerve regeneration in adult rats. J Neurosci 9:1452-1463.

Mimura F, Yamagishi S, Arimura N, Fujitani M, Kubo T, Kaibuchi K, Yamashita T (2006) MAG inhibits microtubule assembly by a Rho-kinase dependent mechanism. J Biol Chem.

Misgeld T, Kerschensteiner M (2006) *In vivo* imaging of the diseased nervous system. Nat Rev Neurosci 7:449-463.

Misgeld T, Nikic I, Kerschensteiner M (2007) *In vivo* imaging of single axons in the mouse spinal cord. Nat Protoc 2:263-268.

Moon LD, Asher RA, Rhodes KE, Fawcett JW (2001) Regeneration of CNS axons back to their target following treatment of adult rat brain with chondroitinase ABC. Nat Neurosci 4:465-466.

Morgenstern DA, Asher RA, Fawcett JW (2002) Chondroitin sulphate proteoglycans in the CNS injury response. Prog Brain Res 137:313-332.

Morris RL, Hollenbeck PJ (1993) The regulation of bidirectional mitochondrial transport is coordinated with axonal outgrowth. J Cell Sci 104 (Pt 3):917-927.

Moskowitz PF, Oblinger MM (1995) Sensory neurons selectively upregulate synthesis and transport of the beta III-tubulin protein during axonal regeneration. J Neurosci 15:1545-1555.

Myers KA, He Y, Hasaka TP, Baas PW (2006) Microtubule transport in the axon: Re-thinking a potential role for the actin cytoskeleton. Neuroscientist 12:107-118.

Neumann S, Woolf CJ (1999) Regeneration of dorsal column fibers into and beyond the lesion site following adult SCI. Neuron 23:83-91.

Neumann S, Bradke F, Tessier-Lavigne M, Basbaum AI (2002) Regeneration of sensory axons within the injured spinal cord induced by intraganglionic cAMP elevation. Neuron 34:885-893.

Ng CE, Tang BL (2002) Nogos and the Nogo-66 receptor: factors inhibiting CNS neuron regeneration. J Neurosci Res 67:559-565.

Niclou SP, Franssen EH, Ehlert EM, Taniguchi M, Verhaagen J (2003) Meningeal cell-derived semaphorin 3A inhibits neurite outgrowth. Mol Cell Neurosci 24:902-912.

Niederost B, Oertle T, Fritsche J, McKinney RA, Bandtlow CE (2002) Nogo-A and myelin-associated glycoprotein mediate neurite growth inhibition by antagonistic regulation of RhoA and Rac1. J Neurosci 22:10368-10376.

Niederost BP, Zimmermann DR, Schwab ME, Bandtlow CE (1999) Bovine CNS myelin contains neurite growth-inhibitory activity associated with chondroitin sulfate proteoglycans. J Neurosci 19:8979-8989.

Nikulina E, Tidwell JL, Dai HN, Bregman BS, Filbin MT (2004) The phosphodiesterase inhibitor rolipram delivered after a spinal cord lesion promotes axonal regeneration and functional recovery. Proc Natl Acad Sci U S A 101:8786-8790.

Okada S, Nakamura M, Katoh H, Miyao T, Shimazaki T, Ishii K, Yamane J, Yoshimura A, Iwamoto Y, Toyama Y, Okano H (2006) Conditional ablation of Stat3 or Socs3 discloses a dual role for reactive astrocytes after SCI. Nat Med 12:829-834.

Pan YA, Misgeld T, Lichtman JW, Sanes JR (2003) Effects of neurotoxic and neuroprotective agents on peripheral nerve regeneration assayed by time-lapse imaging *in vivo*. J Neurosci 23:11479-11488.

Pasterkamp RJ, Anderson PN, Verhaagen J (2001) Peripheral nerve injury fails to induce growth of lesioned ascending dorsal column axons into spinal cord scar tissue expressing the axon repellent Semaphorin3A. Eur J Neurosci 13:457-471.

Pfenninger KH, Maylie-Pfenninger MF (1981) Lectin labeling of sprouting neurons. II. Relative movement and appearance of glycoconjugates during plasmalemmal expansion. J Cell Biol 89:547-559.

Pindzola RR, Doller C, Silver J (1993) Putative inhibitory extracellular matrix molecules at the dorsal root entry zone of the spinal cord during development and after root and sciatic nerve lesions. Dev Biol 156:34-48.

Qiu J, Cafferty WB, McMahon SB, Thompson SW (2005) Conditioning injury-induced spinal axonal regeneration requires signal transducer and activator of transcription 3 activation. J Neurosci 25:1645-1653.

Qiu J, Cai D, Dai H, McAtee M, Hoffman PN, Bregman BS, Filbin MT (2002) Spinal axonal regeneration induced by elevation of cyclic AMP. Neuron 34:895-903.

Ramon y Cajal S (1928) Degeneration and Regeneration of the Nervous System. London: Oxford Univ. Press.

Richardson PM, Issa VM (1984) Peripheral injury enhances central regeneration of primary sensory neurones. Nature 309:791-793.

Richardson PM, Verge VM (1987) Axonal regeneration in dorsal spinal roots is accelerated by peripheral axonal transection. Brain Res 411:406-408.

Sabry J, O'Connor TP, Kirschner MW (1995) Axonal transport of tubulin in Ti1 pioneer neurons in situ. Neuron 14:1247-1256.

Sabry JH, O'Connor TP, Evans L, Toroian-Raymond A, Kirschner M, Bentley D (1991) Microtubule behavior during guidance of pioneer neuron growth cones in situ. J Cell Biol 115:381-395.

Schaefer AW, Kabir N, Forscher P (2002) Filopodia and actin arcs guide the assembly and transport of two populations of microtubules with unique dynamic parameters in neuronal growth cones. J Cell Biol 158:139-152.

Schnell L, Schwab ME (1990) Axonal regeneration in the rat spinal cord produced by an antibody against myelin-associated neurite growth inhibitors. Nature 343:269-272.

Schwab ME (2002) Repairing the injured spinal cord. Science 295:1029-1031.

Schwab ME (2004) Nogo and axonal regeneration. Curr Opin Neurobiol 14:118-124.

Schwab ME, Bartholdi D (1996) Degeneration and regeneration of axons in the lesioned spinal cord. Physiol Rev 76:319-370.

Schwamborn JC, Puschel AW (2004) The sequential activity of the GTPases Rap1B and Cdc42 determines neuronal polarity. Nat Neurosci 7:923-929.

Schweigreiter R, Walmsley AR, Niederost B, Zimmermann DR, Oertle T, Casademunt E, Frentzel S, Dechant G, Mir A, Bandtlow CE (2004) Versican V2 and the central inhibitory domain of Nogo-A inhibit neurite growth via p75NTR/NgR-independent pathways that converge at RhoA. Mol Cell Neurosci 27:163-174.

Seijffers R, Allchorne AJ, Woolf CJ (2006) The transcription factor ATF-3 promotes neurite outgrowth. Mol Cell Neurosci 32:143-154.

Shewan D, Dwivedy A, Anderson R, Holt CE (2002) Age-related changes underlie switch in netrin-1 responsiveness as growth cones advance along visual pathway. Nat Neurosci 5:955-962.

Silver J, Miller JH (2004) Regeneration beyond the glial scar. Nat Rev Neurosci 5:146-156.

Sivasankaran R, Pei J, Wang KC, Zhang YP, Shields CB, Xu XM, He Z (2004) PKC mediates inhibitory effects of myelin and chondroitin sulfate proteoglycans on axonal regeneration. Nat Neurosci 7:261-268.

Smith DS, Skene JH (1997) A transcription-dependent switch controls competence of adult neurons for distinct modes of axon growth. J Neurosci 17:646-658.

Song H, Ming G, He Z, Lehmann M, McKerracher L, Tessier-Lavigne M, Poo M (1998) Conversion of neuronal growth cone responses from repulsion to attraction by cyclic nucleotides. Science 281:1515-1518.

Steinmetz MP, Horn KP, Tom VJ, Miller JH, Busch SA, Nair D, Silver DJ, Silver J (2005) Chronic enhancement of the intrinsic growth capacity of sensory neurons combined with the degradation of inhibitory proteoglycans allows functional regeneration of sensory axons through the dorsal root entry zone in the mammalian spinal cord. J Neurosci 25:8066-8076.

Steward O, Zheng B, Tessier-Lavigne M (2003) False resurrections: distinguishing regenerated from spared axons in the injured central nervous system. J Comp Neurol 459:1-8.

Suter DM, Forscher P (1998) An emerging link between cytoskeletal dynamics and cell adhesion molecules in growth cone guidance. Curr Opin Neurobiol 8:106-116.

Suter DM, Errante LD, Belotserkovsky V, Forscher P (1998) The Ig superfamily cell adhesion molecule, apCAM, mediates growth cone steering by substrate-cytoskeletal coupling. J Cell Biol 141:227-240.

Tan AM, Colletti M, Rorai AT, Skene JH, Levine JM (2006) Antibodies against the NG2 proteoglycan promote the regeneration of sensory axons within the dorsal columns of the spinal cord. J Neurosci 26:4729-4739.

Tanaka EM, Kirschner MW (1991) Microtubule behavior in the growth cones of living neurons during axon elongation. J Cell Biol 115:345-363.

Tang S, Woodhall RW, Shen YJ, deBellard ME, Saffell JL, Doherty P, Walsh FS, Filbin MT (1997) Soluble myelin-associated glycoprotein (MAG) found *in vivo* inhibits axonal regeneration. Mol Cell Neurosci 9:333-346.

Tang X, Davies JE, Davies SJ (2003) Changes in distribution, cell associations, and protein expression levels of NG2, neurocan, phosphacan, brevican, versican V2, and tenascin-C during acute to chronic maturation of spinal cord scar tissue. J Neurosci Res 71:427-444.

Tom VJ, Steinmetz MP, Miller JH, Doller CM, Silver J (2004) Studies on the development and behavior of the dystrophic growth cone, the hallmark of regeneration failure, in an *in vitro* model of the glial scar and after SCI. J Neurosci 24:6531-6539.

Villringer A, Them A, Lindauer U, Einhaupl K, Dirnagl U (1994) Capillary perfusion of the rat brain cortex. An *in vivo* confocal microscopy study. Circ Res 75:55-62.

Vogt L, Giger RJ, Ziegler U, Kunz B, Buchstaller A, Hermens W, Kaplitt MG, Rosenfeld MR, Pfaff DW, Verhaagen J, Sonderegger P (1996) Continuous renewal of the axonal pathway sensor apparatus by insertion of new sensor molecules into the growth cone membrane. Curr Biol 6:1153-1158.

Westermann S, Weber K (2003) Post-translational modifications regulate microtubule function. Nat Rev Mol Cell Biol 4:938-947.

Wigston DJ (1989) Remodeling of neuromuscular junctions in adult mouse soleus. J Neurosci 9:639-647.

Yamada KM, Spooner BS, Wessells NK (1970) Axon growth: roles of microfilaments and microtubules. Proc Natl Acad Sci U S A 66:1206-1212.

Yiu G, He Z (2006) Glial inhibition of CNS axonal regeneration. Nat Rev Neurosci 7:617-627.

You SW, Chen BY, Liu HL, Lang B, Xia JL, Jiao XY, Ju G (2003) Spontaneous recovery of locomotion induced by remaining fibers after spinal cord transection in adult rats. Restor Neurol Neurosci 21:39-45.

Young W (2002) Spinal cord contusion models. Prog Brain Res 137:231-255.

Zang DW, Cheema SS (2003) Leukemia inhibitory factor promotes recovery of locomotor function following SCI in the mouse. J Neurotrauma 20:1215-1222.

Zhang Y, Bo X, Schoepfer R, Holtmaat AJ, Verhaagen J, Emson PC, Lieberman AR, Anderson PN (2005) Growth-associated protein GAP-43 and L1 act synergistically to promote regenerative growth of Purkinje cell axons *in vivo*. Proc Natl Acad Sci U S A 102:14883-14888.

Zheng B, Ho C, Li S, Keirstead H, Steward O, Tessier-Lavigne M (2003) Lack of enhanced spinal regeneration in Nogo-deficient mice. Neuron 38:213-224.

Zhou FQ, Cohan CS (2001) Growth cone collapse through coincident loss of actin bundles and leading edge actin without actin depolymerization. J Cell Biol 153:1071-1084.

Curriculum vitae

Personal Data:

Name: Ali Ertürk

Birth data / place: 28 September 1980 / Sakarya, Turkey

Contact info:

E-mail: erturk@neuro.mpg.de ; karasusakarya@yahoo.com

Call: +49 0176 7677 9660 or +49 89 8578 3462

Present Address:

Max-Planck Institute für Neurobiologie

Am Klopferspitz 18, 82152 Martinsried, Germany

Home-Address:

Kraepelinstr. 12 80804 München, Germany

Education:

- 1994-1997: Sakarya Super High School
- 1997-1998: Adapazari Isik Collage
- 1998-2003: Bachelor of Science, Bilkent University, Faculty of Science, Department of Molecular Biology and Genetics
- 2003-2007: Graduate (Ph.D.) student at Max-Planck Institute of Neurobiology

Achievements and Awards:

- Graduated from the primary and high school as the most successful student.
- Participated in math and physics Olympiads to represent my high school.
- Became 345th most successful student among approximately 1,500,000 students (0.02%) who participated in the national university entrance exam with a total of 571 points over

approximately 589 points.

- Full scholarship awarded by Bilkent University (1998-2003).
- Full scholarship awarded by TUBITAK (Turkey Science And Technology Institute), (1998-2000).
- Early Stage Researcher Fellowship from Marie Curie Foundation as a member of Nervous System Repair research training network (2004 Sep-2007 Aug).

Computer knowledge:

- Experiences in Java, Basic, UNIX, Microsoft office, Windows and Mac applications, Photoshop, Illustrator, Canvas, Amira and several other software.

Experimental skills:

- Basic Molecular cell biology, Biochemistry and Microbiology techniques
- PCR, RT-PCR, Agarose gel electrophoresis, Transformation of bacteria, Transfection of mammalian cell, Miniprep, Maxiprep, Subcloning
- DNA and Protein isolation, Western blotting, SDS-PAGE
- Cell fixation and staining, micro dissection of mouse brain for neocortex cell culture, neuron culture, perfusion of mouse, spinal cord dissection, tissue sectioning, immunohistochemisty
- SPECT and MRI analysis by computer software
- Spinal cord lesion on rats and mice
- Confocal microscopy, Electron microscopy, *in vivo* live imaging microscopy

Research Experiences:

- Time Period: June 2001-September 2001

  Place: Yale University School of Medicine, summer lab research study, (Blumenfeld Lab)

  Subject: Coregistration of MRI and SPECT images and volumetric statistics on ictal-interictal SPECT changes in cortical and subcortical structures during seizures in the

epilepsy patients

- Time Period: June 2002- September 2002

  Place:Harvard University, Harvard Institutes of Medicine, summer lab research study, (Vartanian Lab)

Subject: Explore novel functions of toll-like receptors in the central nervous system (CNS) by molecular and cellular approaches

- Time Period: September 2002- June 2003

  Place: Bilkent University, Department of Molecular Biology and Genetics, Senior Project, (Ahmed Lab)

  Subject: The roles of LPS in attachment of bacterium *Moraxella catarrhalis* to Human pharyngeal epithelial cell.

- Time Period: October 2003- 2007

  Place: Max-Planck-Institute of Neurobiology, PhD project, (Bradke Group)

  Subject: *In vivo* characterization of retraction bulbs after SCI.

Workshops Attended (Certificates Received):

- SCI training course in Ohio State University, USA (for 3 weeks in 2004)
- "Disease models *in vivo* and *in vitro*" workshop in Lund University, Sweden (for 5 days, in 2005)
- "Genes and Cell Therapies" workshop in EPFL, Switzerland (for 5 days, in 2005)
- "Neurodegenerative Diseases: Mechanisms and Treatments" workshop in MPI Neurobiology, Germany (for 5 days, in 2006)
- Spring School and Nervous System Repair Workshop, university of Cambridge, Centre for Brain Repair, UK (for 5 days in 2006)
- "Stem cells and their usage in Neurodegenerative diseases", workshop in University of Turin, Italy (for 5 days in 2006)
- "Neurodegenerative diseases", workshop in University of Göttingen, Germany (for 4 days in 2007)
- "Technologies in Neuronal System Repair" workshop in Karolinska Istitute, Sweden (for 4 days, in 2007)

- "Nervous System Repair" workshop in Institute of Developmental Biology of Marseilles-Luminy (IBDML) Marseilles, France (for 5 days, in 2007)

Languages:

- English (Fluent) - German (Intermediate) - Turkish (Mother Tongue)

Interests:

- I am interested in many sports, especially football. I like dancing and taking photos (three times chosen as the day of the photographer on the most famous Turkish photography web-site (www.fotokritik.com). (Some of my photographs can be seen at: http://picasaweb.google.com/karasusakarya).

Publications:

Erturk A, Hellal F, Enes J, Bradke F (2007) Disorganized microtubules underlie the formation of retraction bulbs and the failure of axonal regeneration. J Neurosci 27:9169-9180.

Akgul G, **Erturk A**, Turkoz M, Turan T, Ichinose A, Nagatake T, Ahmed K.
Role of lipooligosaccharide in the attachment of Moraxella catarrhalis to human pharyngeal epithelial cells. Microbiol Immunol. 2005;49(10):931-5.

Patents:

Bradke F, Witte H, **Erturk A**. Use of microtubule stabilizing compounds for the treatment of lesions of CNS axons **(WO/2006/094811).**

References:

- **Frank Bradke, Ph.D**

Address: **Office Phone:** + 49-89-8578 3641

Max-Planck Institute of Neurobiology **Fax:** + 49-89-8578 3240

Am Klopferspitz 18 Email: fbradke@neuro.mpg.de

82152 Martinsried, Germany

- **Kamruddin Ahmed , Ph.D**

Address: **Office Phone:** :+81-97-586-5798

Oita University **Fax:** +81-97-586-5719

Dept. of Social and Environmental Medicine **Email:** ahmed@med.oita-u.ac.jp

1-1 Hasama-machi, Yufu-shi, Oita 879-5593, Japan

- **Timothy K. Vartanian, M.D., Ph.D**

Address:

Harvard Institutes of Medicine **Office Phone:** 617-667-0809

77 Avenue Louis Pasteur **Fax:** 617-667-0811

Boston, Massachusetts 02115 **Email:** tvartani@caregroup.harvard.edu

- **Hal Blumenfeld, M.D., Ph.D**

Address:

New Haven, Connecticut **Phone:** (203) 785-3928

06520-8018 **Fax:** (203) 737-2538

United States **Email:**hal.blumenfeld@yale.edu